Hepato-protective role of Fragile X Mental Retardation Protein (FMRP) and Immune Cells in Liver Diseases

Inaugural dissertation

for the attainment of the title of doctor
in the Faculty of Mathematics and Natural Sciences
at the Heinrich Heine University Düsseldorf

presented by

Yuan Zhuang
from Linyi, China

Düsseldorf, 02.12.2019

From the Institute of Molecular Medicine II,
at the Heinrich Heine University Düsseldorf

Published by permission of the
Faculty of Mathematics and Natural Sciences at
Heinrich Heine University Düsseldorf

Supervisor: Prof. Philipp Lang,
Institute of Molecular Medicine II,
Heinrich-Heine-University
Düsseldorf

Co-Supervisor: Prof. Heiner Schaal,
Institute of Virology,
Heinrich-Heine-University
Düsseldorf

Date of the oral examination: 23.01.2020
Place: Düsseldorf

Table of content

DECLARATION AND STATEMENT OF CONTRIBUTION 5
ACKNOWLEDGMENT 6
ABBREVIATIONS 8
SUMMARY 11
1. INTRODUCTION 13
1.1 General Introduction of Liver 13
1.1.1 Anatomy of liver 13
1.1.2 Function of liver 13
1.1.3 Liver diseases 14
1.2 Fragile X mental retardation 15
1.2.1 Fragile X syndrome 15
1.2.2 Function of FMRP in neuronal development and treatment 15
1.2.3 Function of FMRP during infection 16
1.2.4 Function of FMRP in regulating DNA damage response 17
1.3 Tumor necrosis factor (TNF) 18
1.3.1 Discovery 18
1.3.2 Structure of TNF and TNF receptors (TNFRs) 19
1.3.3 TNF-TNFR1 regulates NF-κB signaling 19
1.4 TNF-TNFR1 regulated cell death pathway 21
1.4.1 Discovery of apoptosis and necroptosis 21
1.4.2 Apoptosis and necroptosis signaling 21
1.4.3 Inhibitors of apoptosis and necroptosis 22
1.5 Virus infection and Immune response 23
1.5.1 Lymphocytic choriomeningitis virus (LCMV) 23
1.5.2 Immune response 23
1.5.2.1 Innate immunity 23
1.5.2.1.1 Dendritic cells (DCs) 24
1.5.2.1.2 Macrophages 25
1.5.2.1.3 Red pulp and Marginal zone macrophages 25
1.5.2.1.4 CD169+ macrophages 26
1.5.2.2 Adaptive immune response 27

1.5.2.2.1 B cells....27
1.5.2.2.2 T cells....28
1.6 Liver Cholestasis and fibrosis....30
1.6.1 Bile duct ligation (BDL)....30
1.6.2 Hepatocytes injury and Hepatocellular Proliferation....30
1.6.3 Inflammatory response....31
1.6.4 Liver fibrosis development....31
1.7 Liver regeneration....34
1.7.1 Liver regeneration....34
1.7.2 Cytokines and growth factors during liver regeneration....35
1.7.2.1 IL-6....35
1.7.2.2 TNF....35
1.7.2.3 Lymphotoxins....36
1.7.2.4 Growth factors....37
1.7.2.5 Transforming growth factor....37
1.7.2.6 Other growth factors....37
2. PUBLICATION....39
2.1 Fragile X mental retardation protein protects against tumour necrosis factor-mediated cell death and liver injury....39
2.2 B Cell-Mediated Maintenance of Cluster of Differentiation 169-Positive Cells Is Critical for Liver Regeneration....62
3. DISCUSSION....86
4. REFERENCES....93

Declaration and statement of contribution

I, Yuan Zhuang, declare that the content in this dissertation is original. I have cited appropriate texts and figures wherever necessary. No part of this dissertation is submitted somewhere else for consideration of a degree.

Part of the dissertation is published in the following publications,

1. **Zhuang Y**, Xu HC, Shinde PV, et al., Fragile X mental retardation protein protects against tumour necrosis factor-mediated cell death and liver injury. ***Gut*** August 2019. doi: 10.1136/gutjnl-2019-318215

   I was involved in execution of the experiments, analysis, writing and preparation of the manuscript which consists 25% of the published manuscript.

2. *Behnke, K., ***Zhuang, Y**., Xu, H.C., Sundaram, B et al., B Cell-Mediated Maintenance of Cluster of Differentiation 169–Positive Cells Is Critical for Liver Regeneration. ***Hepatology*** May 2018, 68: 2348-2361. doi:10.1002/hep.30088 (*Shared authorship)

   I was involved in execution of the experiments, analysis, writing and preparation of the manuscript which consists 12.5% of the published manuscript.

Yuan Zhuang

Place: Düsseldorf, Germany

Acknowledgment

First of all, I would like to thank my supervisor **Prof. Philipp Lang**, who provided me with constant guidance and chance to do research in his lab. Throughout the years, he made sure his detailed orientedness and passion for excellence also percolated in his students. Without his support, it would have been a difficult achieve all the goals, which I had set for myself before I began on the path of being a PhD student. I have a deep gratitude and respect towards him. Thank you, Philipp, for showing immense patience and helping me to achieve my goals.

I would like to thank my second supervisor **Prof. Heiner Schaal**, who has patiently listened to my talks and provided me with valuable inputs.

I would like to thank **Chris**, **Prashant** for helping me learn all the methods and critically think about the experiments. Especially, I learned and will keep following how **Chris** designs the experiments extremely well with proper negative and positive controls. **Prashant** thanks for helping me to broaden my horizons of imagination. I wish that I could be like you to explore new things with a peaceful mind. **Bala**, over the years you have been extremely supportive to me and we have special bond I cannot thank you enough for all the helps form you. I would like to thank **Kristina** and **Elisabeth** for helping me learn the various surgical techniques I would also like to thank **Melanie** and **Vitaly**, the lovely couple in the lab for being so joyful and helpful in the lab. **The people now in our lab or left** in between were awesome; I know how to get along with different people with different culture.

Dear **Jun**, **Rui**, **Wei** and **Anfei** thank you for being there for me in the most difficult and stressful times and your company which helped me feel like I was home. I will never forget our get together and delicious weekend lunches and dinners.

Special thanks to my supervisors in China for my Master's thesis, **Prof. Weiwei Zhang** and **Prof. Wei Xiao**; who introduced me to research and teaching me the basics of doing science in the lab. I had got proper scientific training after my Master, which, I believe, is helped me to complete my PhD and will help me throughout my research career.

I would like to thank **Dr. Vijay Tiwari**, I really appreciate that you offered me the position in IMB Mainz, which brought me to Germany and introduced me to epigenetics field. **IMB** is one of the most amazing institutes I have ever seen, with nice communications with each other, advanced technologies and free coffee and food, even though I stayed there only for short time,

I acquired tremendous amount of energy and zeal about the science from the lab mates and others which helped me during my PhD study.

My **mamma** and **baba**, without you all this, I never would have achieved if you hadn't shown your support. I know that you don't understand what I do but still you encouraged me to follow my dreams and do whatever I can to achieve it. What else do you want from your parents? All the years spent away from home I still feel you are close to me.

My brother **Peng Zhuang** and sister in law **Xiaolei Huang**, thank you guys so much for your support during my study and to what you contribute to support our parents and our whole family. I want to say loudly that I love my family so much. I feel like that I am really lucky girl to have so much love from everyone in my family, **my grandparents**, **my aunties** and **my friends** from my bachelor and master, especially **Xiaoqing Gao, Fangfang Li and Juanjuan Wang.**

Finally, **Lang Lang** my lovely nephew, you are too young to read this, but when you do, remember that your aunt missed you a lot and you made her laugh so much because of your shenanigans. You always brightened my day in darkest hours.

Lastly, I thank all the people who helped throughout the years to reach one of the most important milestones of life.

Abbreviations

ALS	Amyotrophic lateral sclerosis
ALT	Alanine aminotransferase
APAP	Acetaminophen
APC	Antigen presenting cells
AST	Aspartate aminotransferase
ATR	Ataxia telangiectasia and Rad3-related protein
α-SMA	α-smooth muscle actin
BAFF	B cell-activating factor
BAFFR	B cell-activating factor receptor
BCL	B-cell lymphoma
BCMA	B-cell maturation factor
BCR	B cell receptors
BDL	Bile duct ligation
BRCA1	Breast cancer type 1 susceptibility protein
CDK	Cyclin-dependent kinases
CHX	Cycloheximide
ConA	Concanavalin A
CXCL	Chemokine CXC ligand
CYLD	Cylindromatosis
DAMP	Damage-associated molecular patterns
DKO	Double knockout
DTR	Diphtheria toxin receptor
ECM	Extracellular matrix
EGF	Epidermal growth factor
ERK	Extracellular signal-regulated kinases
FADD	Fas-associated death domain
FGF	Fibroblast growth factor
FGFR	Fibroblast growth factor receptor
FISH	Fluorescence in situ hybridization
FLIP	FLICE-like inhibitory protein
$FLIP_L$	Long isoform of FLICE-like inhibitory protein

FLIPs	Short isoform of FLICE-like inhibitory protein
FMR1	Fragile X mental retardation 1
FMRP	Fragile X mental retardation protein
FoB	Follicular B cells
FXPOI	Fragile X-associated primary ovarian insufficiency
FXR	Farnesoid X receptor
FXS	Fragile X syndrome
FXTAS	Fragile X associated Tremor/Ataxia Syndrome
HBV	Hepatitis B virus
HCC	Hepatocellular carcinama
HCV	Hepatitis C virus
HGF	Hepatocyte growth factor
HSC	Hepatic stellate cells
ICAM	Intercellular adhesion molecule
IFN	Interferon
IκBα	Inhibitor of κB
IKK	Inhibitor of κBα kinases
IL-6	Interleukin-6
IRF	Interferon regulatory factor
IRHOM	Inactive rhomboid protein
JAK	Janus kinase
JNK	JUN N-terminal kinase
LAG	Lymphocyte-activation gene
LCMV	Lymphocytic choriomeningitis virus
LPC	Liver parenchymal cell
LPS	lipopolysaccharide
LT	Lymphotoxin
LUBAC	Linear ubiquitin chain assembly complex
MAPK	Mitogen-activated protein kinase
M-CSF	Macrophage colony stimulating factor
MDM	Mouse double minute 2 homolog
MHC	Major histocompatibility complex
MLKL	Mixed lineage kinase domain-like protein

MZB	Marginal zone B cells
Nec-1	Necrostatin-1
Nec-1s	7-Cl-O-Necrostatin-1
NEMO	Nuclear factor-κB-essential modulator
NF-κB	Nuclear factor-κB
PAMP	Pathogen associated molecular pattern
PARP	Poly (ADP-ribose) polymerase
PCNA	Proliferating cell nuclear antigen
PD-1	Programmed cell death-1
PD-L1	programmed death-ligand 1
PDGF	Platelet-derived growth factor
PDGFR	Platelet-derived growth factor receptor
PHx	Partial hepatectomy
RAG	Recombination-activating gene
RIPK	Receptor-interacting serine/threonine-protein kinase
RNP	Ribonucleoprotein
ROS	Reactive oxygen species
STAT	Signal transducer and activator of transcription
TAB	TAK-binding protein
TACE	Tumor necrosis factor-alpha-converting enzyme
TAK	Transforming growth factor β -activated kinase
TCR	T cell receptor
TGF	Transforming growth factor
TGR	Takeda G protein receptor
TLR	Toll-like receptor
TNF	Tumor necrosis factor
TNFR	Tumor necrosis factor receptor
TRADD	Tumor necrosis factor receptor type 1-associated death domain protein
TRAF	Tumor necrosis factor receptor-associated factor
TUNEL	Terminal deoxynucleotidyl transferase dUTP nick end labeling
VEGF	Vascular endothelial growth factor
VSV	Vesicular stomatitis virus

Summary

The Fragile X mental retardation (FMR) syndrome is a frequently inherited intellectual disability caused by decreased or absent expression of the FMR protein (FMRP). Lack of FMRP is associated with impaired neuronal development and cognitive dysfunction but its role outside the central nervous system is insufficiently studied. Here, we identify a role of FMRP in liver disease. *Fmr1*^{null} mice exhibited increased liver damage during virus-mediated hepatitis following infection with the lymphocytic choriomeningitis virus (LCMV). Exposure to Tumor necrosis factor (TNF) resulted in severe liver damage due to increased hepatocyte cell death. Consistently, we found increased caspase-8 and caspase-3 activation following TNF stimulation. Furthermore, we demonstrate FMRP to be critically important for regulating key molecules in TNF receptor 1 (TNFR1)-dependent apoptosis and necroptosis including Cylindromatosis (CYLD), short isoform of FLICE-like inhibitory protein (c-FLIP$_S$) and JUN N-terminal kinase (JNK), which contribute to prolonged receptor-interacting serine/threonine-protein kinase 1 (RIPK1) expression. Accordingly, the RIPK1 inhibitor Necrostatin-1s could reduce liver cell death and alleviate liver damage in *Fmr1*^{null} mice following TNF exposure. Consistently, FMRP-deficient mice developed increased pathology during experimentally induced acute cholestasis following bile duct ligation, which coincided with increased hepatic expression of RIPK1, RIPK3 and phosphorylation of mixed lineage kinase domain-like protein (MLKL). In conclusion, we show that FMRP plays a central role in the inhibition of TNF-mediated cell death during infection and liver disease.

The liver has an extraordinary capacity to regenerate through activation of key molecular pathways. However, central regulators controlling liver regeneration remain insufficiently studied. Here, we show that B cell–deficient animals failed to induce sufficient liver regeneration after partial hepatectomy (PHx). Consistently, adoptive transfer of B cells could rescue defective liver regeneration. B cell–mediated lymphotoxin beta production promoted recovery from PHx. Absence of B cells coincided with loss of splenic CD169 positive (CD169+) macrophages. Moreover, depletion of CD169$^+$ macrophages resulted in defective liver regeneration and decreased survival, which was associated with reduced hepatocyte proliferation. Mechanistically, CD169$^+$ macrophages contributed to liver regeneration by inducing hepatic interleukin-6 (IL-6) production and signal transducer and activator of transcription 3 activation. Accordingly, treatment of CD169+ cell–depleted animals with IL-6/IL-6 receptor rescued liver regeneration and severe pathology following PHx. In conclusion,

we identified CD169+ cells to be a central trigger for liver regeneration, by inducing key signaling pathways important for liver regeneration.

1. Introduction

1.1 General Introduction of Liver

1.1.1 Anatomy of liver

Liver is one of the biggest organs in human body, measuring about 2% to 3% of average body weight and located in the upper right part of the abdomen, below the diaphragm (1). Human liver is a dark reddish-brown and wedge-shaped organ, increasing in size from left to right (2). Liver is organized to the form of lobules divided into portal areas in the periphery and the central veins in the center of each lobule.

Hepatic artery, portal vein and common hepatic duct are connected to liver. Blood from hepatic artery and portal vein is the main blood supply to the liver (3). Described by morphologic anatomy and by functional anatomy, human liver has two lobes, which can be divided into 8 segments and each segment having its own arterial supply and venous and biliary drainage (4).

Mice and rats are used as an animal model to study human pathologies and diseases, which plays an integral part of medical research. Several murine models are used to study acute and chronic liver disease such as models of inflammatory liver disease related hepatitis, hepatectomy and alcohol, bile duct ligation and high-fat diet on hepatic fibrosis, as well as hepatocellular carcinoma and metastasis.

1.1.2 Function of liver

The liver plays a critical role on many physiological processes including production of metabolites, synthesizing proteins and producing biochemicals for digestion. The liver is responsible for the metabolism of carbohydrate, proteins, amino acids and lipids, as well as removing waste products from the blood. Additionally, the liver is an accessory digestive organ by producing bile containing cholesterol and bile acids. Bile is stored in the gallbladder and then is transported into the small intestine to complete digestion by the emulsification of fats (3).

The hepatic portal vein supplies 75%-80% of blood entering the liver, by collecting the blood drained from spleen, stomach, intestine, gallbladder and pancreas (5, 6). The substrates provided by these organs are used for synthesis, metabolism and transformation by the liver cell (hepatocytes) (7). Hepatocytes make up the largest mass of the liver with approximately

two thirds of the liver. Most of the rest structure is made up of Kupffer cells, stellate cells, endothelial cells, bile ductular cells, blood vessels and supportive structure (8). Since the liver is the metabolic factory of the body, hepatocytes show multiple and distinct polarities to cope with the diverse functions. The basolateral side is lined with microvilli and helps in pinocytosis. This activity can be active or passive uptake of nutrients such as proteins. The cannicular membranes are formed on the apical surface of the cells and secrete the bile components (7).

1.1.3 Liver diseases

There are many liver diseases, which leads to more than 2 million deaths every year. Viral infection, especially Hepatitis B and C, excessive alcohol uptake and obesity are the most prevalent risk factors for chronic liver diseases worldwide (9). Normally, liver disease progression consists of several stages including inflammation, acute liver damage, hepatic fibrosis and cirrhosis, in some cases result in development of hepatocellular carcinoma (HCC) (10). Increased serum levels of alanine aminotransferase (ALT) and aspartate aminotransferase (AST) caused by hepatocyte death are the most widely used parameters to check and monitor liver damage.

Additionally, it has been shown that hepatocellular death is present in almost all types of human liver diseases (11). *Iredale et al.,* showed that increased hepatocyte cell death contributes to fibrogenesis and it can be resuced by inducing death in the fibrogenic cells i.e. hepatic stellate cells. This is an important mechanism for reducing liver fibrosis (12). During viral infection, T cells as well as natural killer cells contribute to viral clearance by killing infected hepatocytes in patients. However, $CD8^+$ T cells and natural killer cells contribute to hepatocyte apoptosis after Hepatitis B virus (HBV) or Hepatitis C virus (HCV) infection in humans (11, 13, 14). Phosphorylated mixed lineage kinase domain-like protein (MLKL) a potential marker for necroptosis is highly increased in liver tissue of patients induced by drug-induced liver injury which is one of the major causes of acute mediated liver disease (15). Since it has been proven that both apoptosis and necrosis are present during alcohol liver disease, this finding also has clinical relevance for human patients (16-18).

1.2 Fragile X mental retardation

1.2.1 Fragile X syndrome

Fragile X syndrome (FXS) is one of the most common inherited causes of intellectual disability and autism. Clinical phenotypes of FXS include impaired cognition, anxiety, hyperactivity, social phobia, and repetitive behaviors (19). This syndrome was first descried by Martin and Bell in 1943 by investigating certain familial cases of mental deficiency showing X chromosome linked inherited pattern (20). In 1969, *Lubs et al.,* identified a fragile site on the X chromosome (21, 22). It was until 1991 that *Verkerk et al.,* discovered Fragile X mental retardation 1 (FMR1) gene containing CGG triplet repeats on this fragile site, which contribute to FXS (23).

In the same year, *Pieretti et al., reported* that hypermethylation of CGG lead to silencing of the FMR1 gene, which is the reason for FMR-1 mRNA to be absent in the majority of male fragile X patients (24). It is a well-established fact that Fragile X syndrome is caused by lack of fragile mental retardation protein (FMRP) expression encoding by the FMR1 gene (25). Normal populations have 5 to 54 of CGG repeats. In fragile X syndrome patients, there are more than 200 CGGs, termed full mutation. CGGs repeats ranging from 55 to 200 are termed permutation (25).

Most of people with premutation have a normal intellectual ability, but have other medical, psychiatric and neurological problems related to Fragile X associated Tremor/Ataxia Syndrome (FXTAS) and fragile X-associated primary ovarian insufficiency (FXPOI) (26, 27). It has been found both in men and women and tend to be more severe in men and the frequency occurs in about 1 in 4,000 males and 1 in 8,000 females (28).

1.2.2 Function of FMRP in neuronal development and treatment

FMRP is a RNA-binding protein, which associates with polysomes and thought to regulate mRNA translation or localization, which are involved in synapsis development, neural plasticity and brain development (29, 30).

To study FXS, several animal models have been developed including drosophila, zebrafish, mouse and rat model systems (19). *Fmr1* knockout (KO) mice also named *Fmr1*^{null} mice are a widely used model to study FXS. These mice were first generated in

1994 as a tool to study the abnormal behaviors and explore the mechanisms involved in FXS (31). It was shown that FMRP plays essential role in neuron development (29,30).

Absence of FMRP in adult neuronal progenitor cells result in decreased neurogenesis both in vivo (mouse model) and in vitro (cell culture) (32). However, the exact role of FMRP in regulation of neurogenesis is still unclear. In the recent studies it was reported that immature neurons from *Fmr1*^{null} mice displayed reduced dendritic development. Mechanistically they found reduced expression of Huntingtin (Htt), which can induce neurodegeneration in the *Fmr1*^{null} mice as a result of impaired mitochondrial function and increased oxidative stress (33, 34).

Recently many research groups have focused on studying the etiology and therapies for Fragile X syndrome. Nutlin-3, an inhibitor of mouse double minute 2 homolog (MDM2) and p53 interaction has been identified to rescue neurogenic and cognitive deficits in *Fmr1*^{null} mice. FMRP can stimulate the mGluR5 receptors which might contribute to the cognitive deficits and abnormal behaviors (35). Serval groups have evaluated the function of mGluR5 receptor antagonist (AFQ056) in *Fmr1*^{null} mice. They found that AFQ056 rescues various aspects of the fragile X phenotype in the mice model (36-39). This led to further investigations of AFQ056 effects on human patients, whether it would improve the behavior of FXS patients. Unfortunately, it did not elicit the anticipated therapeutic benefits (40).

1.2.3 Function of FMRP during infection

Over the years the function of FMRP outside of neuron development has been limited to few infections in drosophila and mice studies. *Fmr1*^{null} drosophila are highly susceptible to two pathogens: *Streptococcus pneumoniae* or *Serratia marcescens* induced pathology. This phenomenon showed that FMRP plays role in innate immune cell phagocytosis (41). Furthermore, FMRP is also involved in regulating virus infection. Since the influenza A virus's ribonucleoprotein (RNP) is responsible for the transcription and replication of viral RNA in the nucleus, FMRP can interplay with viral RNP and stimulates viral RNP assembly, leading to this virus replication in the host (42). On the contrary, FMRP represses Zika virus infection by inhibiting early synthesis of viral proteins (43).

1.2.4 Function of FMRP in regulating DNA damage response

FMRP is predominantly located in the cytoplasm where it regulates translation of proteins important for neuron development. Only 4% of FMRP is present in the nucleus (44). After analyzing the transcriptome of FXS patients, several DNA damage/repair pathway transcripts have been found (45). In line with this, *Alpatov et al.,* found that FMRP facilitates the DNA damage response by regulating H2A.X phosphorylation, breast cancer type 1 susceptibility protein (BRCA1), ataxia telangiectasia and Rad3-related protein (ATR) recruitment. Loss of *Fmr1* reduces the DNA repair response and genomic stability, as well as increases the cell death after aphidicolin (replication stress inducer) treatment (46). This was further confirmed by the interaction between FMRP and poly (ADP-ribose) polymerase (PARP) which is an important part of DNA repair and maintaining genomic stability (47).

In human patients, telomere shortening, a well-known marker for genomic instability, has been found. These markers play an important role in the DNA repair (48). Similarly, in the absence of FMR1, increased DNA damage and apoptosis was observed in the spermatocytes of $Fmr1^{null}$ mice (49). Pro-survival function of FMRP was further shown by *Jeon et al.*, in inhibiting apoptotic cell death with the presence of FMRP (50).

Above all, FMRP serves as genomic protector to induce DNA damage repair and promote the cell survival. In FXS patients and FMRP-deficient mice, it has been shown that there are disorders in the testes and ovaries outside of brain (51, 52). The role of FMRP apart from these organs is poorly studied. Hence, it is imperative to investigate if FMRP is involved in the pathologies of other organs.

1.3 Tumor necrosis factor (TNF)

1.3.1 Discovery

The discovery of TNF can be tracked back to the late 19th century. Spontaneous tumor remission from some patients were reported by F. Fehleisen from Germany and William B. Coley from the United States. Those patients suffered from simultaneous bacterial infection. In 1893, William B. Coley successfully treated patients with killed bacteria, a mixture of *Streptococcus pyogenes* and *Serratia marcescens*, defined as Coley's toxins (53). Based on this, a number of microbial products have been tested in the laboratory for their antitumor effects. Murray, Shear and colleagues identified the principle component of the toxin, which led to the hemorrhagic necrosis of the tumors caused by Gram-negative bacteria. Later this component was termed as endotoxin or lipopolysaccharide (LPS) (53).

This endotoxin could not kill the cultured tumor cells directly, prompting researchers to find the direct cause of tumor hemorrhagic necrosis (54). Until 1975 it remained a mystery and poorly defined mechanism of the tumor necrosis. Finally, E. A. Careswell and colleagues reported that Bacillus Calmette-Guerin (BCG)-infected mice treated with endotoxin/LPS derived from *Escherichia coli* produce a substance and can be detected in the serum, defined at tumor necrosis factor (TNF) which causes tumors necrosis (55).

It was also shown that the TNF-positive serum could induce necrosis of the sarcoma Meth A and other transplanted tumors (55). TNF is cytotoxic to some of transformed cell lines in culture for example L cells (NCTC Clone 929, L929 cells) and Meth A Sarcoma cell, but not toxic for other cell cultures, e.g. mouse embryonic fibroblast cultures (55-58). Furthermore, the role of macrophages as the main source of TNF production also has been characterized in vivo (murine model) and in vitro (cell culture) against tumors (55, 57, 59). Aggarwal and colleagues isolated 2 cytotoxic factors: TNF from macrophages and lymphotoxin from lymphocytes both of them shared 50% homology so it was named as TNF alpha (TNF) and TNF beta (Lymphotoxin) (56, 60).

Until now, based on the sequence of TNF, 19 members of the TNF superfamily and 29 their interacting receptors have been found (60). The roles of TNF superfamily interacting along with receptors have been identified in various aspects including inflammation, proliferation, apoptosis, necroptosis, metastasis, angiogenesis and morphogenesis within the last decades.

1.3.2 Structure of TNF and TNF receptors (TNFRs)

TNFRs have an extracellular domain which binds to ligands and an intracellular domain which regulates the biological signaling (61, 62). Regarding the biological activities, most of the receptors act as activating receptors and induce nuclear factor κB (NF-κB) and mitogen-activated protein kinase (MAPK) pathways. Only 8 out of 29 are death receptors work which have a cytoplasmic death domain in the intracellular region that can induce cell death (63-65). Well known death receptors are TNFR1 and Fas. Among the TNF superfamily and TNFRs, TNF and its two receptors TNFR1 and TNFR 2 are very well receptors. TNFRs form homotrimers upon binding towards TNF (66, 67).

TNF is expressed as transmembrane protein and can be cleaved to be soluble form by the metalloproteinase TNF-converting enzyme (TACE or ADAM17) (68-70). Inactive rhomboid protein 2 (IRHOM2) interacts with TACE and promotes the maturation of TACE, leading to trafficking of TACE from endoplasmic reticulum to cell membrane to cleave TNF (71, 72). sTNF and membrane bound TNF can both bind to either TNFR1 or TNFR2 to regulate its biological activities. However, *Grell et al.,* found that inflammatory responses of mTNF is mainly regulated by TNFR2 (73).

1.3.3 TNF-TNFR1 regulates NF-κB signaling

TNFR1 can activate the NF-κB and MAPK pathway, as well as the cell death pathway. The death domain of TNFR1 can recruit the adaptor TNFR1-associated death domain protein (TRADD). In turn TRADD can recruit receptor-interacting serine/threonine-protein kinase 1 (RIPK1) and ubiquitin E3 ligases, TNFR-associated factor 2 (TRAF2) or TRAF5, cellular inhibitor of apoptosis protein 1 (cIAP1) or cIAP2 and the linear ubiquitin chain assembly complex (LUBAC) to form TNFR1 signaling complex I. RIPK1 can add Lys-63 (K63) ubiquitinating Met1-linked linear ubiquitin chains with the help of ubiquitin E3 ligases in the signaling complex 1 (74) (Graphical Figure 1).

Ubiquitinated RIPK1 recruits IκB kinases (IKKs) consisting of two catalytic subunits IKKα and IKKβ and the scaffolding subunit IKKγ (also termed NFκB-essential modulator (NEMO)) as well as transforming growth factor (TGF) β -activated kinase 1 (TAK1), TAK-binding protein 1 (TAB1) and TAB2 (74, 75). The complex of NEMO and IKKs regulate phosphorylation of inhibitor of κB (IκBα) and subsequently IκBα is degraded by the proteasome, and eventually nuclear factor-κB (NF-κB) is activated (Graphical Figure 1). TAK1 can phosphorylate and activate the MAPKs (JUN N-terminal kinase (JNK) and p38 (74, 75). Once

NF-κB is released from IκBα and it subsequently translocates into the nucleus and promotes the expression of pro-survival and pro-inflammatory genes transcripts (Graphical Figure 1).

Graphical Figure 1: *Figure depicting TNF/TNFR1 mediated NF-κB pathway. Adapted from Yuan et al., (76)*

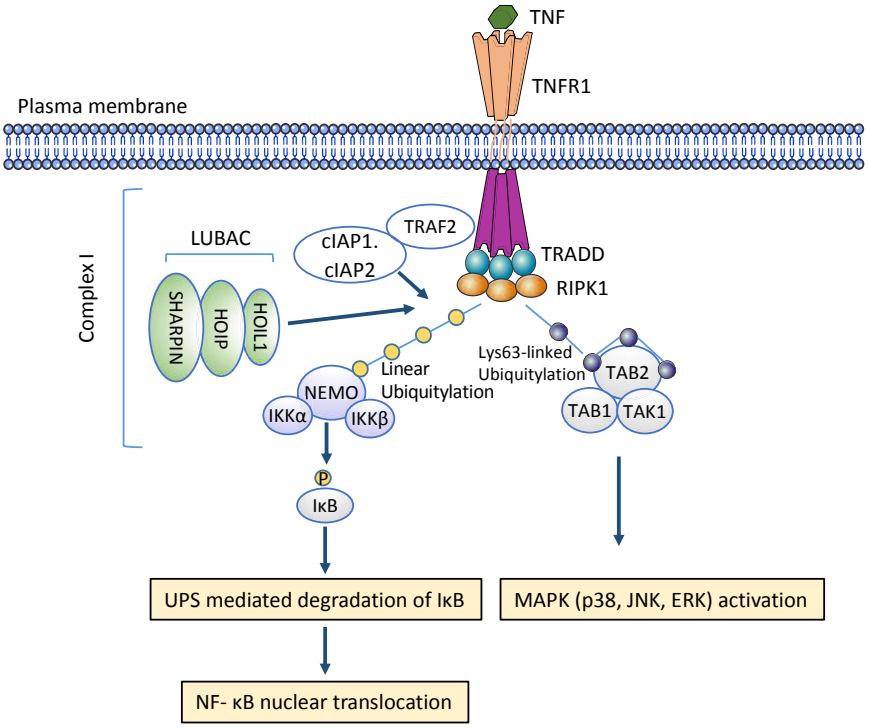

1.4 TNF-TNFR1 regulated cell death pathway

1.4.1 Discovery of apoptosis and necroptosis

Apoptosis was first termed by *Kerr et. al* in 1972 to describe natural cell death (77). Since then, apoptosis was considered as the mechanism of developmental and homeostatic cell death through activation of a specific class of proteases and caspases for many years (78). It was not until *Laster et.al* found TNF also induce the balloon-like plasma membrane and a lack of nuclear disintegration of the cell, which was named necroptosis because it differs from apoptosis in morphology (79). Numerous molecules have been identified to play role in regulating apoptosis and necroptosis over the past two decades. Sydney Brenner, H Robert Horvitz and John E. Sulston shared the 2002 Nobel Prize in medicine or physiology for their discovery of genes involved in the regulation of apoptosis.

1.4.2 Apoptosis and necroptosis signaling

Several deubiquitinated-enzymes can regulate the ubiquitin status RIPK1, for instance, A20 and CYLD remove the ubiquitin chains from RIPK1 in the complex 1. The deubiquitylated RIPK1 moves from the membrane to the cytoplasm, which leads to cytosolic TNFR1 complex IIa and complex IIb to mediate cell death (Graphical Figure 2) (80-82). Complex IIa includes deubiquitinated RIPK1, TRADD, FAS-associated death domain protein (FADD), and pro-caspase 8 to mediate apoptosis (80-82).

FADD interacts with pro-caspase 8 and removes the caspase 8 pro-domains, leading to release of an activated caspase 8. On one hand, activated caspase 8 cleaves pro-caspase 3 into activated caspase 3, which subsequently actives poly (ADP-ribose) polymerase (PARP-1), on the other hand, activated caspase 8 can cleave RIPK1 and RIPK3 as well, which ultimately results in apoptosis (83-85). The long isoform of FLICE-like inhibitory protein ($FLIP_L$) as cell death inhibitor forms heterodimers with pro-caspase 8 to inhibit cell death and promote cell survival (Graphical Figure 2) (80-82).

RIPK1 recruits RIPK3 to form complex IIb, named necrosome or ripoptosome to regulate necroptosis (86). This complex relies on RIPK1 and RIPK3 kinase activities. RIPK3 phosphorylates MLKL at T357/S35 and promotes its oligomerization, leading to disruption of the plasma membrane integrity (Graphical Figure 2) (15, 87).

Graphical Figure 2: *Figure depicting TNF/TNFR1 mediated apoptosis and necroptosis pathway. Adapted from Yuan et al., (76).*

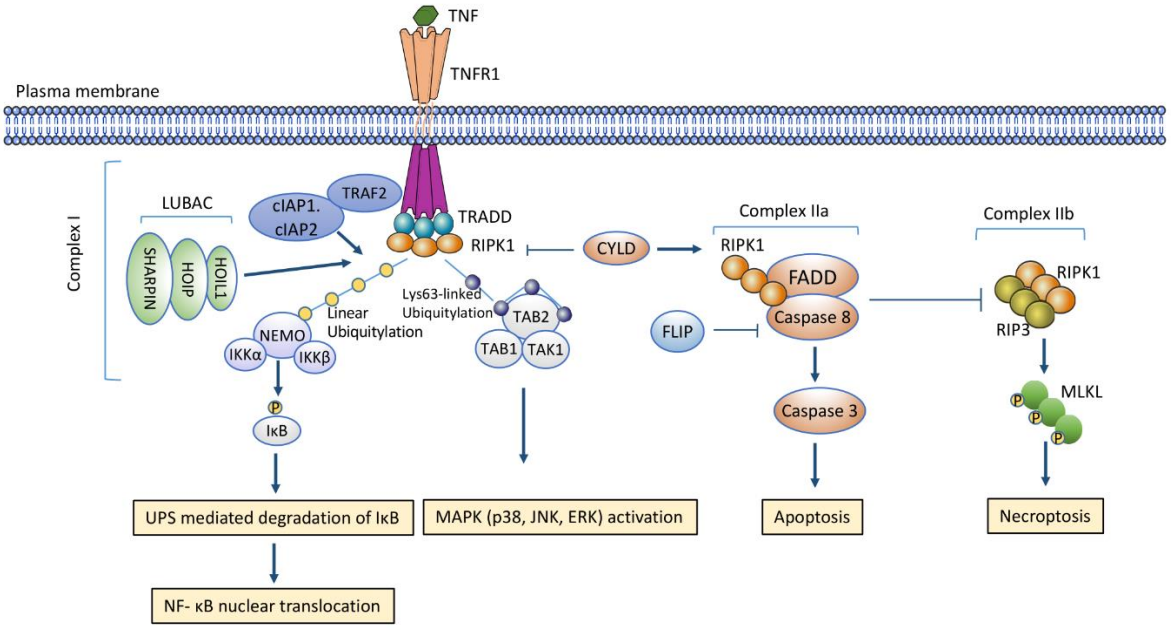

1.4.3 Inhibitors of apoptosis and necroptosis

Apoptosis and necroptosis are well studied and serval molecules which inhibit those pathways have been characterized. Based on this, small molecules/ compounds are produced which bind to the active site of the enzymes. z-VAD-fluoromethylketone (z-VAD-FMK) is a pan caspases inhibitor to inhibit reversibly or irreversibly their catalytic site. It is a widely used chemical for apoptosis research (88). Smac mimetics is antagonist of cIAPs to induce RIPK1-dependent apoptosis via mimicking of Smac/Diablo protein to induce cIAPs ubiquitination and degradation (89, 90). Necrostatin-1 (Nec-1), a RIPK1 inhibitor, is widely used in blocking RIPKI kinase-dependent regulated cell death including apoptosis and necroptosis not only in cell lines but also used in vivo such as mice as well. Moreover, 7-Cl-O-Nec-1 (Nec1-s) an analog of Nec-1 is more specific and highly stable in vivo (mice model) (91-93).

1.5 Virus infection and Immune response

1.5.1 Lymphocytic choriomeningitis virus (LCMV)

LCMV is one of the most widely used model systems to study viral persistence, viral pathogenesis and immune response to viral infections. LCMV belongs to the arenavirus family of single stranded RNA viruses. The LCMV genome consists of a large (L) segment and a small (S) segment, which are negative-sense single-stranded RNA segments (94, 95). The S segment codes three major structural proteins: the nucleoprotein (NP) and two mature virion glycoproteins (GP-1, GP-2) (96). GP1 and GP2 are on the virion surface, GP-1 is peripheral membrane protein and GP-2 is transmembrane protein. Tetramers of GP-1 and GP-2 make up the spikes on the virion envelope.

It has been shown that GP-1 regulates host receptor recognition and GP-2 regulates virus and host membrane fusion (95, 97, 98). *Cao et al.,* identified α-dystroglycan (α-DG) as the receptor for LCMV on host cells (99). The L segment encodes the RNA polymerase and the small polypeptide Z with a RING finger motif (100, 101). The NP enclose viral RNA (vRNA) to form the nucleocapsid as the template for the viral RNA polymerase to regulate transcription and replication (101).

LCMV is able to infect a wide range of hosts including humans and can cause persistent or acute infections. Until now several strains have been isolated from infected organisms (102). The LCMV mouse model has been widely used to study mechanisms of viral persistence and concepts of virus-induced immunity and immunopathology.

1.5.2 Immune response

All the vertebrates are threatened by pathogenic microorganisms. Pathogens can be eliminated with the help of immune system. There are two major branches of the immune system: the innate immune system and the adaptive immune system. Innate immune system is the first barrier of host defense against pathogens.

1.5.2.1 Innate immunity

The innate immune system as first line of defense is responsible for rapid defense against invading pathogens and assist to promote an adaptive immune response. During pathogen invasion, they release components known as pathogen-associated molecular patterns (PAMPs) (103). PAMPs are recognized by germline-encoded pattern-recognition receptors

(PRRs) which are expressed on innate immune cells such as dendritic cells (DCs), macrophages and neutrophils. There are several PRRs, including Toll-like receptors (TLRs), RIG-I-like receptors (RLRs), NOD-like receptors (NLRs) and DNA receptors (cytosolic sensors for DNA) (104, 105).

Sensing of PAMPs by PRRs rapidly activate host immune responses by inducing complex signals including various inflammatory cytokines, chemokines and type I interferons. Those responses also initiate the development of pathogen-specific, long-lasting adaptive immunity through B and T lymphocytes (103, 106).

1.5.2.1.1 Dendritic cells (DCs)

DCs as antigen presenting cells (APCs) are crucial to both innate and adaptive immune systems. In 1973 *Steinman et al.,* discovered a novel type of cells from adherent cell populations derived from mouse peripheral lymphoid organs, termed dendritic cell (107). Later on, they identified the role of DCs in controlling immunity and was awarded Nobel prize in 2011 (108).

Over the years, DCs are well studied of their role in antigen uptake, antigen presentation and activation or tolerance of the immune system (109, 110). DCs can be divided into two groups conventional dendritic cell (cDC) and plasmacytoid dendritic cell (pDC) regarding their capacity of antigen presentation and Type I interferon (IFN-I) production (109, 111). DCs express Toll-like receptors (TLR) to specifically recognize the different pathogens such as virus and bacteria and promote pro-inflammatory cytokine and IFN-I production, as well as enhanced antigen presentation to naive T cells through major histocompatibility complex (MHC)–peptide complexes on their surface (109, 112, 113).

After viral infection, cDCs induce pro-inflammatory cytokines and IFNs-1 through TLR3-dependent and retinoic acid-inducible gene I (RIG-I)-dependent pathways. In pDCs, TLR7 and TLR9 recognize viral ssRNA and DNA, respectively and upregulate the expression of IFN genes in a MyD88 dependent manner (109). It has been reported that pDCs produce higher amount of IFN-I (114, 115).

To study the role in DCs in vivo (mice model), CD11c-diphtheria toxin receptor (CD11c-DTR) mice was generated in which $CD11c^+$ DCs can be depleted by diphtheria toxin (DT) treatment. By using these mice, *Jung et al.,* found DCs to promote the priming of CD8+ T cells, suggesting a critical role of DCs for the adaptive immune defense (116).

1.5.2.1.2 Macrophages

Macrophages play a key role in innate immune defense by recognizing and eliminating pathogens. Macrophages can also remove the damaged or dead cells and cellular debris from the body. In addition, as APCs, macrophages have the ability to present antigens to T cells (117-119).

Macrophages rapidly ingest pathogens which can be trapped in the phagosome. The phagosome fuses with lysosomes to form a phagolysosome where the pathogen is broken down by enzymes and toxic peroxides. While macrophages are professional phagocytes (120, 121), DCs have limited ability for lysosomal degradation of phagocytosed material (122, 123).

Based on their function, macrophages can be broadly divided into two groups: M1 macrophages (classically activated macrophages) and M2 macrophages (alternatively activated macrophages) (124). In general, M1 macrophages secrete pro-inflammatory cytokines, clear pathogens and phagocytosis. PAMPs, DAMPs, and inflammatory cytokines such as TNF-α and IFN-γ activate M1 macrophages, which destroy pathogens and secrete high levels of pro-inflammatory cytokines (125, 126). In contrast, M2 macrophages have anti-inflammatory functions. Anti-inflammatory cytokines such as interleukin-10 (IL-10), IL-4, and IL-13 activate M2 macrophages (127).

1.5.2.1.3 Red pulp and Marginal zone macrophages

In the spleen red pulp macrophages, marginal zone macrophages and metallophilic marginal macrophages can be found. All those macrophages express different surface markers and show specialized functions (128).

Red pulp macrophages in mice can be characterized by expression of $F4/80^{high}CD68^{+}CD11b^{low/-}$ (129) and play role in removing senescent red blood cells (130). According to the expression of different surface markers, marginal zone macrophages can be further divided into marginal zone and metallophilic macrophages. Marginal zone macrophages express the C-type lectin SIGN-related 1 (131) and macrophage receptor with collagenous structure (MARCO) and marginal metallophilic zone macrophages express the sialic acid-binding Ig-like lectin-1 (CD169). Both capture microbes and viruses from blood circulation (132).

Recent studies shed light on understanding of the precise roles of different macrophages.

1.5.2.1.4 CD169+ macrophages

In 1980s, *Kraal et al.,* firstly detected a specific macrophage population localized at the marginal metallophilic zone of the spleen by using the monoclonal (MOMA-1) antibody. This antibody binds to the surface molecule CD169 (133). $CD169^+$ macrophages can be found on the subcapsular sinus of the lymph node as well, functionally which enables them to defence against pathogens and foreign antigens (133).

To study the role of $CD169^+$ macrophages, *Miyake et al.,* firstly generated the CD169-diphtheria toxin receptor (DTR) mice, which show depletion of $CD169^+$ macrophages with DT treatment (134). By using these mice, they found that $CD169^+$ macrophages have the capacity to capture and clear apoptotic cells (134). Several studies also show the role of these cells in bacterial and viral infections. $CD169^+$ macrophages not only rapidly capture *Listeria monocytogenes* but also transport the bacteria to the T cell zones. Their absence resulted in bacterial growth and spread, which ultimately lead to death of the infected animals (135).

Honke et al., found that $CD169^+$ macrophages in spleen tissue enforce early viral replication to promote innate immune recognition and antigen presentation in a Usp18-dependent manner after VSV infection (136). Furthermore, BAFFR and TNFR1 were shown to be also crucial for maintenance of active $CD169^+$ macrophages after VSV infection (137, 138). It was found that B-cell-derived lymphotoxin alpha (Ltα) and lymphotoxin beta (Ltβ) promote the development and maintenance of $CD169^+$ macrophages in spleen and lymph node tissue (139). Hence, mice lacking B cells show fewer $CD169^+$ macrophages in the naïve stage and limited immune activation after viral infection, including the defective production of IFN-I after vesicular stomatitis virus (VSV) infections (137, 138, 140). *Junt et al.,* also showed that $CD169^+$ macrophages in the subcapsular sinus rapidly capture viral particles to promote B cell mediated immunity (141). All these studies highlighted the importance of $CD169^+$ macrophages in preventing bacterial and viral infections.

Since, most of the past studies have focused on the role of $CD169^+$ macrophages in the subcapsular sinus of the lymph node and the marginal zone of the spleen during ininfection, a role of $CD169^+$ macrophages out of these findings is less clear, prompting us to explore the novel functions of this cell population.

1.5.2.2 Adaptive immune response

The adaptive immune responses specialize in eliminating pathogens with two core competencies, specificity and immunological memory. Adaptive immune cells recognize a great variety of different specific antigens. Lymphocytes including T and B cells expresses diverse antigen receptors generated by somatic recombination to recognize specific pathogens (142). It is well known that in jawed vertebrates, B cell receptors (BCR)/immunoglobulin (Ig) and T cell receptors (TCR) repertoire diversity is generated by variable (V)-diversity(D)–joining(J) rearrangement (VDJ rearrangement) with the help of the recombination-activating gene (RAG) (143-146).

1.5.2.2.1 B cells

a) Development of B cells

In general, mammalian development of B cells initiates from hematopoietic precursor cells in primary lymphoid tissue such as bone marrow, following migration it matures in secondary lymphoid tissue such as lymph nodes and spleen where they can be activated. In the bone marrow during development the stages of hematopoietic precursor cells, progenitor-B cell, precursor-B cell and immature B cell depends on RAG1 rearrangement of VDJ genes segment. RAG initiates the rearrangement of D and J gene segments to form the heavy chain (H-chain) which first can form pre-BCRs, followed by V and J gene segment rearrangement of the light chain (L-chain) with the help of RAG (143-146).

L-chains pair with H chain form a complete immunoglobulin B cell receptor expressed on the cell surface, termed as immature B (147). Expression of IgM on the surface changes the expression pattern of many genes in immature B cells and promotes these cells to egress from the bone morrow and migrate to the spleen, where B cells interact with antigens and mature into Follicular B cells (FoB), Marginal zone B cells (MZB) and B1 cells (148, 149).

b) Mediators during B cell development and differentiation

Many factors contribute to the development of B cells, including IL-7 and chemokine CXC ligand 12 (CXCL12) produced by bone marrow stromal cells, which interact with pre-B cells and regulate the early stage of B development (150). *Schneider et al.,* identified that B-cell activator of the TNF-α family (BAFF) promotes B cell proliferation and controls B cell function (151). *Thompson et al.,* further found that BAFF receptor (BAFFR) specifically binds

to BAFF and regulates B cell survival (152). During the differentiation, B cell lymphoma 6 (BCL-6) is highly expressed in germinal center (GC) B cells and promotes proliferation of GC B cells (153).

Furthermore, transcript factor interferon regulatory factor (IRF)-4 also has been found in regulating GC formation and playing role in immunoglobulin class switching (154). It was shown that lymphotoxin is expressed by B cells (155). Lymphotoxin deficient mice display abnormal development of peripheral lymphoid organs with impaired presence of lymph nodes and Peyer's patches, and impaired spleen architecture with disorganized B and T cells, and without germinal centers (156-158).

c) Activation of B cells

One of the main function of B cells are production of antibodies, which are produced by terminally differentiated B cell plasmablasts and plasma cells. MZB and B1 cells respond to T cell-independent antigens, while FoB cells additionally respond to T cell-dependent antigens (148, 149). Upon antigen activation, FoB cells divide and differentiate into short-lived plasmablasts that secrete antibodies and also may undergo immunoglobulin class switching, Activated B cells with the help of specialized T follicular helper cells enter a lymphoid follicle and form a germinal center (GC) where B cells undergo proliferation, immunoglobulin class switching, and affinity maturation trigged by somatic hypermutation (149).

Ultimately GCs generate long-live plasma cells, which can secrete high amounts of antibodies and form memory cells (149, 159, 160). Naïve mature B cells express IgM and IgD, after activation by antigens. Following class switch B cells can produce IgG, IgA or IgE antibodies (161).

1.5.2.2.2 T cells

T cells develop from hematopoietic precursor cells from the bone marrow and migrate through the bloodstream to the thymus where they are matured (162). In the thymus, at least 3 main types of T cells are developed: $CD4^+$ αβ T cells, $CD8^+$ αβ and γδ T cells and including subsets of lineages, such as regulatory T cells and natural killer (NK) T cells (163). During the development, T cell receptors undergo V(D)J recombination as well. Through selection, only T cells showing low-affinity to self major histocompatibility complex (MHC) survive (164). MHC complexes bind to antigens and display them on the antigen-presenting cell surface for recognition by T-cells (165).

T cells play a central role in controlling virus infections. In addition to bind to MHC-peptide complex, co-stimulatory molecules can promote T cell activation. For example, CD80/CD86 expressed on DCs can bind to CD28 on $CD8^+$ T cells. Eventually, recognition of the MHC-I peptide complex by the virus specific-TCR and CD28 signaling will result in the activation of $CD8^+$ T cells (166-168).

Cytotoxic $CD8^+$ T cells can kill virus-infected cells as well as cancer cells. Cytotoxic T cells produce cytotoxic granules such as perforin and granzymes which trigger programmed cell death of target cells (169, 170). Perforin promotes to form a pore in the target cell membrane and triggers granzymes enter to the cells (169, 170). Granzyme B can induce the activation of caspase-3 to regulate cell death, resulting in target cell destruction (169, 170). Furthermore, cytotoxic T cells can express Fas ligand and TNF which can bind to their receptors on the target cells and then promote cell death (171). *Moskophidis et al.,* found that LCMV strains such as docile persist after infection due to exhaustion of antiviral $CD8^+$ cytotoxic T cells (172).

Using the LCMV model system, other two groups also found exhaustion of virus-specific T cells during persistent LCMV infection of mice (173, 174). Mechanistically, *Barber et al.,* identified programmed cell death-1 (PD-1) as one critical factor in regulating T cell exhaustion. PD-1 is markedly upregulated by exhausted $CD8^+$ T cells after clone 13 infection. Interestingly, blockage of PD-L1 could restore cytotoxic T cells (175). However, when programmed death-ligand 1($PD\text{-}L1^{-/-}$) mice were infected with clone 13, they succumbed due to damage caused by immunopathology (175). *Blackburn et al.,* found Lymphocyte-activation gene 3 (LAG-3) to regulate T cell exhaustion (176). In contrary, *Kaech et al.,* identified that $CD8^+$ T cells which express high IL-7R would survive longer and become memory cells (177).

1.6 Liver Cholestasis and fibrosis

1.6.1 Bile duct ligation (BDL)

Liver fibrosis is a global health problem. It can be caused by multiple etiologies. Upon liver damage, complex interactions between inflammatory signals, neutrophils and macrophages activates hepatic stellate cells to transdifferentiate to myofibroblasts, accumulate extracellular matrix (ECM) and then form hepatic fibrosis and late stage cirrhosis (10, 178).

Bile acids emulsify absorbed fat, digest lipids in the small intestine and also facilitate cholesterol breakdown (179). It has been shown that farnesoid X receptor (FXR) and Takeda G protein receptor 5 (TGR5) work as a receptor of bile acid and can be activated by bile acids to regulate bile acids synthesis and bile acid transporter expression (180, 181). Surgical ligation of bile duct results in blockage of the biliary system followed by liver pathology with severe cholestasis and inflammation leading to fibrosis in rodents (178). Bile duct ligation (BDL) is a well-established model to study liver fibrosis.

Ligation of bile duct in murine models such as rat and mice to surgically mimic obstructive cholestatic induced liver injury and liver fibrosis has been carried out in the laboratory for decades (182). Following BDL, there are approximately 2 major events which lead to fibrosis including initiation of acute liver injury phase (first 7 days) and the fibrotic progression phase (7-20 days) (Graphical Figure 3). Acute hepatocyte injury and hepatocyte proliferation occur in the initial days following BDL, which contributes to establishment of liver fibrosis (178, 183).

1.6.2 Hepatocytes injury and Hepatocellular Proliferation

Following BDL, bile acids cannot be secreted in the intestine and accumulate in the liver and serum which lead to hepatocytes death and liver injury. These biliary infarcts can be detected 8 hours after surgery and increase in size and numbers around day 3 (183). Lysis of hepatocytes releases intracellular enzymes into the serum including alanine aminotransferase (ALT) and aspartate aminotransferase (AST), which are clinical markers for liver damage. ALT and AST levels reach their peak levels at day 2 following surgery (183).

Another event which takes place following BDL is hepatocytes proliferation. Two established hepatocytes proliferation markers are Ki67 and proliferating cell nuclear antigen (PCNA) (184). Moreover, growth factors regulating hepatocyte proliferation, such as hepatocyte growth factor (HGF) and TGF-α are secreted after BDL (185). It is known that the

gene expression level of HGF rapidly increases and reaches peak levels at day 3 after BDL. Transcripts of TGFα also rapidly increase and reach peak levels at day1 after BDL (183).

1.6.3 Inflammatory response

Inflammation is found during acute and chronic cholestatic liver injury. BDL leads to high infiltration of immune cells into the area of biliary infarcts (area of hepatocyte death). It has been shown that neutrophils are the predominantly infiltrating cell type around injured hepatocytes in the first 3 days after BDL (183). Whereas no significant changes in numbers and distribution of Kupffer cells were observed during early time after BDL, but increased presence of Kupffer cells can be detected at 2 weeks following BDL (183). One group identified that Kupffer cell engulfment of apoptotic bodies promotes inflammation and fibrogenesis. They found decreased neutrophil infiltration, stellate cell activation, hepatocytes death, bile infarcts and serum ALT levels following BDL after eliminating macrophages by treating mice daily with gadolinium chloride (GdCl3, a Kupffer cell toxicant) (186). However, on other study showed increased hepatocellular necrosis, serum ALT and bilirubin levels in BDL mice upon intravenous treatment with multilamellar liposome-encapsulated dichloromethylene diphosphonate (Cl_2MDP-L), which can specifically deplete resident liver macrophages in mice (187). These contradictory results suggest heterogeneity in macrophage populations in the liver and their function.

Increasing numbers of T cells and a slight increase in B cells were detected on day 5 after BDL. T cells were detectable until 6 weeks after BDL, however B cells were not detectable in the late time points after BDL (Graphical Figure 3) (183). Reduced liver fibrosis in the absence of B cells was demonstrated by markedly reduced collagen expression in B cell–deficient as compared with wild-type mice after 6 weeks treatment of CCl4 (188).

1.6.4 Liver fibrosis development

BDL is a well-established model to induce fibrosis in the liver and rapidly upregulate expression of fibrosis related genes: tissue inhibitor of metalloproteinases-1 (TIMP-1), type I collagen and TGF-β1 (189, 190). It has been shown that expression of TIMP-1 has an initial first peak at day 3 after BDL, reaches the second peak at day 7 (183). TGF-β1 and type I collagen expression show the same pattern with TIMP-1 expression only at early time points but reach the second peak at day 14 (183).

αSMA is one of the markers of liver fibrosis. αSMA positive cells were first detectable around biliary infarcts at day 3, subsequently found in portal tracts and around the resolving biliary infarcts from day 5 after BDL. However, there are less αSMA-positive cells at 28 to 45 days following BDL (183). Other marker for activated hepatic stellate cells (HSC) is the deposition of collagen, which can be observed until day 14, with no further increase. During development of fibrosis, decreased expression levels of collagen, TIMP-1 and TGF-β1 are consistent with the reduced number of αSMA-positive cells (183).

Furthermore, since establishment of fibrosis is regulated by multiple cells types, multiple factors and signaling pathways contribute to HSC activation, proliferation, migration and ECM deposition. It has been shown that damage-associated molecular patterns (DAMPs) from damaged or injured hepatocytes, reactive oxygen species (ROS), acetaldehyde and lipid peroxidation products following liver injury strongly initiate HSCs activation (191). Mediators such as TNFα, platelet-derived growth factor (PDGF) produced by Kupffer cells, neutrophils, platelets also induce HSC activation and proliferation. TNF and LPS promote proliferation and survival of HSCs by activating NF-κB and down-regulating pro-apoptotic genes (191, 192).

To study the role of TNF and its receptor TNFR1 and TNFR2 in the BDL induced fibrosis model, BDL was performed on wide type, TNFR1 knockout (KO) mice, TNFR2 KO mice and TNFR-double KO (TNFR-DKO) mice. The extent of the liver damage was assessed after BDL. The liver damage and fibrosis were decreased in TNFR1 KO mice and TNFR-DKO compared to wild-type or TNFR2 KO mice after BDL, suggesting TNF-TNFR1 not TNFR2 is critical for HSC activation and liver fibrosis (193). It is known that PDGF is a crucial driver for HSCs proliferation and migration. PDGF binds to its receptor and stimulates multiple signaling cascades including the expression of signal transducer and activator of transcription1 (STAT-1) through phosphatidylinositol 3-kinase (PI3K) signaling, NF-κB and extracellular signal-regulated kinases (ERK)-MAPK pathway. Deleting β-PDGFR on hepatic stellate cells showed decreased expression of αSMA and collagen α1, decreased their proliferation upon injury (194).

Graphical Figure 3: *Figure depicting dynamic changes following bile duct ligation in mice. adapted from Georgiev et al., (183)*

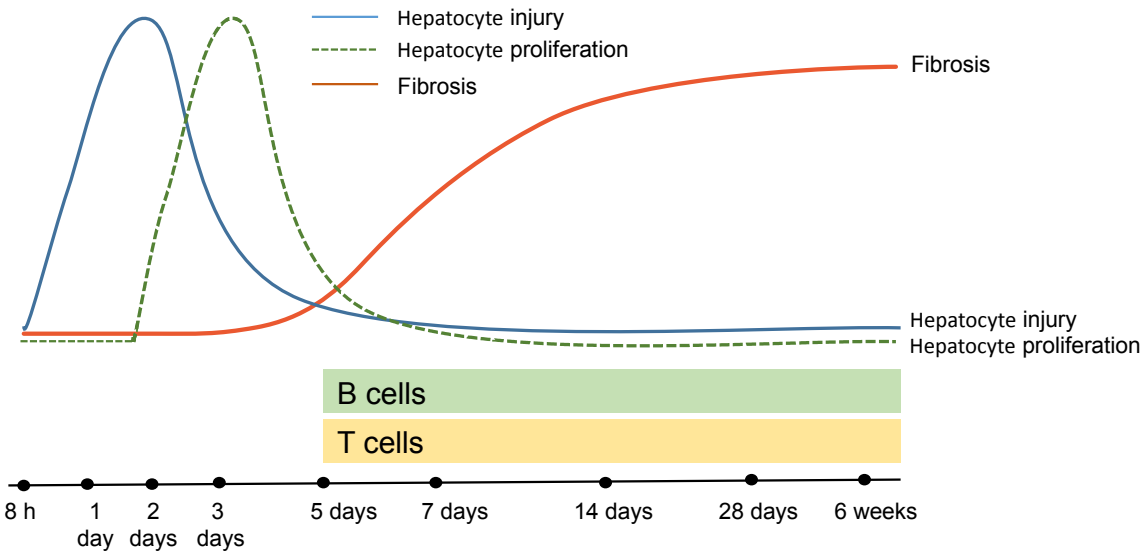

1.7 Liver regeneration

1.7.1 Liver regeneration

It has been more than 80 years since Higgins and Anderson's first report of the procedure of 70% partial hepatectomy (PHx) in rats (195). Until now, PHx is a widely used tool to explore the mechanisms during liver regeneration (195, 196). The remaining liver lobes will grow through hepatocyte proliferation and reach its original liver mass within 10 days after surgery. However, newly formed liver mass do not differentiate into liver lobes in its original form (195, 197).

In naïve conditions, most of the adult hepatocytes are quiescent. Once liver is damaged, hepatocytes start proliferating under the influence of cell cycle genes and undergo cell division (198). In experimental hepatology, removal of 70% liver mass is a well-studied technique for hepatocyte proliferation and to mimic cell cycle regulation to toxin injury and infection. Recovery of the original liver mass in mice can be divided into 3 phases. The initiation phase is around the first 6 hours when hepatocytes prepare to start the cell cycle. The following phase is characterized by DNA replication and cell proliferation. The last phase shows arrest of hepatocyte proliferation after reaching the original liver mass. The classical proliferation markers Ki67 and PCNA, indicate cell proliferation (195, 199).

Pro-inflammatory cytokines, growth factors and their related nuclear transcription factors are involved in signaling pathways, which can drive cell cycle progression (200). Cytokines include tumor necrosis factor (TNF), lymphotoxins (LTs) and IL-6. Growth factors includes HGF, epidermal growth factor (EGF) and TGF. The nuclear transcription factors include nuclear factor-kappa B (NF-κB), signal transducer and activator of transcription 3 (STAT3), extracellular signal-regulated kinases (Erk), c-Jun and c-Myc. However, liver cells stops proliferating when the liver mass is reconstituted to the approximate size of the original lobes (197).

Hepatocytes are the first cells to enter into DNA replication and cell cycle. It has been reported that, approximately 60% of hepatocytes undergo one round of DNA synthesis, which peaks at 24h for the rat and at around 36h for the mouse following PHx. However, the other round of DNA synthesis and proliferation only happens in a small number of hepatocytes (201, 202).

To evaluate the importance of cell cycles related gene, it has been reported that Brahma-related gene 1 (Brg1), which is involved in cell proliferation, promotes liver regeneration by

regulating several cell cycle genes including cyclin B1 and CDK1 (203). Moreover, Forkhead boxM 1b (Foxm1b) knock out mice showed reduced-DNA replication after PHx. Mechanistically, FoxM1b regulates cyclin B1 and promotes activation of Cdc25b to dephosphorylate Cdc2 (204).

1.7.2 Cytokines and growth factors during liver regeneration

1.7.2.1 IL-6

Interleukin-6 (IL-6) is an important cytokine during liver regeneration. The IL-6 pathway includes classic and trans-signaling. For the classic pathway, IL-6 directly binds to the membrane-bound IL-6R to induce dimerization with glycoprotein (gp130), which results in activation the downstream signaling cascade (Janus kinase (JAK)-STAT3, MAPK and phosphoinositide 3 (PI3) kinase). For trans-signaling, IL-6 binds to soluble IL-6 receptor and forms a complex to bind cell membrane bound gp130 (205). Notably, neither IL-6 nor IL-6R can bind to gp130 directly. Only IL-6/IL-6R form a complex can bind to gp130. Hyper-IL-6 is a fusion protein of IL-6 and soluble IL-6 receptor, which can act as an activator of gp130. In addition, to block trans-signal, soluble gp130 which is a fusion protein of the extracellular fragment of gp130 and a Fc fragment of human IgG1 antibody (sgp130Fc) can be used (205, 206).

Expression of IL-6 together with TNF is highly upregulated at early time after PHx. In addition, TNF can further induce IL-6 expression via TNFR1 pathway. Consequently, impaired liver regeneration of TNFR1 deficient mice can be rescued by a single injection of IL-6 (202). IL-6 knockout mice showed impaired liver regeneration and increased liver necrosis following PHx (207). Furthermore, IL-6 trans-signaling and not the classic signal was identified for contributing to liver regeneration after PHx (208). Since STAT3 is one key regulator in the IL-6 signaling pathway, mice lacking this gene specifically in the hepatocytes, showed reduced DNA synthesis and hepatocytes proliferation (Graphical Figure 4) (209).

1.7.2.2 TNF

TNF expressions increase after 30-120 mins. Consistently, following PHx, inhibition of NF-κB activation leads to increased liver injury and decreased hepatocyte proliferation (Graphical figure 4) (202, 210). One of the inducers to promote of TNF production is gut-derived lipopolysaccharide (LPS), which is recognized by Toll-like receptor 4 (211, 212).

Activation of the complement component, a C5a receptor can also induce TNF and IL-6 production following PHx. After C5a blockage, NF-κB gene expression was impaired. Furthermore, an increase in the liver damage and mortality was observed in the C5a knockout mice (213). Moreover, TNF and IL-6 expression were lower and resulted in decreased liver regeneration in the intracellular adhesion molecule 1 (ICAM-1) deficient mice after PHx (214).

After administration of TNF neutralizing antibodies to block TNF signaling before PHx, IL-6 expression was downregulated and hepatocyte proliferation was reduced (215). Consistently, less DNA synthesis and delayed hepatocyte proliferation was found in TNFR1 deficient mice after PHx. Mechanistically, reduced activation of NF-κB and STAT3 was observed which then lead to reduced IL-6 production. Giving IL-6 to TNFR1 knockout mice could rescue the deficiency in hepatocyte proliferation by restoring STAT3 activation but not NF-kB activation, which suggesting that TNF could be a prime factor to initiate cascade events for the following DNA synthesis and cell mitosis (216). However, there is no defect in TNFR2 knock out mice following PHx (217).

1.7.2.3 Lymphotoxins

Lymphotoxin-α (LT-α) and LT-β are members of the TNF superfamily. Both of them can be produced by activated B cells, T cells and natural killer T cells (218, 219). Functionally, lymphotoxins are crucial for the development of peripheral lymphoid organs (156, 220). They also play a critical role during liver regeneration (221, 222). LT-α can activate TNFR1 signaling. Consequently, TNF and LT-α double knock out mice display reduced liver regeneration, which is consistent with TNFR1 deficient mice (222). LT-β deficient mice show increased liver damage, impaired DNA synthesis and increased mortality (223). T cells can produce lymphotoxins to promote liver regeneration, which is shown by T cell-specific deletion of LT-β mice (223).

Since both LT-α and LT-β can both active LT-βR, LT-βR deficient mice showed increased liver damage and reduced liver regeneration following 70% PHx (221, 224). The importance of LT-βR for liver regeneration was strengthened after observations that anti- LT-βR agonistic antibody treatment alleviated the defects of liver regeneration in T cell deficient mice after PHx (223).

LT-βR shares the same downstream signaling pathway with TNFR1 after PHx (Graphical Figure 4). Hence, LT-βR deficient mice showed severe disease after treatment with

Etanercept (224). These studies suggested a cooperative role of LT-βR and TNFR1 during liver regeneration.

1.7.2.4 Growth factors

Hepatocyte growth factor (HGF) is a prominent hepatocyte mitogen, which can bind and activate receptor the c-Met (225). Several studies have shown that HGF is involved in liver regeneration. For instance, concentration of HGF increased 10-20 fold in the serum after PHx (226). Following PHx, there are 2 phases according to the expression of HGF. In the first 3 hours active HGF is consumed and then new HGF can be synthesized from 3 to 48 hours (227). Infusion of HGF into mice leads to hepatocytes proliferation and increased liver mass, which is independent of IL-6 (228). Administration of HGF in the hepatocyte culture medium causes increased DNA synthesis and cell proliferation. c-Met can be activated after PHx and depletion of HGF in rats by using RNA interference causes moderate suppression of hepatocytes proliferation (229).

However, depletion of c-Met in rats by using RNA interference leads to complete cell cycle arrest at 24 hours after PHx (230). c-Met deficiency in albumin-cre expressing cells in mice showed increased mortality after PHx with severe liver necrosis and jaundice (231). Considering these studies, HGF and its receptor c-Met regulate hepatocytes proliferation and play a critical role in liver regeneration.

1.7.2.5 Transforming growth factor

There are three types of Transforming growth factor (TGF-β). TGF-β1, TGF-β2 and TGF-β3 bind and activate their receptor. TGF-β acts also as growth inhibitor of epithelial cells and hepatocytes. To evaluate the role of TGF-β during liver regeneration, hepatocyte specific deletion of TGF-β type II receptor in mice was used and these mice displayed increased hepatocyte proliferation and liver weight / body weight ratio (232).

1.7.2.6 Other growth factors

There are several other growth factors which play a role during liver regeneration, such as, EGFs, fibroblast growth factors (FGFs) and vascular endothelial growth factors (VEGFs). Studies have shown that growth factors from these families promote liver regeneration after

PHx either in mice or rats. For example, EGF overexpression transgenic mice displayed highly increased hepatocyte proliferation and accelerated liver regeneration (233). The FGF family has 22 members which binds to four receptors (FGFR1-4). *Fgf15* transgenic mice displayed increased hepatocyte proliferation through activation of the NF-κB pathway, mitogen-activated protein kinase pathway and STAT3 following PHx (234). Mice lacking FGFR1 and FGFR2 in hepatocytes show increased mortality after PHx (20603121). FGF2 deficient mice showed reduced liver regeneration until day 4. However, the overall liver regeneration was not affected, which might be compensated by elevated expression of VEGFs which can interact with their receptors to regulate vasculogenesis, angiogenesis and lymphangiogenesis (235). Lack of VEGFs and its receptors also caused impaired liver regeneration (235).

Taken together, cytokines and growth factors promote liver regeneration.

Graphical Figure 4: *Figure depicting molecules regulate liver regeneration. Adapted from Ohkohchi et al., (236)*

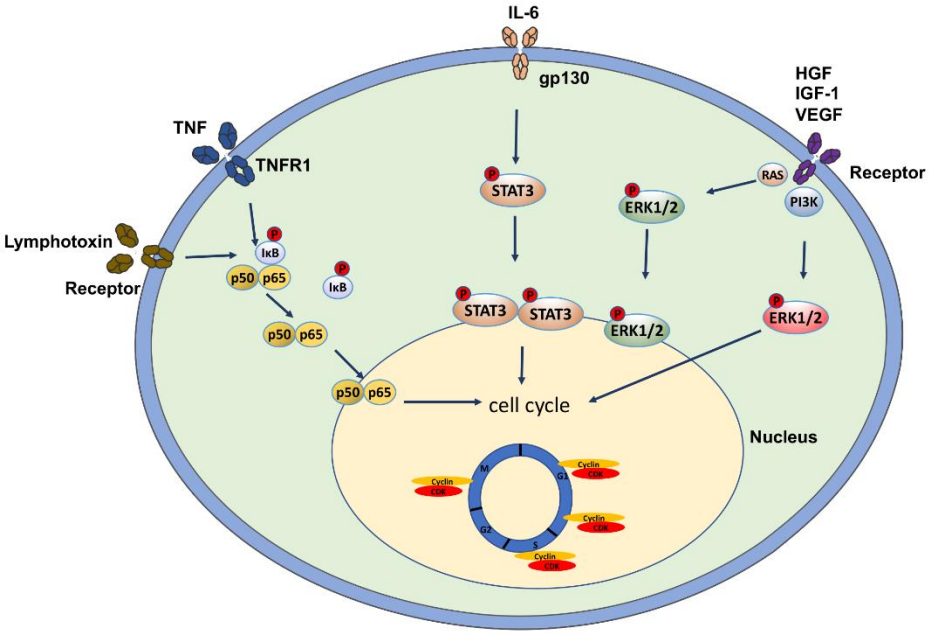

2. Publication

2.1 Fragile X mental retardation protein protects against tumour necrosis factor-mediated cell death and liver injury

Hepatology

OPEN ACCESS

ORIGINAL ARTICLE

Fragile X mental retardation protein protects against tumour necrosis factor-mediated cell death and liver injury

Yuan Zhuang,[1] Haifeng C Xu,[1] Prashant V Shinde,[1] Jens Warfsmann,[2] Jelena Vasilevska,[1] Balamurugan Sundaram,[1] Kristina Behnke,[1] Jun Huang,[1] Jessica I Hoell,[2] Arndt Borkhardt,[2] Klaus Pfeffer,[3] Mohamed S Taha,[4,5] Diran Herebian,[6] Ertan Mayatepek,[6] Dirk Brenner,[7,8,9] Mohammad Reza Ahmadian,[5] Verena Keitel,[10] Dagmar Wieczorek,[11] Dieter Häussinger,[10] Aleksandra A Pandyra,[1,10] Karl S Lang,[12] Philipp A Lang[1]

► Additional material is published online only. To view please visit the journal online (http://dx.doi.org/10.1136/gutjnl-2019-318215).

For numbered affiliations see end of article.

Correspondence to
Dr Philipp A Lang, Department of Molecular Medicine II, Medical Faculty, Heinrich Heine University, Universitätsstr 1, Düsseldorf 40225, Germany; philipp.lang@med.uni-duesseldorf.de

KSL and PAL contributed equally.

Received 3 January 2019
Revised 22 July 2019
Accepted 24 July 2019

To cite: Zhuang Y, Xu HC, Shinde PV, *et al*. *Gut* Epub ahead of print: [*please include* Day Month Year]. doi:10.1136/gutjnl-2019-318215

ABSTRACT

Objective The Fragile X mental retardation (FMR) syndrome is a frequently inherited intellectual disability caused by decreased or absent expression of the FMR protein (FMRP). Lack of FMRP is associated with neuronal degradation and cognitive dysfunction but its role outside the central nervous system is insufficiently studied. Here, we identify a role of FMRP in liver disease.

Design Mice lacking *Fmr1* gene expression were used to study the role of FMRP during tumour necrosis factor (TNF)-induced liver damage in disease model systems. Liver damage and mechanistic studies were performed using real-time PCR, Western Blot, staining of tissue sections and clinical chemistry.

Results *Fmr1*^{null} mice exhibited increased liver damage during virus-mediated hepatitis following infection with the lymphocytic choriomeningitis virus. Exposure to TNF resulted in severe liver damage due to increased hepatocyte cell death. Consistently, we found increased caspase-8 and caspase-3 activation following TNF stimulation. Furthermore, we demonstrate FMRP to be critically important for regulating key molecules in TNF receptor 1 (TNFR1)-dependent apoptosis and necroptosis including CYLD, c-FLIP$_s$ and JNK, which contribute to prolonged RIPK1 expression. Accordingly, the RIPK1 inhibitor Necrostatin-1s could reduce liver cell death and alleviate liver damage in *Fmr1*^{null} mice following TNF exposure. Consistently, FMRP-deficient mice developed increased pathology during acute cholestasis following bile duct ligation, which coincided with increased hepatic expression of RIPK1, RIPK3 and phosphorylation of MLKL.

Conclusions We show that FMRP plays a central role in the inhibition of TNF-mediated cell death during infection and liver disease.

Significance of this study

What is already known on this subject?
- ► Viral infection, septic shock and cholestasis can trigger liver damage.
- ► Tumour necrosis factor (TNF) pathway is well studied in promoting liver damage and fibrosis.

What are the new findings?
- ► Fragile X mental retardation protein (FMRP) is critical for preventing TNF-induced cell death.
- ► FMRP negatively regulates RIPK1 to prevent cell death.
- ► FMRP-deficient mice developed severe pathology during acute cholestasis, septic shock and virally induced hepatitis.
- ► The RIPK1 inhibitor Necrostatin-1s could alleviate disease in the absence of FMRP.

How might it impact on clinical practice in the foreseeable future?
- ► Patients exhibiting sequence alterations in the *Fmr1* gene may exhibit increased liver cell death in severe hepatotoxic situations.

INTRODUCTION

Liver damage can be triggered by hepatic infections, immune activation and intoxication.[1–3] Prolonged tissue damage can result in fibrosis, cirrhosis and liver failure, which affects more than one million casualties worldwide.[1] Tumour necrosis factor α (TNF) is a central cytokine during liver damage.[1 3] Consistently, injection of TNF can cause severe liver damage and septic shock, when applied in combination with D-Gal, which is dependent on TNFR1.[3] Notably, TNF has been shown to promote liver damage and fibrosis in a variety of animal models including acute cholestasis and toxic liver damage.[4 5] Mechanistically, TNF binds to TNFR1, which can mediate cell activation via NF-κB, and apoptosis via caspase activation.[6] On TNF binding, TNFR1 forms a complex with TRADD and RIPK1 with latter being the central molecular switch guided by its ubiquitination status.[6] Non-ubiquitinated RIPK1 dissociates from the cell membrane to form cytosolic complexes termed IIa, IIb or IIc that promote cell death rather than NF-κB activation.[6] Hence, either the lack of cIAPs that can ubiquitinate RIPK1 or the deubiquitination enzyme cylindromatosis

(CYLD) results in reduced K63-linked polyubiquitin chains conserving non-ubiquitinated RIPK1 and promoting cell death.[7–9] Non-ubiquitinated RIPK1 can recruit RIPK3, which is an elementary switch from apoptosis to necroptosis.[10–12] Necroptosis depends on the kinase activity of RIPK3, which can be alleviated by caspase-mediated cleavage of the kinase domain.[13] Accordingly, inhibition of caspase activity by c-FLIP$_S$ cannot inactivate RIPK3 and promotes necroptosis.[14 15]

During viral infections of the liver, viral-specific cytotoxic CD8$^+$ T cells target infected hepatocytes to limit viral replication and induce tissue damage rather than direct cytolytic effects of the virus. Consistently, the murine, poorly cytolytic, lymphocytic choriomeningitis virus (LCMV) model system induces a CD8$^+$ T-cell-mediated hepatitis, which is associated with increased liver cell enzymes in the blood stream.[16] Hence, depletion of CD8$^+$ T cells results in absent tissue damage during LCMV infection, although high viral load can be detected in the liver.[16] CD8$^+$ T-cell-mediated cytokine production such as secretion of TNF triggers liver damage following viral hepatitis.[17] Consistently, viral-specific CD8$^+$ T-cells induce liver cell death coinciding with activation of caspase-3 (Casp3).[18]

The leading cause for inherited intellectual disability is the Fragile X mental retardation (FMR) syndrome, caused by CGG repeats in the locus Xq27.3.[19 20] Insertion at the folate-sensitive fragile site causes genetic instability of the *Fmr1* gene, leading to reduced or absent expression of the FMR protein (FMRP).[21 22] *Fmr1* knockout (KO) mice exhibit learning deficits and deregulation of presynaptic and postsynaptic proteins.[23] Additionally, *Fmr1*^{null} mice exhibit macroorchidism and increased ovarian weight.[23 24] FMRP is an RNA-binding protein known to regulate translation of over 40 proteins in the central nervous system (CNS). Additionally, FMRP was shown to bind over 6000 transcripts.[24–26] Interestingly, increased expression of *Fmr1* mRNA levels and FMRP correlates with prognostic indicators denoting aggressive breast and lung cancers.[27] However, despite its ubiquitous expression, the physiological role of FMRP outside the CNS remains poorly understood.

Expression of FMRP in secondary lymphoid organs raised the question whether it affects anti-viral immunity. We therefore infected *Fmr1*^{null} mice with LCMV and monitored increased CD8$^+$ T-cell-mediated liver damage. No gross immune defects in the anti-LCMV defence pointed to an increased sensitivity of targeted liver cells. Consistently, we found increased liver damage following exposure of *Fmr1*^{null} mice to D-galactosamine (D-Gal)/TNF along with increased presence of cell death markers. Mechanistically, increased expression of RIPK1 resulted in activation of apoptosis and necroptosis pathways. Consistently, treatment with the RIPK1 inhibitor Necrostatin-1s (Nec-1s) could reduce liver cell death and liver damage. During acute cholestasis following bile duct ligation (BDL) in mice, we observed increased presence of RIPK1, RIPK3 and phosphorylation of MLKL with severe RIPK1-dependent pathology.

MATERIALS AND METHODS

Animals

All experiments were performed under the authorisation of LANUV in accordance with German law for animal protection. *Fmr1* KO (*Fmr1*^{null}) mice were purchased from Jackson Laboratories (USA) and maintained under specific pathogen-free conditions. *Fmr1*^{null} mice were on a C57Bl/6 background (F8-F10) and compared with control C57Bl/6 mice. Key experiments were performed with littermate controls. For BDL, laparotomy was performed predominantly on male mice at 10–14 weeks of age, animals were anaesthetised by isoflurane and placed on a heating pad. Animals were shaved and the skin was disinfected with 70% ethanol and povidone-iodine. A midline incision in the upper abdomen was made and the common bile duct and the bile bladder were identified, isolated and ligated with three surgical knots using silk. Abdomen and peritoneum were closed with a running silk suture. Sham treatment was performed similarly but without ligation of the bile duct and bile bladder. Animals were monitored during recovery and treated with carprofen (0.05 mg/kg) after surgical intervention. Mice exhibiting severe disease symptoms where sacrificed and considered as dead. For blood and tissue collection, mice were anaesthetised, bled and serum was collected by retro orbital vein puncture. The organs were stored at −80°C for histology, RNA and protein extraction. For injections, age-matched and sex-matched control and *Fmr1*^{null} mice were intraperitoneally injected with 10 mg D-Gal (Sigma, dissolved in phosphate-buffered saline (PBS) at a concentration of 100 mg/mL) and 15 min later intravenously injected with the indicated doses of rTNFα (R&D Systems, dissolved in PBS at a concentration of 100 µg/mL). For R-7-Cl-O-Nec-1 (Nec-1s) treatment experiments, mice were intraperitoneally injected with 10 mg D-Gal (Sigma) and 6 µg/g Nec-1s (Abcam, dissolved in dimethyl sulfoxide (DMSO) at a concentration of 20 mg/mL) or vehicle (DMSO, Sigma), then 15 min later intravenously injected with 100 ng/mouse rTNFα (R&D Systems). Mice were intraperitoneally injected with FS-7-associated surface antigen (Fas) (clone Jo2, 0.5 mg/mL, BD Pharmingen). Mice were intraperitoneally injected with 100 µg/mouse Etanercept (Pfizer, dissolved at a concentration of 10 mg/mL in PBS) 1 day before LCMV infection, then three times/week during LCMV infection.

Virus

LCMV strain W.E. (WE) was originally obtained from F. Lahmann-Grube (Heinrich Pette Institute). Virus was inoculated via intravenous tail vein injection. Virus titres were measured with a plaque-forming assay as previously described.[16]

Primary hepatocytes isolation

Primary hepatocytes were isolated from C57BL/6J control and *Fmr1*^{null} mice using a collagenase perfusion technique. Briefly, livers were perfused with Hanks' balanced salt solution (HBSS) buffer with 1% glucose and 2.5 mM ethylene glycol-bis(β-aminoethyl ether)-N,N,N′,N′-tetraacetic acid (EGTA) for 4 min. Then, liver tissue was perfused with 0.03 mg/mL collagenase for 6–8 min in HBSS buffer with 1% glucose and 5 mM Cacl2. The isolated primary hepatocytes were cultured in William medium.

Histology

Histological analysis of snap-frozen tissue was performed as previously described.[16] Snap-frozen tissue sections were stained with anti-alpha smooth muscle actin (αSMA; abcam), anti-F4/80, Ly6G (eBioscience), anti-active Casp3 (BD Biosciences), anti-proliferating cell nuclear antigen (PCNA; Cell Signaling). Casp3 activity was performed with a fluorescence assay according to the manufacturer's instructions (Cell Signaling). Terminal deoxynucleotidyl transferase dUTP nick end labelling (TUNEL) staining was performed on liver sections according to the manufacturer's instructions (Roche). Fluorescence images were taken with an Axio Observer fluorescence microscope (Zeiss). Quantification of fluorescence staining was analysed by ImageJ, with either measurement of the mean fluorescent intensity (MFI) or the numbers of positive signals.

Flow cytometry

Different immune populations were identified from single cell solutions harvested from organ as indicated. Experiments were performed on BD LSRFortessa and analysed using FlowJo software. For tetramer staining, singly suspended cells were incubated with tetramer-glycoprotein (gp)33 and nucleoprotein (np)396 for 15 min, or incubated with tetramer-gp61 for 30 min at 37°C. After incubation, surface anti-CD8 (eBioscience) or anti-CD4 (eBioscience) antibodies were added for 30 min at 4°C. For intracellular cytokine staining, single suspended cells were stimulated with LCMV-specific peptide gp33, and gp61 for 1 hour after which Brefeldin A (eBiocience) was added for another 5 hours and incubated at 37°C, followed by permeabilisation and addition of anti-interferon gamma (IFNγ) or anti-TNFα antibodies (eBioscience).

Bile acids analysis

Bile acids and their glycine and taurine derivatives were analysed by ultra performance liquid chromatography - tandem mass spectrometer (UPLC-MS/MS). The system consists of an Acquity UPLC-I Class (Waters) coupled to a Waters Xevo-TQS tandem mass spectrometer equipped with an electrospray ionization source in the negative ion mode. Data were collected in the multiple reaction monitoring mode.

Casp3 activity assay

Casp3 activity assay kit (Cell Signaling, #5723) was used on liver tissue lysates by following the manufacturer's instructions.

Quantitative real-time PCR

RNA was isolated using Trizol (Invitrogen; 15596018) and real-time PCR analyses were performed according to the manufacturer's instructions (Applied Biosystems). For analysis, expression levels were normalised to *GADPH* (ΔCt). Gene expression values were then calculated based on the ΔΔCt method, using the mean naive mice as a control to which all other samples were compared. Relative quantities (RQ) were determined using the equation: RQ=2^-ΔΔCt.

Immunoblotting

Liver tissue was lysed in PBS containing 1% Triton X-100 lysis buffer, protease inhibitors cocktail and PhosSTOP (Roche). Equal amounts of the total protein were separated by sodium dodecyl sulfate–polyacrylamide gel electrophoresis (SDS-PAGE) and transferred to a nitrocellulose membrane, after blocking probed with specific primary and secondary antibodies. The blots were developed using enhanced chemiluminescence (ECL) western blotting substrates (Thermo Fisher) or Li-COR. The following antibodies from Abcam were used: ASK1, FMRP, PARP, Phospho-MLKL. The following antibodies from Santa Cruz were used: $FLIP_{S/L}$ and cylindromatosis. The following antibodies from Cell Signaling were used: cleaved-caspase-8 (Casp8), Casp3, IκBα, c-IAP1, XIAP, SMAC, FMRP, Phospho-ASK1, MKK4, Phospho-MKK4, SAPK/JNK, Phospho-SAPK/JNK, Phospho-c-Jun, Phospho-Erk1/2, RIPK1, PCNA, RIPK3 and MLKL.

Immunoprecipitation

To monitor phosphorylation and ubiquitination of RIPK1, we used TNF-Flag treatment.[28] Liver tissue was homogenised in buffer containing 25 mM 4-(2-hydroxyethyl)-1-piperazineethanesulfonic acid-Potassium hydroxide pH7.5, 0.2% NP-40, 120 mM NaCl, 0.27M sucrose, 1 mM EDTA, 1 mM EGTA, 50 mM NaF, 10 mM β-glycerophosphate, 5 mM sodium pyrophosphate, 2 mM Na3VO4, cOmpleteTM Protease Inhibitor Cocktail, 2 mM phenylmethylsulfonyl fluoride and 10 mM N-Ethylmaleimide. Samples were either incubated with anti-FLAG M2 magnetics beads (Sigma) for 4 hours or RIPK1 antibody (Cell Signaling) overnight followed by 2 hours incubation with magnetics beads (Bio-rad) at 4°C. The beads were washed and proteins were eluted in 70°C with sample buffer and the eluted proteins were fractionated by SDS-PAGE gels. Proteins were detected by immunoblotting as described above.

Bioinformatic analyses

Target genes of FMRP were selected on the basis of enrichment in Rip-chip data published previously.[24] The biological classification of associated genes in terms of their biological processes was obtained by Gene Ontology (GO) analysis using the Protein Analysis through Evolutionary Relationships (PANTHER) classification system (PANTHER V.9.0; http://www.pantherdb.org).[29 30]

Statistical analyses

Data are expressed as mean±SEM. Statistically significant differences were determined with a Student's t-test, a one-way analysis of variance (ANOVA), two-way ANOVA and Log-rank (Mantel-Cox). All the quantifications were analysed by ImageJ.

RESULTS

Absence of FMRP results in increased $CD8^+$ T-cell-mediated liver damage during viral hepatitis

FMRP expression in spleen, liver and lymph node tissue prompted us to investigate whether *Fmr1* also plays a critical role during viral infection (online supplementary figure 1). On infection of control and $Fmr1^{null}$ mice with LCMV-WE, we observed higher activity of the enzyme alanine aminotransferase (ALT) along with increased bilirubin concentrations in the serum of $Fmr1^{null}$ mice (figure 1A, B). Liver tissue harvested from $Fmr1^{null}$ animals exhibited increased presence of highly nucleated cells when compared with liver tissue from control animals (figure 1C). Furthermore, we observed increased expression of αSMA, an indicator of fibrosis, in the liver tissue of $Fmr1^{null}$ mice compared with control animals (figure 1D). During infection with LCMV, infected hepatocytes are targeted by viral-specific $CD8^+$ T cells, and this is followed by cell death of infected cells.[16 18] Liver sections of $Fmr1^{null}$ mice exhibited increased DNA fragmentation indicating cell death, following infection (figure 1E). Notably, the infiltration of macrophages or granulocytes into liver tissue following infection appeared similar between $Fmr1^{null}$ and control mice (online supplementary figure 2A). Due to the increased liver damage in $Fmr1^{null}$ mice, we wondered whether anti-viral $CD8^+$ T-cell immunity was increased in the absence of FMRP. As expected, increased liver damage in $Fmr1^{null}$ mice was dependent on cytotoxic T-cell immunity as depletion of $CD8^+$ T cells blunted liver damage in both control and $Fmr1^{null}$ mice (figure 2A). However, we did not observe a difference in the numbers of circulating viral-specific $CD8^+$ or $CD4^+$ T cells (figure 2B). Furthermore, the surface expression of interleukin 7 receptor which is associated with T-cell survival and programmed cell death-1 along with other surface molecules associated with T-cell exhaustion,[31] was similar on anti-viral T cells, suggesting that anti-viral T-cell immunity was unaffected by FMRP (online supplementary figure 2B). Consistently, the proportion of effector, effector memory and central memory T cells was similar between control and $Fmr1^{null}$ mice (online supplementary figure 2C). IFNγ and TNF production in $CD8^+$ T cells following re-stimulation with LCMV-specific epitopes was not dependent on the presence of FMRP in spleen or liver tissue,

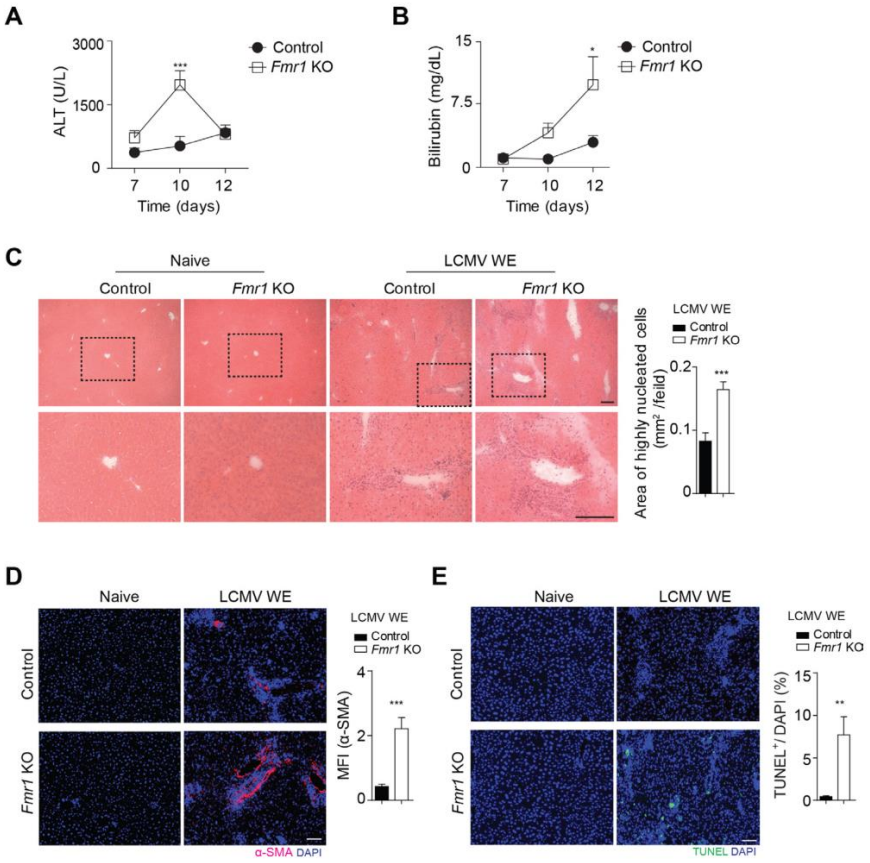

Figure 1 FMRP alleviates virally induced hepatitis LCMV infection. (A–E) Mice were infected with 2×10^6 pfu of LCMV-WE. (A) ALT activity was measured in serum of control and *Fmr1*^{null} (*Fmr1* KO) mice at the indicated time points (n=5–7). (B) Bilirubin was measured in the serum of control and *Fmr1*^{null} mice infected with LCMV-WE at the indicated time points (n=4). (C) Haematoxylin and eosin staining was performed on liver sections of control and *Fmr1*^{null} mice at day 12 post-infection (n=4, scale bar=50 µm). Representative sections are shown. Right panel indicates quantification. (D) Liver tissue sections harvested from control and *Fmr1*^{null} mice were stained for αSMA at day 12 post-infection (n=4, scale bar=100 µm). Representative sections are shown. Right panel indicates quantification. (E) Sections from liver tissue harvested from control and *Fmr1*^{null} mice at day 12 post-infection were stained for TUNEL (n=4, scale bar=100 µm). Representative sections are shown. Right panel indicates quantification. *p<0.05, **p<0.01, ***p<0.001. ALT, alanine aminotransferase; αSMA, alpha smooth muscle actin; FMRP, Fragile X mental retardation protein; KO, knockout; LCMV, lymphocytic choriomeningitis virus; TUNEL, terminal deoxynucleotidyl transferase dUTP nick end labelling.

which was consistent with similar frequencies of LCMV-specific CD8$^+$ T cells in both groups (figure 2C,D, online supplementary figure 2D, E). These data indicate that cytotoxic T-cell immunity was not affected by lack of FMRP. In further support of this, CD4$^+$ T-cell frequencies were similar in spleen and liver tissue between control and *Fmr1*^{null} animals (online supplementary figure 2F). Hence, we concluded that FMRP is dispensable for induction of viral-specific immunity against LCMV and wondered whether FMRP might influence LCMV replication. However, we observed no significant difference in viral titres in organs harvested from control and *Fmr1*^{null} mice following infection (figure 2E). The presence of LCMV nucleoprotein (NP) was similar between liver tissue of control and *Fmr1*^{null} mice (figure 2F). Since T cells secrete TNF during LCMV infection, and TNF can contribute to aggravated LCMV-induced liver damage,[17] we speculated that blockage of TNF signalling might reduce severe liver damage in absence of FMRP. Consistently, when we applied TNFR2-Fc fusion protein (Etanercept) as TNF inhibitor, we found reduced presence of liver enzymes including ALT, aspartate aminotransferase (AST) and lactate dehydrogenase (LDH) in the sera of infected *Fmr1*^{null} mice when compared with untreated *Fmr1*^{null} animals (figure 2G). Taken together, these data indicate that FMRP is important for reducing liver damage during viral infection but does not affect the induction of anti-viral immunity in this setting.

TNF-mediated liver damage can be alleviated by FMRP

TNF can induce liver damage via TNFR1 signalling when injected in combination with D-Gal.[3] Following injection of TNF and D-Gal into C57Bl/6 mice, we observed increased expression levels of *Fmr1* in liver tissue (figure 3A). Consistently, protein expression of FMRP was increased in liver tissue following TNF/D-Gal treatment (figure 3B). We therefore hypothesised that FMRP might be upregulated as a protection mechanism against TNF-mediated damage. When challenged with D-Gal/TNF, the survival of *Fmr1*^{null} mice was reduced compared with control mice (figure 3C), while exposure to D-Gal alone did not cause severe pathology (online supplementary figure 3A). ALT and AST activities in the serum of *Fmr1*^{null} mice were increased

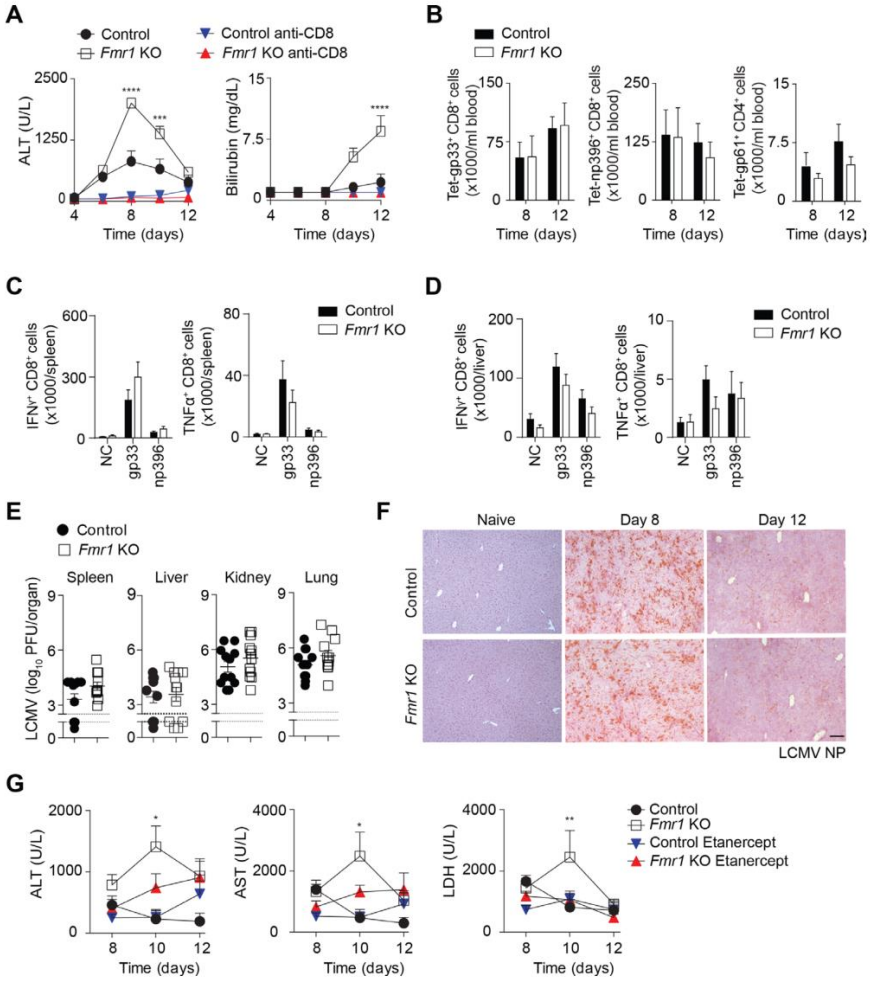

Figure 2 Increased liver damage in absence of FMRP is triggered by CD8$^+$ T cells and TNF. (A) CD8$^+$ T cells were depleted in control and *Fmr1*^{null} (*Fmr1* KO) mice. ALT activity and total bilirubin concentration were measured after infection at the indicated time points (n=4). (B) Anti-viral T-cell response was measured in blood samples using T-cell-specific tetramers of gp33, np396 and gp61 in control and *Fmr1*^{null} mice at indicated time points after infection (n=5-10). (C) Spleen and (D) liver tissue were harvested from control and *Fmr1*^{null} mice at day 12 post-infection. Single cell suspensions were stimulated with gp33 and np396 peptides followed by staining with anti-IFNγ and anti-TNFα antibodies in CD8$^+$ T cells (n=12). (E) LCMV titres were measured in different organs from control and *Fmr1*^{null} mice at day 12 post-infection (n=12). (F) Liver tissue sections harvested from control and *Fmr1*^{null} mice were stained for LCMV-NP (clone VL4) (n=3–6, scale bar=50 µm). Representative sections are shown. (G) Control and *Fmr1*^{null} mice were treated with Etanercept. ALT, AST and LDH activities were measured after infection as indicated (n=3–4). *p<0.05, **p<0.01, ***p<0.001. ALT, alanine aminotransferase; AST, aspartate aminotransferase; FMRP, Fragile X mental retardation protein; gp33, glycoprotein 33; IFN, interferon; KO, knockout; LCMV, lymphocytic choriomeningitis virus; LDH, lactate dehydrogenase; NC, negtive control; np396,nucleoprotein 396; TNF, tumour necrosis factor.

when compared with control mice (figure 3D). The livers of *Fmr1*^{null} mice appeared macroscopically enlarged and dark red when compared with control liver tissue (figure 3E). Moreover, histological analysis showed the disruption of hepatic organisation and reduced presence of nuclei in liver tissue from *Fmr1*^{null} mice when compared with control mice (figure 3F).[32] We did not observe a difference in the infiltration of macrophages or granulocytes (online supplementary figure 3B). Next, we wondered whether FMRP inhibits liver damage induced by other receptors than that for TNF such as the well-studied death receptor CD95.[33] When we exposed control and *Fmr1*^{null} mice to an anti-CD95 activating antibody, there was no difference between survival or ALT/AST activity in the sera between the two groups (figure 3G, H). Taken together, while we determined that FMRP is important in reducing TNF-mediated liver damage and incurring protection from lethal septic shock, it remained unclear whether these effects could affect cell death.

Absence of FMRP results in increased TNF-mediated cell death

A higher degree of DNA fragmentation was observed in liver tissue harvested from *Fmr1*^{null} mice when compared with control animals after D-Gal/TNF stimulation (figure 4A). DNA damage can be repaired by the enzyme Poly(ADP—ribose)-Polymerase 1 (PARP).[34] PARP is cleaved during cell death to prevent DNA repair.[35] We observed increased PARP cleavage in protein lysates harvested from liver tissue of *Fmr1*^{null} animals when compared

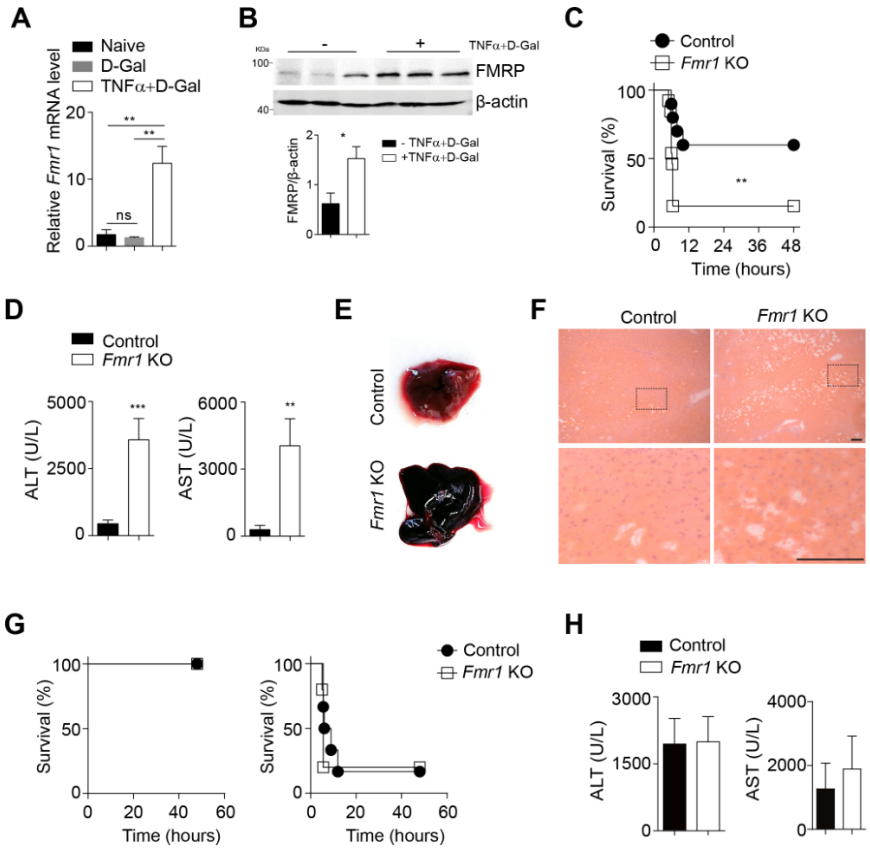

Figure 3 Lack of FMRP triggers increased susceptibility towards TNF-induced septic shock. (A) *Fmr1* gene expression was quantified in liver tissue of C57Bl/6 mice 3 hours post D-Gal (10 mg/mouse) and rTNF (100 ng/mouse) injection (n=4–5). (B) Liver lysates were probed for FMRP at 3 hours post D-Gal/rTNF injection. Bottom panels indicate quantification. (C–F) Control and *Fmr1*^{null} (*Fmr1* KO) mice were treated with D-Gal (10 mg/mouse) and rTNF (100 ng/mouse). (C) Survival of control and *Fmr1*^{null} mice was monitored (n=14). (D) ALT (n=15) and AST (n=6) activities were measured in serum samples of control and *Fmr1*^{null} mice 5 hours post-injection. (E) Morphology of whole liver tissue from control and *Fmr1*^{null} mice was assessed 5 hours after treatment. (F) Haematoxylin and eosin staining of liver tissue sections from control and *Fmr1*^{null} mice 5 hours after treatment (n=3, scale bar=50 µm). Representative sections are shown. (G) Control and *Fmr1*^{null} mice were treated with 0.28 µg/g (left panel, n=3) and 0.56 µg/g (right panel, n=6-7) Fas antibody and survival was monitored. (H) ALT (n=9) and AST(n=3) activities were measured in serum samples of control and *Fmr1*^{null} mice 3 hours post-Fas antibody treatment (0.56 µg/g). *p<0.05, **p<0.01, ***p<0.001. ALT, alanine aminotransferase; AST, aspartate aminotransferase; FMRP, Fragile X mental retardation protein; KO, knockout; TNF, tumour necrosis factor.

with controls (figure 4B, online supplementary figure 4A). PARP cleavage is mediated by Casp3, a common effector caspase shared by the intrinsically and extrinsically induced cell death pathways.[6] As expected, we observed increased cleavage and activity of Casp3 in liver tissue of *Fmr1*^{null} mice when compared with control animals (figure 4B–D). Effector caspases are activated by initiator caspases such as Casp8 during TNFR1-mediated cell death.[6] We observed increased Casp8 cleavage in D-Gal/TNF stimulated *Fmr1*^{null} mice in comparison to control animals (figure 4E, F). These in vivo effects were corroborated in vitro as we also found more cleaved PARP and Casp8 in primary hepatocytes harvested from *Fmr1*^{null} mice than in hepatocytes from control mice stimulated with cyclohexamide and TNF (figure 4G).

TNFR1 activation can result in both Casp8-mediated apoptosis and NF-κB activation. NF-κB is retained in the cytosol by binding to an inhibitor of κB α (IκBα). Accordingly, proteasomal degradation of IκBα results into release of NF-κB, which can translocate to the nucleus to induce transcription of pro-inflammatory cytokines.[6] Degradation of IκBα was observed in both FMRP-deficient and control mice following stimulation with TNF (figure 4H). Consistently, we monitored similar translocation of the NF-κB subunit p65 into the nucleus in liver tissue from *Fmr1*^{null} and control mice over time (online supplementary figure 4B). Moreover, expression levels of genes typically induced by NF-κB were similar in liver tissue from control or *Fmr1*^{null} mice (figure 4I). Notably, at later time points, we observed a slightly but significantly increased expression of *Il2*, *Ccl2*, *Cxcl10* and *Cxcl12* in *Fmr1*^{null} liver tissue when compared with controls (online supplementary figure 4C). These data indicate that in the absence of FMRP while TNF-mediated cell death is highly increased, TNF-mediated NF-κB activation is only marginally affected.

Inhibition of RIPK1 reduces TNF induced cell death in absence of FMRP

Next, we investigated the molecular mechanism by which FMRP inhibits cell death. A previous study identified over 6000 transcripts that can potentially bind to FMRP through the binding consensus sequences ACU (G or U) or (A or U) GGA.[24] By GO

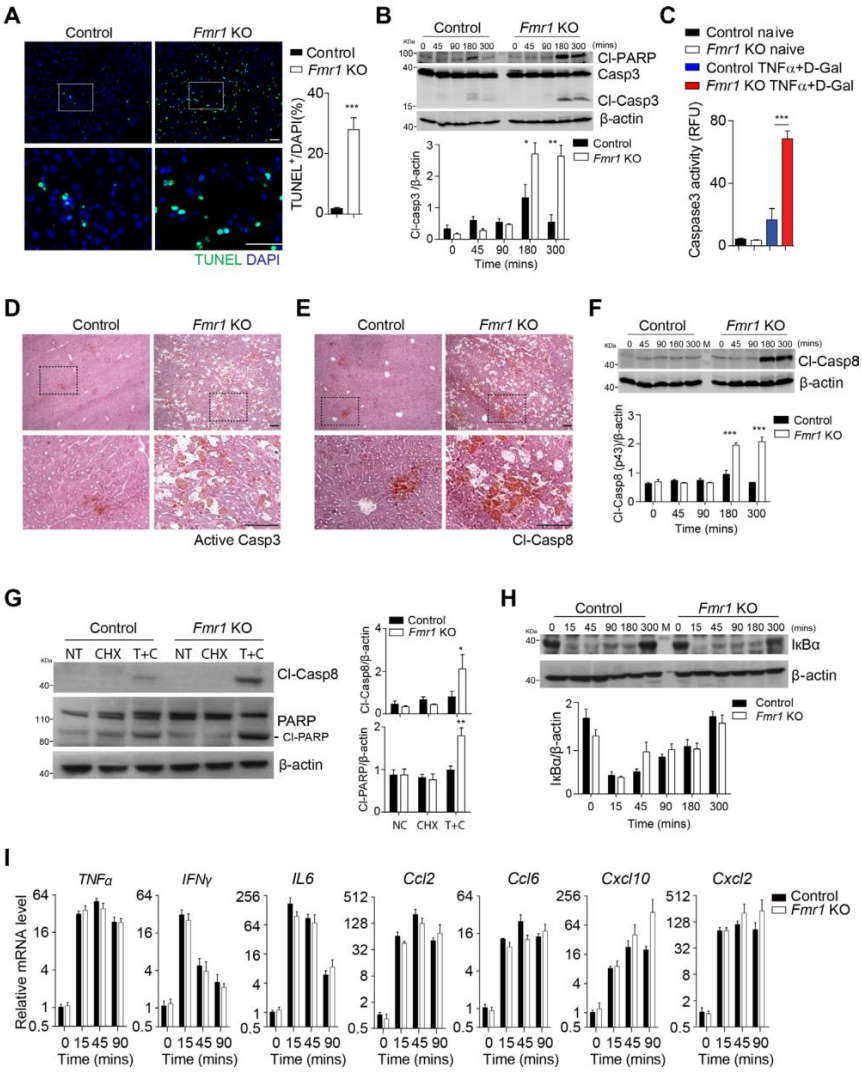

Figure 4 *Fmr1*^{null} mice exhibit increased TNF-mediated cell death. (A) TUNEL staining of liver tissue sections from control and *Fmr1*^{null} (*Fmr1* KO) mice 5 hours post D-Gal (10 mg/mouse) and rTNF (100 ng/mouse) treatment. Right panel indicates quantification (n=5, one representative picture is shown, scale bar=100 µm). (B) Liver tissue homogenates from control and *Fmr1*^{null} mice were assessed for expression of cleaved-PARP and Casp3 (one representative immunoblot of n=3 is shown). Bottom panel indicates quantification for cleaved-Casp3. (C) Casp3 activity in liver tissue homogenates was performed in control and *Fmr1*^{null} mice 5 hours post D-Gal/rTNF treatment (n=5). (D–E) Sections of liver tissue from control and *Fmr1*^{null} mice were stained for active Casp3 (D) and cleaved-Casp8 (E) 5 hours post D-Gal/rTNF treatment (n=5, scale bar=100 µm). Representative sections are shown. (F) Liver tissue homogenates harvested from Control and *Fmr1*^{null} mice were analysed for expression of cleaved-Casp8 at the indicated time points (one representative set of n=3 immunoblots is shown). Bottom panel indicates quantification. (G) Primary hepatocytes were isolated from naive control and *Fmr1*^{null} mice and treated with cyclohexamide (10 µg/mL) and rTNF (40 ng/mL) for 8 hours. Cell lysates were analysed for the presence of cleaved-Casp8 and PARP (one representative immunoblot of n=4 is shown). Right panels indicate quantification. (H) Liver tissue homogenates from control and *Fmr1*^{null} mice were assessed for expression of IκBα (one representative immunoblot of n=3 is shown). (I) Expression levels of genes as indicated were quantified in control and *Fmr1*^{null} mice at indicated time points after D-Gal/rTNF treatment (n=3–4). *p<0.05, **p<0.01, ***p<0.001. Casp3, caspase-3; Casp8, caspase-8; IκBα; inhibitor of κB α; KO, knockout; PARP, poly(ADP—ribose)-polymerase 1; TNF; tumour necrosis factor; TUNEL, terminal deoxynucleotidyl transferase dUTP nick end labelling.

analysis using the PANTHER classification system, about 6% of these genes clustered in the 'response to stimulus' category (online supplementary figure 5A). Functional categories identified targets encoding for genes involved in cell death and the TNF signalling pathway (online supplementary figure 5B), with multiple binding consensus sites in genes involved in cell death (figure 5A). We found increased RNA expression levels of *Casp8* in *Fmr1*^{null} mice compared with control animals following stimulation with TNF, but not in other genes encoding for proteins critical for cell death, which were measured (figure 5B). At the protein level, we found protein expression of cIAP1, cIAP2, XIAP, SMAC and A20 to be comparable between both groups after TNF/D-Gal challenge (online supplementary figure 6A-E). As FMRP-binding sites were observed in genes involved in the

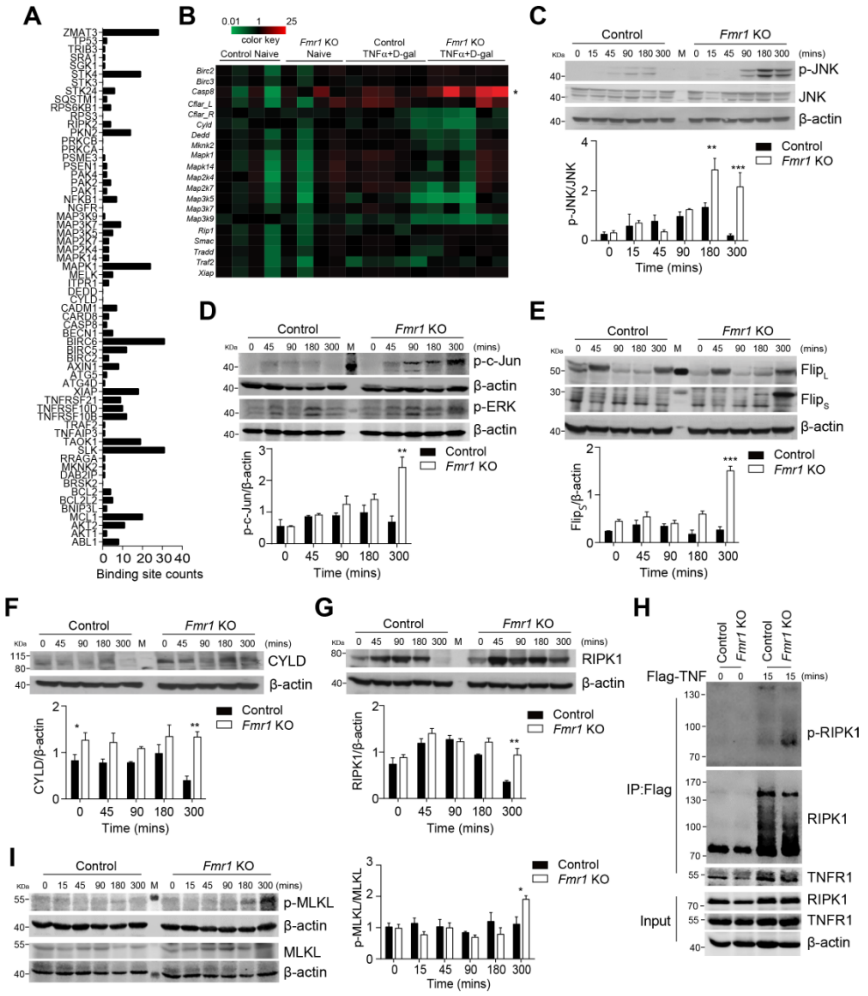

Figure 5 Expression of RIPK1 is increased during TNF-induced liver damage in absence of FMRP. (A) FMR1-binding sites on apoptosis-related genes derived from the publically available FMR1 PAR-CLIP data[6] were analysed. (B) Control and *Fmr1*^{null} (*Fmr1* KO) mice were treated with D-Gal (10 mg/mouse) and rTNF (100 ng/mouse). Gene expression was quantified as indicated in liver tissue 3 hours post-treatment (n=4–5). (C–G) Control and *Fmr1*^{null} mice were treated with TNF and D-Gal and liver tissue was harvested at the indicated time points. Liver lysates were assessed for expression of JNK and phosphorylated JNK (C), phosphorylated c-Jun and p-ERK (D), FLIP$_L$ and FLIP$_S$ (E), CYLD (F), RIPK1 (G). One representative set of immunoblots of n=3 is shown. Bottom panels show quantification as indicated. (H) Control and *Fmr1*^{null} mice were treated with Flag-mTNFα (200 ng/mouse). TNF-complex was immunoprecipitated using anti-Flag beads and RIPK1, p-RIPK1 and TNFR1 were analysed by immunoblotting. One representative of n=4 is shown. (I) Control and *Fmr1*^{null} mice were treated with TNF and D-Gal and liver tissue was harvested at the indicated time points. Liver lysates were assessed for expression of p-MLKL and MLKL. One representative set of immunoblots of n=3 is shown. Right panel shows quantification as indicated. *p<0.05, **p<0.01, ***p<0.001. CYLD, cylindromatosis; FMRP, Fragile X mental retardation protein; TNF, tumour necrosis factor.

MAPK signalling pathway, we next evaluated the effects of FMRP deficiency on this pathway following TNF stimulation (figure 5A). We observed increased expression and phosphorylation of ASK1, along with increased phosphorylation of MKK4 following stimulation with TNF (online supplementary figure 6F, G). Moreover, sustained JNK activation has been shown to be associated with increased TNF-dependent cell death and hepatitis.[36–38] Consistently, we observed increased phosphorylation of JNK, and the transcription factor Jun after TNF exposure in absence of FMRP when compared with controls (figure 5C, D, online supplementary figure 6H), while activation of ERK was unaffected (figure 5D, online supplementary figure 6I). Activated JNK was previously shown to induce turnover of c-FLIP$_{LONG}$, which inhibits TNF-mediated apoptosis.[39] However, we did not see a significant difference in c-FLIP$_{LONG}$ (figure 5E, online supplementary figure 6J).

In turn, the deubiquitinase CYLD promotes TNF-induced JNK activation and might contribute to increased phosphorylation of JNK and Jun.[40] CYLD also inhibits tumour cell proliferation and *Cyld*$^{-/-}$ mice suffer from increased tumour susceptibility.[41 42] Consistent with enhanced JNK phosphorylation, increased protein expression of CYLD was observed in untreated and TNF stimulated liver tissue of *Fmr1*^{null} mice when compared with controls (figure 5F). Furthermore, CYLD catalyses deubiquitination of RIPK1, which consequently dissociates from the TNFR1 complex and is released into the cytosol in order to form a complex with fas-associated protein with death domain (FADD) and Casp8 to promote cell death.[6 7] RIPK1

protein expression was increased in the absence of FMRP following exposure to TNF when compared with controls (figure 5G). Increased RIPK1 expression correlates with a higher susceptibility to cell death.[6] In addition, $FLIP_S$ is upregulated in FRMP-deficient cells (figure 5E). $FLIP_S$ is also known to promote formation of the riptoptosome and accordingly necroptotic cell death.[14 15] In contrast to $FLIP_L$, which forms a catalytic active heterodimer with Casp8 that cleaves and inactivates RIPK1, the heterodimer between Casp8 and $FLIP_S$ does not cleave RIPK1. This leads to $FLIP_S$-dependent stabilisation of RIPK1 and RIPK1-mediated necroptosis induction.[14 15] Hence, we speculated that increased presence of RIP1K resulted in enhanced susceptibility towards TNF-mediated apoptosis and necroptosis in the absence of FMRP. Consistently, we observed increased phosphorylation and reduced ubiquitination of RIPK1 following immunoprecipitation of TNF-Flag from liver tissue of *Fmr1*^{null} mice compared with control mice after treatment (figure 5H). During necroptosis, the pseudokinase MLKL is phosphorylated.[43] Accordingly, p-MLKL levels were increased in liver tissue harvested from *Fmr1*^{null} mice compared with control mice (figure 5I). Taken together, these data indicate that absence of FMRP results in increased apoptosis and necroptosis pathways following TNF/D-Gal treatment.

RIPK1 can be inhibited by Necrostatin-1, and, with higher affinity by 7-Cl-O-Nec-1 (Nec-1s), which is also suitable for animal models.[44] Following treatment of *Fmr1*^{null} mice with Nec-1s, we observed reduced phosphorylation of RIPK1 (figure 6A). Accordingly, application of Nec-1s resulted in reduction of p-MLKL in liver tissue of *Fmr1*^{null} mice (figure 6B). Moreover, reduced presence of active Casp3 was detected in liver tissue of Nec-1s treated *Fmr1*^{null} mice compared with untreated *Fmr1*^{null} mice (figure 6C). Consequently, TUNEL staining in liver tissue sections from Nec-1s treated *Fmr1*^{null} mice was reduced when compared with *Fmr1*^{null} mice (figure 6D). Consistently, when we administered Nec-1s during D-Gal/TNF injections, we observed reduction of liver enzyme activity including ALT, AST and LDH in the sera of treated *Fmr1*^{null} mice when compared with untreated animals (figure 6E). These findings were also obtained using the inhibitor Nec-1 (online supplementary figure 6K). Taken together, the RIPK1 inhibitor Nec-1s can reduce the presence of proteins indicating apoptosis and necroptosis and consequently reduce liver damage following TNF/D-Gal treatment in *Fmr1*^{null} mice.

Expression of FMRP alleviates liver damage and disease during BDL

Next, we wondered whether FMRP modulated liver cell death during another disease model such as acute cholestasis following BDL, a model system for liver fibrosis. TNF has been shown to contribute towards liver fibrosis following BDL.[4] As expected, we found increased expression levels of *Tnfa* in mice following BDL (figure 7A). Consistently, we also identified increased expression of FMRP in liver tissue from BDL-operated animals, when compared with tissue from Sham-operated mice (figure 7B). Notably, we did not find a difference in circulating conjugated bile acids in control or *Fmr1*^{null} mice following BDL (figure 7C). However, we identified increased levels of unconjugated bile acids 4 days after BDL (figure 7D). Furthermore, we found increased activity of liver enzymes in the blood stream in FMRP-deficient mice when compared with control mice, suggesting increased liver damage (figure 7E). Histological analyses showed increased disruption of the hepatic organisation in liver tissue harvested from *Fmr1*^{null} mice compared with control mice following BDL (figure 7F). Notably, we did not find a major difference in granulocyte infiltration or expression of pro-inflammatory cytokines in this setting (online supplementary figure 7A-C). However, following BDL, FMRP-deficient mice showed decreased survival compared with control animals (figure 7G).

Next, we wondered by which mechanism FMRP-deficient mice exhibited high susceptibility towards acute cholestasis. We did not observe any significant differences in the expression levels of *Cola1*, *Cola3* and *Acta2* between control and *Fmr1*^{null} mice (online supplementary figure 8A). Consistently, we did not find any difference in hepatic αSMA expression between *Fmr1*^{null} and control mice at these early time points (online supplementary figure 8B). Notably, we found a transient increase in $TUNEL^+$ cells in absence of FMRP (figure 8A). Furthermore, histological analyses of the proliferation marker Ki67 showed reduced expression in liver tissue harvested from *Fmr1*^{null} mice when compared with control animals (figure 8B). Consistently, RNA expression levels of *Ki67* were reduced in FMRP-deficient mice (figure 8C). These findings were further supported by the reduced expression of PCNA, which is associated with hepatocyte proliferation following liver damage (figure 8D). Notably, we did not observe increased presence of cleaved Casp3 or cleaved Casp8 in *Fmr1*^{null} mice following BDL (online supplementary figure 8C, D). In contrast, LCMV infection resulted in increased presence of cleaved Casp3 in liver tissue of *Fmr1*^{null} mice compared with control mice (online supplementary figure 9A, B). Consistent with the increased cell death and reduced proliferation during BDL, we found increased presence of RIPK1 in FMRP-deficient mice when compared with control animals following BDL (figure 8E). RIPK1- dependent recruitment of RIPK3 is a critical step in TNF-mediated necroptosis.[10–12] We observed increased RIPK3 expression in absence of FMRP when compared with FMRP competent mice (figure 8F). RIPK3 can phosphorylate the pseudokinase MLKL, which mediates necroptosis.[43] Consistently, we detected increased presence of p-MLKL in *Fmr1*^{null} liver tissue when compared with control tissue (figure 8G). Furthermore, we observed increased presence of RIPK1, RIPK3 and p-MLKL following LCMV infection (online supplementary figure 9C-E). Treatment of *Fmr1*^{null} animals with Nec-1s could improve the pathology observed following BDL (figure 8H). Taken together, absence of FMRP results in increased expression of RIPK1 and accordingly increased pathology following acute cholestasis.

DISCUSSION

This study shows that lack of FMRP results in prolonged presence of RIP1K affecting TNFR signalling and consequently leading to increased susceptibility towards TNF-mediated liver cell death. Hence, *Fmr1*^{null} mice exhibited increased TNF-mediated liver damage, septic shock, LCMV-induced hepatitis and pathology during BDL. Application of the RIP1K inhibitor Nec-1s could alleviate liver damage following TNF challenge or pathology during BDL in *Fmr1*^{null} mice.

Despite its ubiquitous expression, little is known about the FMRP function outside the CNS. *Fmr1*^{null} mice exhibit macroorchidism and increased ovarian weight.[23 24] Moreover, increased expression of *Fmr1* correlates with aggressive cancer growth.[27] Furthermore, in hepatocellular carcinoma tissue, *FMR1* expression levels were increased when compared with tumour-free tissue.[45] Considering our data, increased presence of FMRP could affect RIPK1 expression and accordingly prevent susceptibility of cancer cells towards TNF-mediated cell death. Hence, strategies to inhibit FMRP might increase the susceptibility of cancer cells towards therapies involving TNF including immunotherapies.

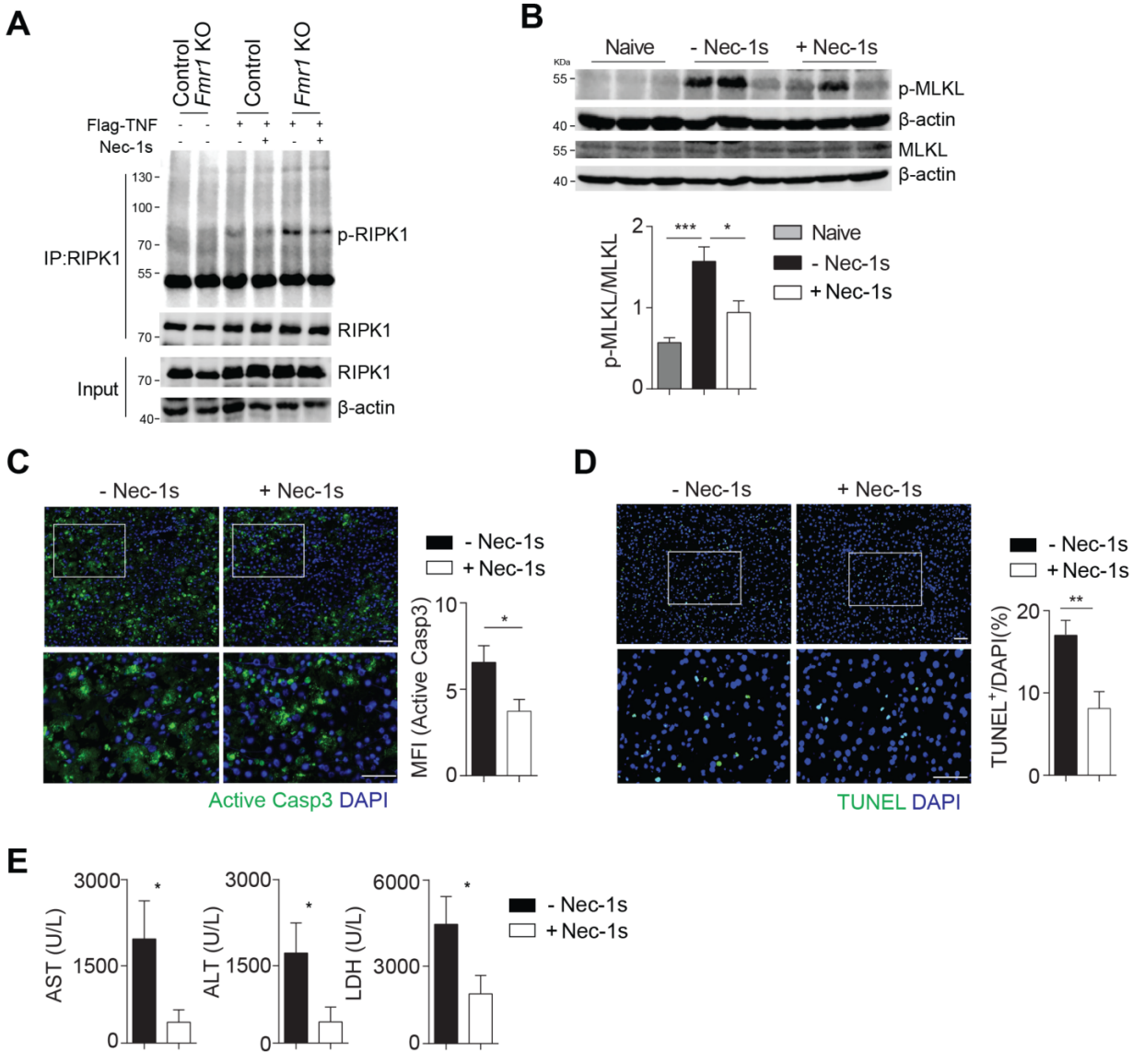

Figure 6 Nec-1s treatment reduced TNF-induced liver damage in absence of FMRP. (A) Control and *Fmr1*^{null} (*Fmr1* KO) mice were treated with Flag-mTNFα (200 ng/mouse) with Nec-1s (6 µg/g) or without Nec-1s. RIPK1 was immunoprecipitated followed by immunoblotting of p-RIPK1 and RIPK1 (one representative of n=4 is shown). (B) p-MLKL and MLKL expression were detected in liver tissue lysates from *Fmr1*^{null} mice and Nec-1s treated *Fmr1*^{null} mice 5 hours post D-Gal/rTNF treatment. Lower panel shows quantification from n=6 mice. (C) Active-caspase-3 and (D) TUNEL staining of liver tissue sections from *Fmr1*^{null} mice and Nec-1s treated *Fmr1*^{null} mice 5-hour post D-Gal/rTNF treatment. Right panel indicates quantification (n=6, one representative picture is shown, scale bar=100 µm). (E) ALT, AST and LDH activities were measured in serum samples of *Fmr1*^{null} mice and Nec-1s treated *Fmr1*^{null} mice 5 hours post D-Gal/rTNF treatment (n=6). Error bars in all graphs indicate SEM. *p<0.05, **p<0.01, ***p<0.001. ALT, alanine aminotransferase; AST, aspartate aminotransferase; FMRP, Fragile X mental retardation protein; LDH, lactate dehydrogenase; Nec-1s, necrostatin-1s; TNF, tumour necrosis factor; TUNEL, terminal deoxynucleotidyl transferase dUTP nick end labelling.

Whether patients suffering from Fragile X syndrome exhibit increased liver damage is not sufficiently studied. Notably, we did not observe increased liver enzymes or gross defects in liver tissue in naïve mice. Only following stimulation with TNF-dependent disease models *Fmr1*^{null} mice exhibited increased liver damage and disease. Patients carrying CGG repeats in the locus Xq27.3 might also be asymptomatic and would not exhibit gross liver damage. However, during infections or intoxication TNF-mediated liver damage might be increased. Future studies on patient cohorts are needed to address the role of FMRP during liver damage and disease.

Absence of FMRP triggers TNF-mediated apoptosis and necroptosis in liver tissue. Positive TUNEL staining and caspase activation cannot distinguish between apoptosis or necroptosis.[6] Notably, the deubiquitinase CYLD was increased in *Fmr1*^{null} mice compared with controls. Presence of CYLD triggers deubiquitination of RIPK1 resulting in presence of non-ubiquitinated RIPK1 and preventing its degradation.[7 9]

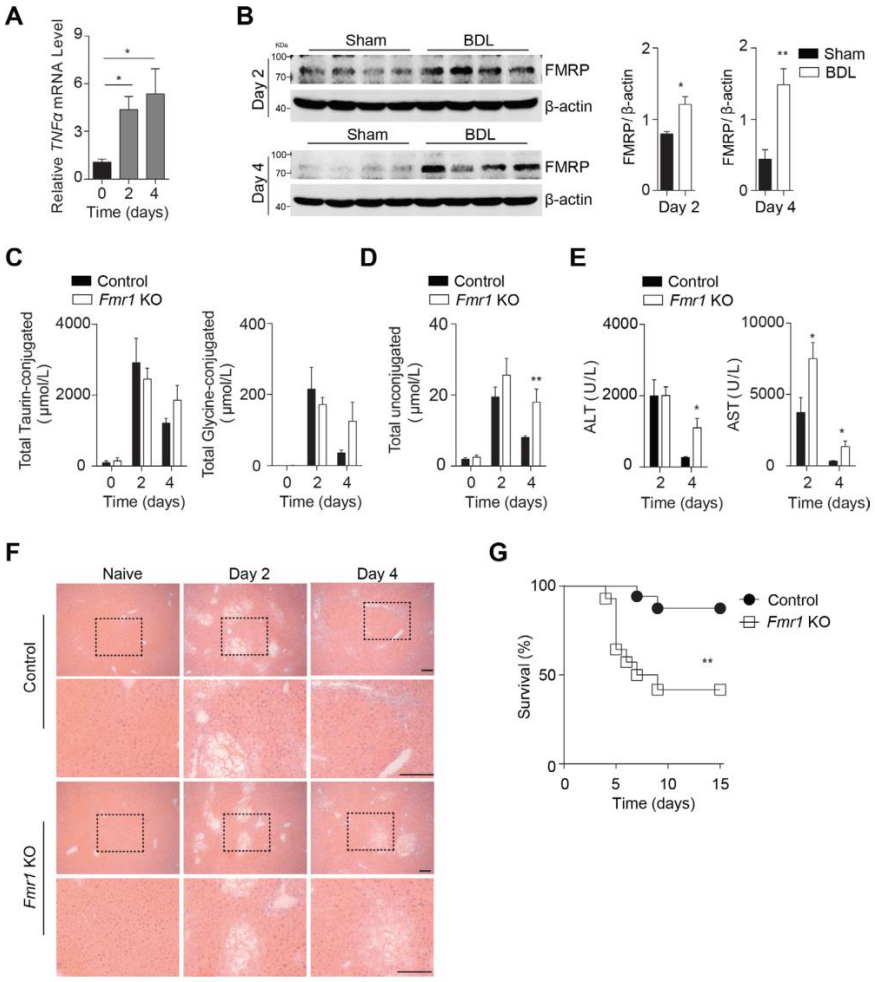

Figure 7 Lack of FMRP triggers increased susceptibility towards BDL-induced liver damage. (A) *Tnfα* gene expression was quantified in liver tissue at indicated time points post-BDL (n=3–4). (B) Liver lysates were probed for FMRP at the indicated time points from Sham and BDL mice. Right panels indicate quantification of n=4 mice. (C) Total taurin-conjugated and glycine-conjugated bile acids, and (D) unconjugated bile acids were measured in serum samples of control and *Fmr1*^{null} (*Fmr1* KO) mice at indicated time points post-BDL (n=4–10). (E) ALT and AST activities were measured in serum samples of control and *Fmr1*^{null} mice at indicated time points post-BDL (n=5–7). (F) Haematoxylin and eosin staining of liver tissue sections of control and *Fmr1*^{null} mice at indicated time points post-BDL (one representative set of n=5–7 is shown, scale bar=50 µm). (G) Survival of control and *Fmr1*^{null} mice after BDL was monitored (n=14–17). *p<0.05, **p<0.01, ***p<0.001. ALT, alanine aminotransferase; AST, aspartate aminotransferase; BDL, bile duct ligation; FMRP, Fragile X mental retardation protein; KO, knockout; TNF, tumour necrosis factor.

Hence, we observed increased expression of RIPK1, a central switch towards necroptosis.[6] Moreover, FLIP$_S$ expression was increased in the absence of FMRP, which triggers formation of the riptoptosome, promoting recruitment of RIPK3 and accordingly induction of necroptosis.[14 15] Consistently, we observed increased presence of p-MLKL during TNF/D-Gal treatment, LCMV infection and BDL in *Fmr1*^{null} mice when compared with control animals. During TNF/D-Gal treatment and LCMV infection, we also observed increased cleaved Casp3, which we did not observe during BDL. Hence, we speculate that FMRP can affect both apoptosis and necroptosis, which is likely context specific. Since treatment with Nec-1s can alleviate pathology during TNF/D-Gal stimulation and BDL in *Fmr1*^{null} mice, RIPK1 is likely involved.

The function of TNF during FMRP deficiency might reach beyond liver pathology. Necroptosis and activation of RIPK1 are associated with a variety of neurological diseases including Alzheimers disease, amyotrophic lateralsclerosis (ALS) and multiple sclerosis.[46] Hence, TNFR1-deficient animals exhibit reduced amyloid β generation and disease symptoms during Alzheimer model systems.[47] RIPK1 mediated the microglial response, which is associated with disease.[48] Moreover, activation of necroptosis can be observed in patient cohorts suffering from Alzheimer disease.[49] Consistently, RIPK1 mediates axonal degradation during ALS.[50] Accordingly, suppression of RIPK1 is associated with later onset of ALS.[28] Furthermore, pathological TNF levels cause synaptic alterations resulting in memory impairment, which is dependent on TNFR1 on astrocytes.[51] In line with this, TNF exacerbates neurotoxic effects during liver disease and acute ammonia intoxication.[52] It is tempting to speculate that increased effects of TNF on neurons contribute to the phenotypical changes of neurons in absence of FMRP. Considering our data, absence of FMRP in neurons might trigger increased degradation during infection or intoxication. Nec-1 or other inhibitors of RIPK1 might be beneficial, not only in preventing liver pathology but also to improve neurological

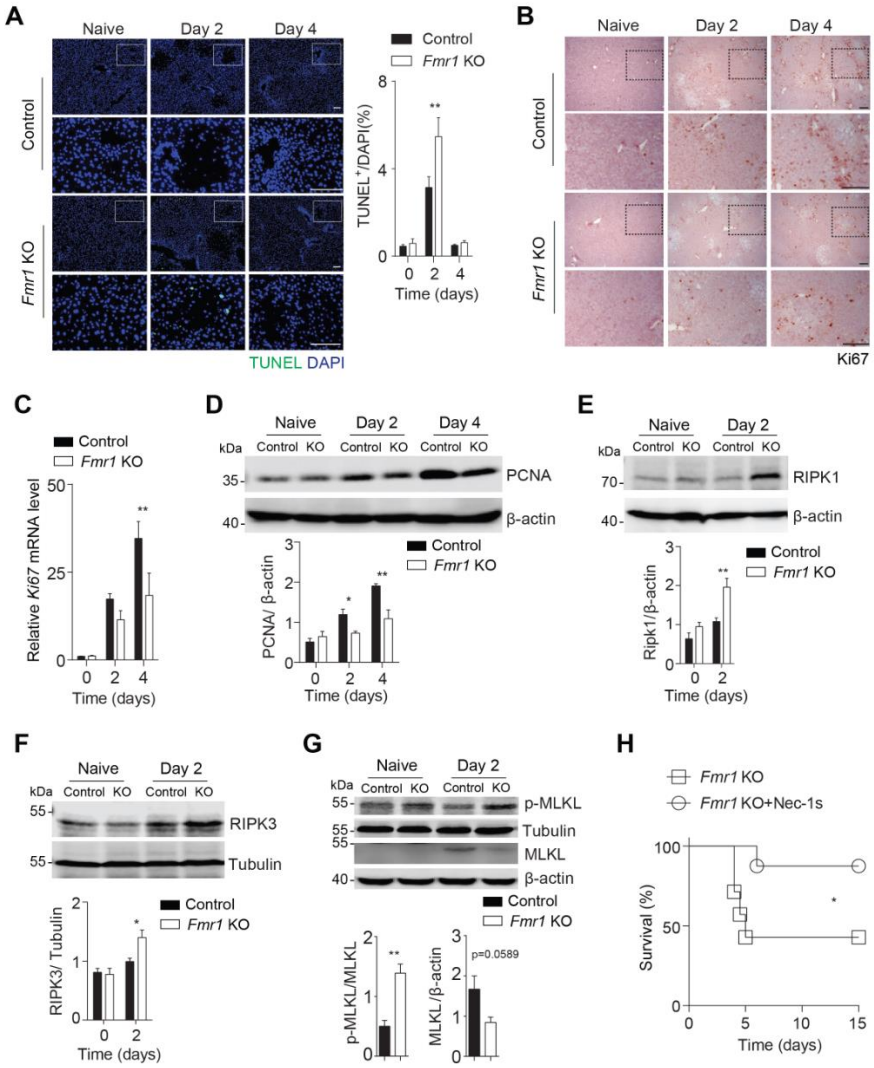

Figure 8 Increased expression of RIPK1 triggers BDL-induced pathology in absence of FMRP. (A) TUNEL staining of liver tissue sections harvested from control and *Fmr1*^{null} (*Fmr1* KO) mice at indicated time points after BDL. Right panel indicates quantification (n=5–7, one representative set of pictures is shown, scale bar=50 µm). (B) Sections of liver tissue harvested from control and *Fmr1*^{null} mice were stained for Ki67 at indicated time points after BDL (n=5–7, scale bar=50 µm). Representative images are shown. (C) *Ki67* gene expression was quantified in liver tissue harvested from control and *Fmr1*^{null} mice at indicated time points post-BDL (n=5–7). (D) PCNA expression was detected at the indicated time points from BDL control and FMRP-deficient mice (one representative set of immunoblots of n=4 is shown). Bottom panels indicate quantification. (E–G) RIPK1 (E), RIPK3 (F), p-MLKL and MLKL (G) expression were detected in liver tissue lysates from control and *Fmr1*^{null} mice at the indicated time points (one representative set of immunoblots of n=3–4 is shown). Bottom panels indicate quantification of day 2. (H) Survival of *Fmr1*^{null} and Nec-1s treated *Fmr1*^{null} mice after BDL was monitored (n=7–8). *p<0.05, **p<0.01. BDL, bile duct ligation; FMRP, Fragile X mental retardation protein; KO, knockout; PCNA, proliferating cell nuclear antigen; TUNEL, terminal deoxynucleotidyl transferase dUTP nick end labelling.

defects. While inhibition of RIPK1 could prevent neuronal degradation during infection, it remains unclear whether a long-term treatment would be possible and/or beneficial. However, the function of FMRP might also be cell type specific and our observations unrelated to neurological defects.

Taken together, we identified a protective role of FMRP in TNF-mediated liver damage and during liver disease.

Author affiliations
[1]Department of Molecular Medicine II, Medical Faculty, Heinrich Heine University, Düsseldorf, Germany
[2]Department of Pediatric Oncology, Hematology and Clinical Immunology, Center for Child and Adolescent Health, Heinrich Heine University, Medical Faculty, Düsseldorf, Germany
[3]Institute of Medical Microbiology and Hospital Hygiene, University Hospital, Heinrich-Heine-University, Düsseldorf, Germany
[4]Research on Children with Special Needs Department, Medical research Branch, National Research Centre, Cairo, Egypt
[5]Institute of Biochemistry and Molecular Biology II, Medical Faculty, Heinrich Heine University, Düsseldorf, Germany
[6]Department of General Pediatrics, Neonatology and Pediatric Cardiology, Medical Faculty, Heinrich Heine University Düsseldorf, Düsseldorf, Germany
[7]Department of Infection and Immunity, Experimental & Molecular Immunology, Luxembourg Institute of Health, Esch-sur-Alzette, Luxembourg
[8]Department of Dermatology and Allergy Center, Odense Research Center for Anaphylaxis (ORCA), Odense University Hospital, University of Southern Denmark, Odense, Denmark
[9]Luxembourg Centre for Systems Biomedicine (LCSB), University of Luxembourg, Belvaux, Luxembourg

[10]Department of Gastroenterology, Hepatology, and Infectious Diseases, Medical Faculty, Heinrich-Heine-University Düsseldorf, Düsseldorf, Germany
[11]Institute of Human Genetics, Medical Faculty, Heinrich-Heine-University Düsseldorf, Düsseldorf, Germany
[12]Institute of Immunology, Medical Faculty, University of Duisburg-Essen, Essen, Germany

Contributors YZ designed and conducted the experiments and analysed the data. HCX, PVS, JW, JV, BS, KB, JH, JIH, AB and KP conducted the experiment and analysed the data. MST, DH, EM, DB, MRA, VK, DW, DH, AAP and KSL analysed the data. AAP and KSL supervised the study and edited the manuscript. PAL designed the whole project, supervised the study and wrote the manuscript.

Funding This study was supported by the German Research Council (SFB974, KFO217, LA-2558/5-1). Furthermore, this study was supported by the Jürgen Manchot Graduate School MOI III and the Research Committee of the Medical Faculty of the Heinrich-Heine University Düsseldorf (grant number: 9772690), DB is supported by the FNR-ATTRACT program (A14/BM/7632103).

Competing interests None declared.

Patient consent for publication Not required.

Ethics approval Landesamt für Natur, Umwelt und Verbraucherschutz (LANUV), North Rhine-Westphalia, Germany. State Office for Nature, Environment and Consumer Protection.

Provenance and peer review Not commissioned; externally peer reviewed.

Data availability statement All data relevant to the study are included in the article or uploaded as supplementary information.

REFERENCES

1 Koyama Y, Brenner DA. Liver inflammation and fibrosis. *J Clin Invest* 2017;127:55–64.
2 Nagy LE, Ding W-X, Cresci G, *et al*. Linking Pathogenic Mechanisms of Alcoholic Liver Disease With Clinical Phenotypes. *Gastroenterology* 2016;150:1756–68.
3 Luedde T, Kaplowitz N, Schwabe RF. Cell death and cell death responses in liver disease: mechanisms and clinical relevance. *Gastroenterology* 2014;147:765–83.
4 Tarrats N, Moles A, Morales A, *et al*. Critical role of tumor necrosis factor receptor 1, but not 2, in hepatic stellate cell proliferation, extracellular matrix remodeling, and liver fibrogenesis. *Hepatology* 2011;54:319–27.
5 Yin M, Wheeler MD, Kono H, *et al*. Essential role of tumor necrosis factor alpha in alcohol-induced liver injury in mice. *Gastroenterology* 1999;117:942–52.
6 Brenner D, Blaser H, Mak TW. Regulation of tumour necrosis factor signalling: live or let die. *Nat Rev Immunol* 2015;15:362–74.
7 Wang L, Du F, Wang X. TNF-α Induces Two Distinct Caspase-8 Activation Pathways. *Cell* 2008;133:693–703.
8 Bertrand MJM, Milutinovic S, Dickson KM, *et al*. cIAP1 and cIAP2 facilitate cancer cell survival by functioning as E3 ligases that promote RIP1 ubiquitination. *Mol Cell* 2008;30:689–700.
9 Hitomi J, Christofferson DE, Ng A, *et al*. Identification of a molecular signaling network that regulates a cellular necrotic cell death pathway. *Cell* 2008;135:1311–23.
10 He S, Wang L, Miao L, *et al*. Receptor interacting protein kinase-3 determines cellular necrotic response to TNF-alpha. *Cell* 2009;137:1100–11.
11 Cho YS, Challa S, Moquin D, *et al*. Phosphorylation-Driven assembly of the RIP1-RIP3 complex regulates programmed necrosis and virus-induced inflammation. *Cell* 2009;137:1112–23.
12 Zhang D-W, Shao J, Lin J, *et al*. RIP3, an energy metabolism regulator that switches TNF-induced cell death from apoptosis to necrosis. *Science* 2009;325:332–6.
13 Feng S, Yang Y, Mei Y, *et al*. Cleavage of RIP3 inactivates its caspase-independent apoptosis pathway by removal of kinase domain. *Cell Signal* 2007;19:2056–67.
14 Feoktistova M, Geserick P, Kellert B, *et al*. cIAPs block Ripoptosome formation, a RIP1/caspase-8 containing intracellular cell death complex differentially regulated by cFLIP isoforms. *Mol Cell* 2011;43:449–63.
15 Tenev T, Bianchi K, Darding M, *et al*. The RIPoptosome, a signaling platform that assembles in response to genotoxic stress and loss of IAPs. *Mol Cell* 2011;43:432–48.
16 Lang PA, Contaldo C, Georgiev P, *et al*. Aggravation of viral hepatitis by platelet-derived serotonin. *Nat Med* 2008;14:756–61.
17 Wohlleber D, Kashkar H, Gärtner K, *et al*. Tnf-Induced target cell killing by CTL activated through cross-presentation. *Cell Rep* 2012;2:478–87.
18 Guidotti LG, Inverso D, Sironi L, *et al*. Immunosurveillance of the liver by intravascular effector CD8(+) T cells. *Cell* 2015;161:486–500.
19 Bagni C, Tassone F, Neri G, *et al*. Fragile X syndrome: causes, diagnosis, mechanisms, and therapeutics. *J Clin Invest* 2012;122:4314–22.
20 Martin JP, Bell J. A pedigree of mental defect showing sex-linkage. *J Neurol Psychiatry* 1943;6:154–7.
21 Fu YH, Kuhl DP, Pizzuti A, *et al*. Variation of the CGG repeat at the fragile X site results in genetic instability: resolution of the Sherman paradox. *Cell* 1991;67:1047–58.
22 Pieretti M, Zhang FP, Fu YH, *et al*. Absence of expression of the FMR-1 gene in fragile X syndrome. *Cell* 1991;66:817–22.
23 Bakker CE. Fmr1 knockout mice: a model to study fragile X mental retardation. The Dutch-Belgian fragile X Consortium. *Cell* 1994;78:23–33.
24 Ascano M, Mukherjee N, Bandaru P, *et al*. FMRP targets distinct mRNA sequence elements to regulate protein expression. *Nature* 2012;492:382–6.
25 Pasciuto E, Bagni C. Snapshot: FMRP mRNA targets and diseases. *Cell* 2014;158:1446–6.
26 Darnell JC, Van Driesche SJ, Zhang C, *et al*. Fmrp stalls ribosomal translocation on mRNAs linked to synaptic function and autism. *Cell* 2011;146:247–61.
27 Lucá R, Averna M, Zalfa F, *et al*. The fragile X protein binds mRNAs involved in cancer progression and modulates metastasis formation. *EMBO Mol Med* 2013;5:1523–36.
28 Xu D, Jin T, Zhu H, *et al*. Tbk1 suppresses RIPK1-Driven apoptosis and inflammation during development and in aging. *Cell* 2018;174:1477–91.
29 Mi H, Muruganujan A, Casagrande JT, *et al*. Large-Scale gene function analysis with the panther classification system. *Nat Protoc* 2013;8:1551–66.
30 Thomas PD, Campbell MJ, Kejariwal A, *et al*. Panther: a library of protein families and subfamilies indexed by function. *Genome Res* 2003;13:2129–41.
31 Wherry EJ. T cell exhaustion. *Nat Immunol* 2011;12:492–9.
32 Pfeffer K, Matsuyama T, Kündig TM, *et al*. Mice deficient for the 55 kD tumor necrosis factor receptor are resistant to endotoxic shock, yet succumb to L. monocytogenes infection. *Cell* 1993;73:457–67.
33 Ram DR, Ilyukha V, Volkova T, *et al*. Balance between short and long isoforms of cFLIP regulates Fas-mediated apoptosis in vivo. *Proc Natl Acad Sci U S A* 2016;113:1606–11.
34 Dantzer F, Amé J-C, Schreiber V, *et al*. Poly(ADP-ribose) polymerase-1 activation during DNA damage and repair. *Methods Enzymol* 2006;409:493–510.
35 Boulares AH, Yakovlev AG, Ivanova V, *et al*. Role of poly(ADP-ribose) polymerase (PARP) cleavage in apoptosis. Caspase 3-resistant PARP mutant increases rates of apoptosis in transfected cells. *J Biol Chem* 1999;274:22932–40.
36 Kamata H, Honda S-I, Maeda S, *et al*. Reactive oxygen species promote TNFalpha-induced death and sustained JNK activation by inhibiting MAP kinase phosphatases. *Cell* 2005;120:649–61.
37 Das M, Sabio G, Jiang F, *et al*. Induction of hepatitis by JNK-mediated expression of TNF-alpha. *Cell* 2009;136:249–60.
38 Deng Y, Ren X, Yang L, *et al*. A JNK-dependent pathway is required for TNFα-induced apoptosis. *Cell* 2003;115:61–70.
39 Chang L, Kamata H, Solinas G, *et al*. The E3 ubiquitin ligase itch couples JNK activation to TNFalpha-induced cell death by inducing c-FLIP(L) turnover. *Cell* 2006;124:601–13.
40 Xue L, Igaki T, Kuranaga E, *et al*. Tumor suppressor CYLD regulates JNK-induced cell death in Drosophila. *Dev Cell* 2007;13:446–54.
41 Massoumi R, Chmielarska K, Hennecke K, *et al*. Cyld inhibits tumor cell proliferation by blocking Bcl-3-dependent NF-kappaB signaling. *Cell* 2006;125:665–77.
42 Zhang J, Stirling B, Temmerman ST, *et al*. Impaired regulation of NF-kappaB and increased susceptibility to colitis-associated tumorigenesis in CYLD-deficient mice. *J Clin Invest* 2006;116:3042–9.
43 Murphy JM, Czabotar PE, Hildebrand JM, *et al*. The pseudokinase MLKL mediates necroptosis via a molecular switch mechanism. *Immunity* 2013;39:443–53.
44 Ofengeim D, Yuan J. Regulation of RIP1 kinase signalling at the crossroads of inflammation and cell death. *Nat Rev Mol Cell Biol* 2013;14:727–36.
45 Liu Y, Zhu X, Zhu J, *et al*. Identification of differential expression of genes in hepatocellular carcinoma by suppression subtractive hybridization combined cDNA microarray. *Oncol Rep* 2007;18:943–51.
46 Yuan J, Amin P, Ofengeim D. Necroptosis and RIPK1-mediated neuroinflammation in CNS diseases. *Nat Rev Neurosci* 2019;20:19–33.
47 He P, Zhong Z, Lindholm K, *et al*. Deletion of tumor necrosis factor death receptor inhibits amyloid β generation and prevents learning and memory deficits in Alzheimer's mice. *J Cell Biol* 2007;178:829–41.
48 Ofengeim D, Mazzitelli S, Ito Y, *et al*. RIPK1 mediates a disease-associated microglial response in Alzheimer's disease. *Proc Natl Acad Sci U S A* 2017;114:E8788–E8797.
49 Caccamo A, Branca C, Piras IS, *et al*. Necroptosis activation in Alzheimer's disease. *Nat Neurosci* 2017;20:1236–46.
50 Ito Y, Ofengeim D, Najafov A, *et al*. RIPK1 mediates axonal degeneration by promoting inflammation and necroptosis in ALS. *Science* 2016;353:603–8.
51 Habbas S, Santello M, Becker D, *et al*. Neuroinflammatory TNFα impairs memory via astrocyte signaling. *Cell* 2015;163:1730–41.
52 Odeh M, Sabo E, Srugo I, *et al*. Relationship between tumor necrosis factor-alpha and ammonia in patients with hepatic encephalopathy due to chronic liver failure. *Ann Med* 2005;37:603–12.

Supplementary Figure 1

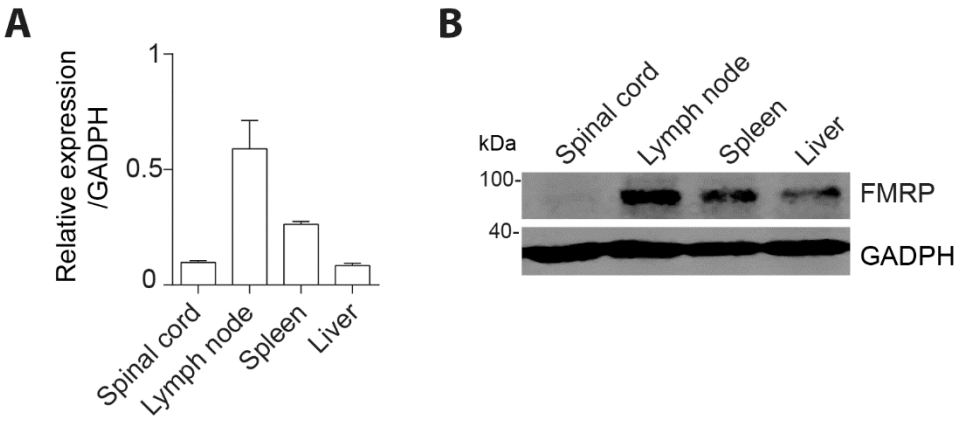

Supplemental Figure 1: FMRP is expressed in spinal cord, lymph node, spleen and liver tissue. (A) Tissue samples were harvested from indicated organs from C57BL/6J mice and homogenized followed by RNA isolation. *Fmr1* gene expression was quantified using RT-PCR (n=3). **(B)** Tissue samples were isolated from indicated organs and lysates were subjected to Western blot analysis and probed for FMRP (one representative immunoblot of n=3 is shown). Error bar in all graphs indicate SEM.

Supplementary Figure 2

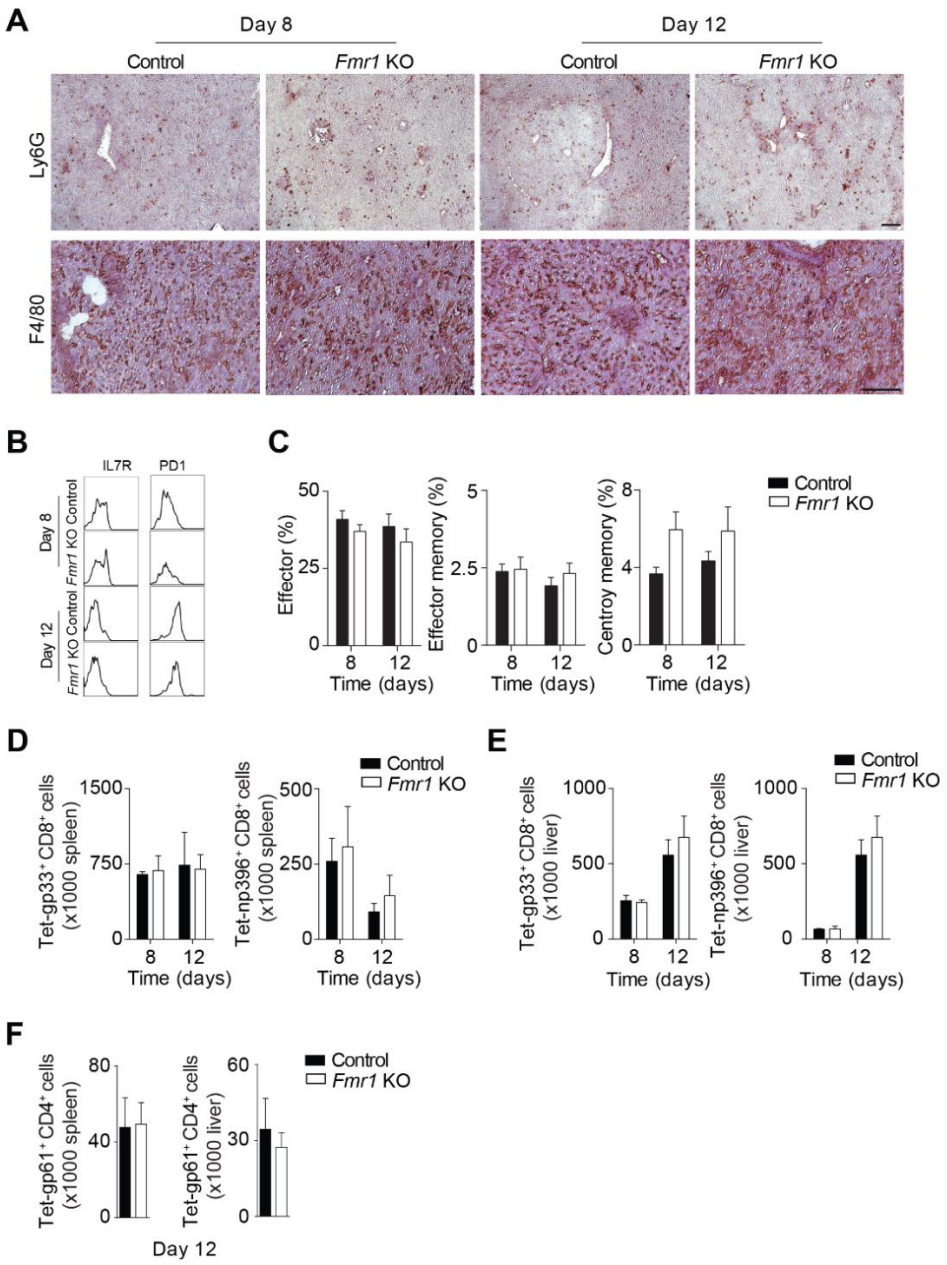

Supplemental Figure 2: FMRP is dispensable for hepatic immune cell infiltration and anti-viral T cell immunity during LCMV infection. (**A**) Sections of snap frozen liver tissue harvested from control and *Fmr1*^{null} (*Fmr1* KO) mice were stained for anti-F4/80, anti-Ly6G (Gr1) (one representative set of n=3 is shown, scale bar=50µm). (**B**) Expression of IL7R and PD1 surface markers were measured on Gp33 specific T cells in control and *Fmr1*^{null} mice at indicated time points after infection (n=7-8). (**C**) Analysis of effector (CD62-L^{-}IL7-R^{-}KLRG-1^{+}), effector memory (CD62-L^{-}L7-R^{+}KLRG-1^{-}) and central memory (CD62-L^{+}IL7-R^{+}KLRG-1^{-}) T cell response was carried out in control and *Fmr1*^{null} mice at indicated time points after infection (n=7-8). (**D-E**) Anti-viral T cell responses were measured in spleen (D) and liver (E) of control and *Fmr1*^{null} mice using T cell specific tetramers as indicated post infection (n=5-6). (**F**) Anti-viral CD4^{+} T cell responses were measured in spleen and liver of control and *Fmr1*^{null} mice using T cell specific tetramers as indicated at day 12 after infection (n=5-6). Error bar in all graphs indicate SEM.

Supplementary Figure 3

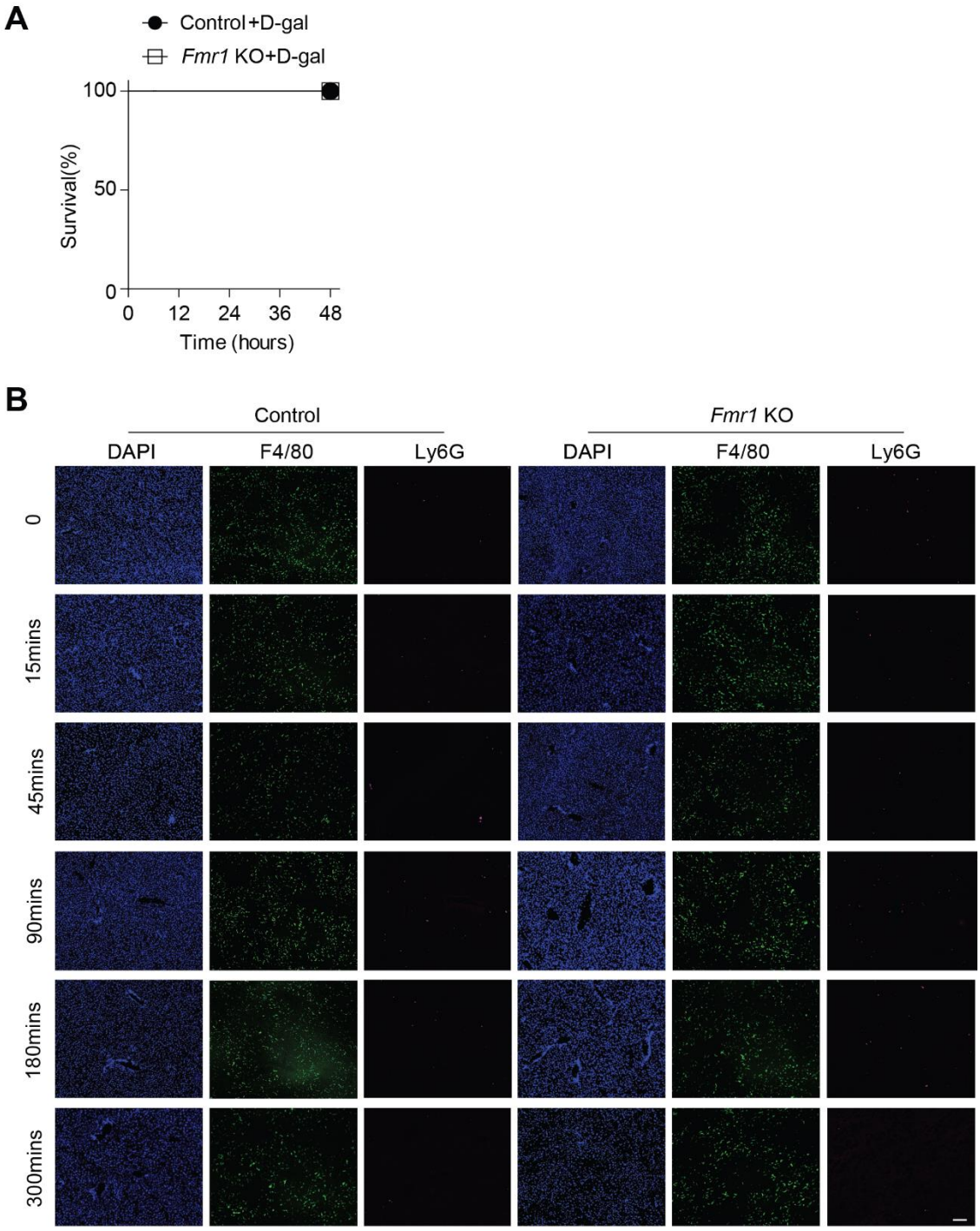

Supplemental Figure 3: FMRP is dispensable for macrophage or granulocyte infiltration following TNF treatment. **(A)** Survival of control and *Fmr1*^{null} (*Fmr1* KO) mice was monitored after treatment with D-Gal (10mg/mouse, n=4). **(B)** Sections of snap frozen liver tissue were stained for anti-F4/80 and anti-Ly6G at indicated time points after TNFα/D-Gal treatment (n=3-5, scale bar=50µm).

Supplementary Figure 4

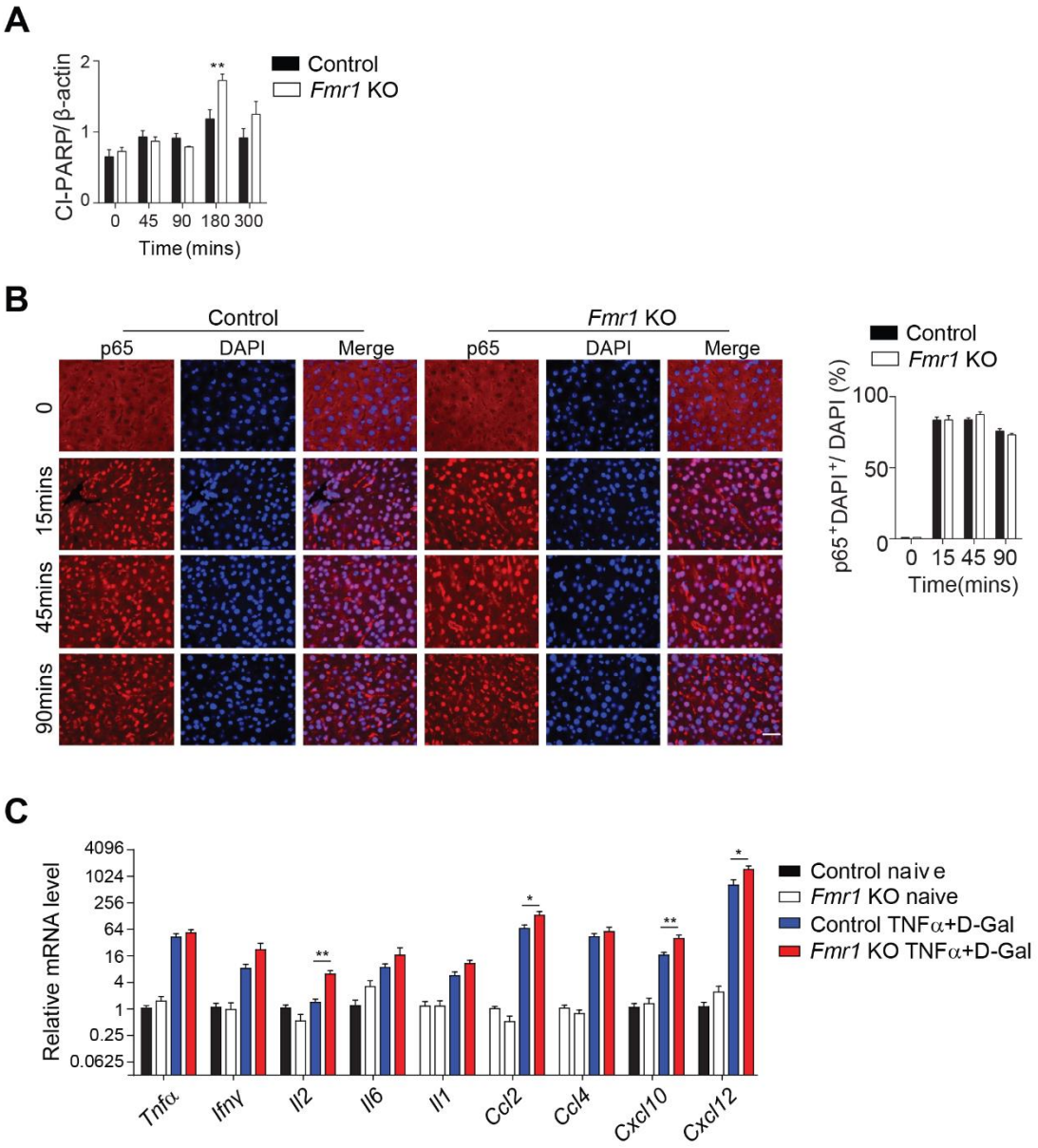

Supplemental Figure 4: FMRP affects cleavage of PARP but not nuclear translocation of p65. (A) Liver tissue homogenates harvested from control and *Fmr1*^{null} (*Fmr1* KO) mice were probed for expression of cleaved PARP at the indicated time points as shown in Figure 4B (n=3). **(B)** Sections of snap frozen liver tissue were stained for p65 and DAPI at indicated time points after TNFα/D-Gal treatment (one representative set of n=3 is shown, scale bar=100μm). Graph indicates p65^{+}DAPI^{+}/DAPI^{+} (n=3). **(C)** Expression of NF-κB pathway genes was quantified in control and *Fmr1*^{null} mice at 3 hours after D-Gal/rTNF treatment (n=4-5). Error bar in all graphs indicate SEM. **P* < 0.05, ***P* < 0.01.

Supplementary Figure 5

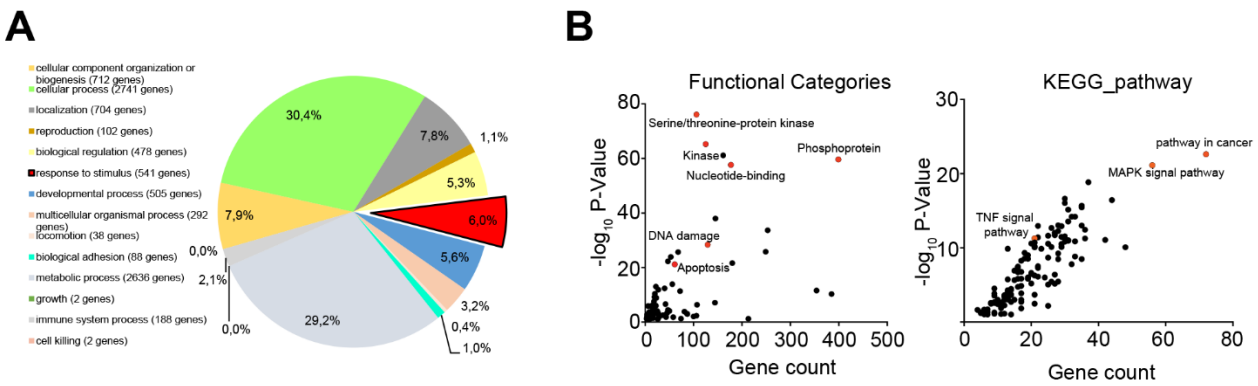

Supplemental Figure 5: Genes involved in TNF signaling exhibit FMRP binding sites. (A) Pie chart showing the percentage of gene enrichment analysis derived from the publically available FMR1 PAR-CLIP data *(6)*. **(B)** Genes in the 'response to stimulus' section from (A) were further analysed using DAVID for functional categories and KEGG pathways. Gene counts were plotted on the x-axis and corresponding p-values on the y-axis.

Supplementary Figure 6

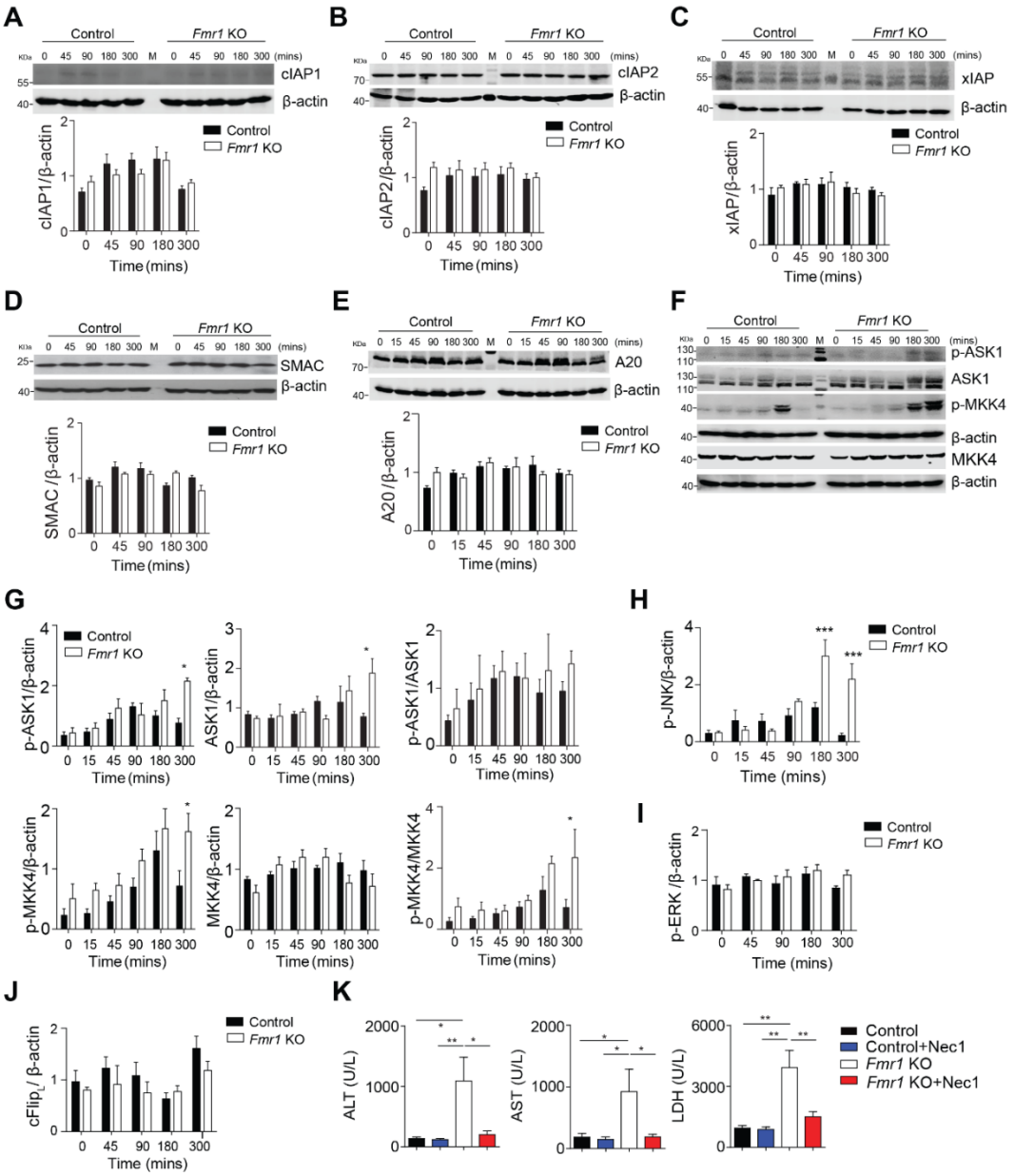

Supplemental Figure 6: Altered TNF mediated signaling in absence of FMRP. (A-J) Liver lysates harvested from control and *Fmr1*^{null} (*Fmr1* KO) mice at indicated time points after D-Gal (10mg/mouse) and TNFα treatment (100ng/mouse) were assessed for expression of cell death and survival related proteins. **(A)** cIAP1, **(B)** cIAP2, **(C)** xIAP, **(D)** SMAC, and **(E)** A20 is shown. Bottom panels indicate quantification (n=3). **(F)** Lysates were assessed for expression of proteins involved in the MAPK pathway including total and phosphorylated ASK1, MKK4. **(G)** Quantitative analysis of the western blots from F (n=3). **(H)** Quantitative analysis of p-JNK from main Figure 5C (n=3). **(I)** Quantitative analysis of p-ERK from main Figure 5D (n=3). **(J)** Quantitative analysis of FLIP$_L$ (long form) from main Figure 5E (n=3). (**K**) ALT, AST and LDH activities were measured in serum samples of control and *Fmr1*^{null} mice and Necrostatin-1 treated control and *Fmr1*^{null} mice 5h post D-Gal/rTNF treatment (n=6-9). Error bar in all graphs indicate SEM. **P* < 0.05; ***P* < 0.01.

Supplementary Figure 7

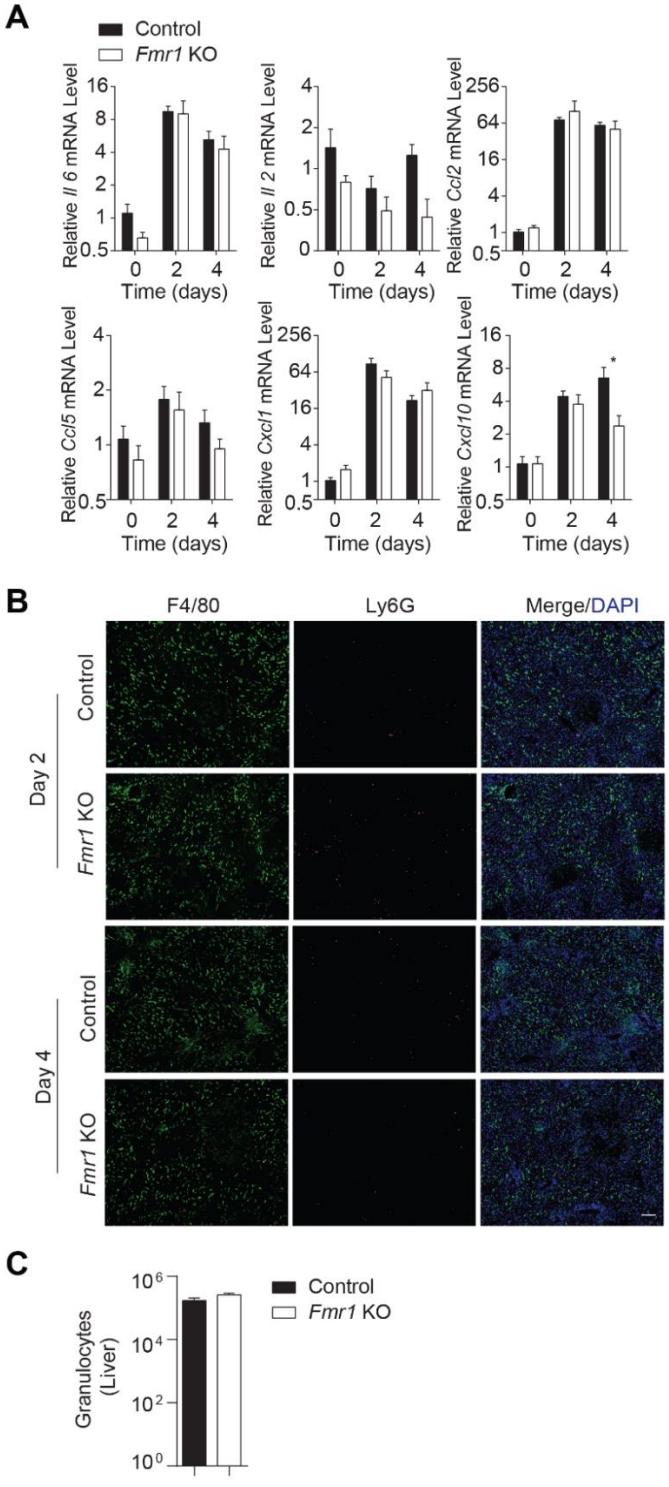

Supplemental Figure 7: Hepatic immune cell infiltration during BDL is similar in absence or presence of FMRP. (A) Cytokines and chemokines were quantified using RT-PCR in control and *Fmr1*^{null} (*Fmr1* KO) mice at indicated time points after BDL (n=4-7). **(B)** Sections of snap frozen liver tissue harvested from control and *Fmr1*^{null} mice were stained with anti-F4/80 and anti-Ly6G at indicated time points following BDL (n=5-7, scale bar=50µm). **(C)** Granulocytes (Ly6G^{+}) were measured in liver tissue of control and *Fmr1*^{null} mice 1 day after BDL by flow cytometry (n=3). Error bar in all graphs indicate SEM; **P* < 0.05.

Supplementary Figure 8

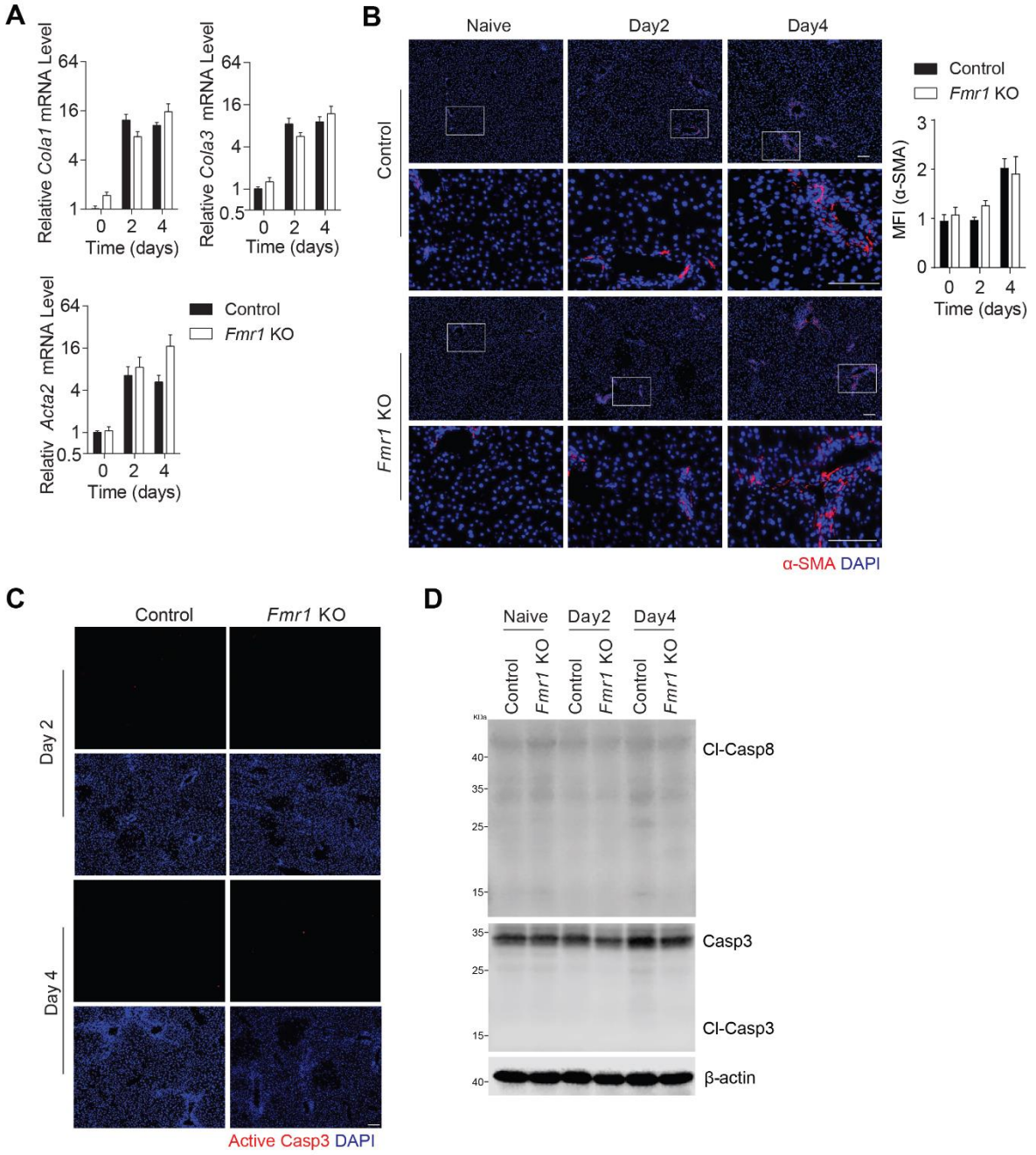

Supplemental Figure 8: FMRP is dispensable for liver fibrosis during early time points after BDL. (A) Fibrosis markers were quantified using RT-PCR in control and *Fmr1*^{null} (*Fmr1* KO) mice at indicated time points after BDL (n=4-7). **(B)** Sections of snap frozen liver tissue harvested from control and *Fmr1*^{null} mice were stained for αSMA expression at indicated time points following BDL (n=3, scale bar=50µm). Right panel indicates the quantification. (**C**) Sections of liver tissue from control and *Fmr1*^{null} mice were stained for active caspase-3 (n=3, scale bar=50µm). (**D**) Liver tissue homogenates from control and *Fmr1*^{null} mice were assessed for expression of cleaved-caspase-8 and caspase-3 at indicated time points post BDL (n=4). Error bar in all graphs indicate SEM.

Supplementary Figure 9

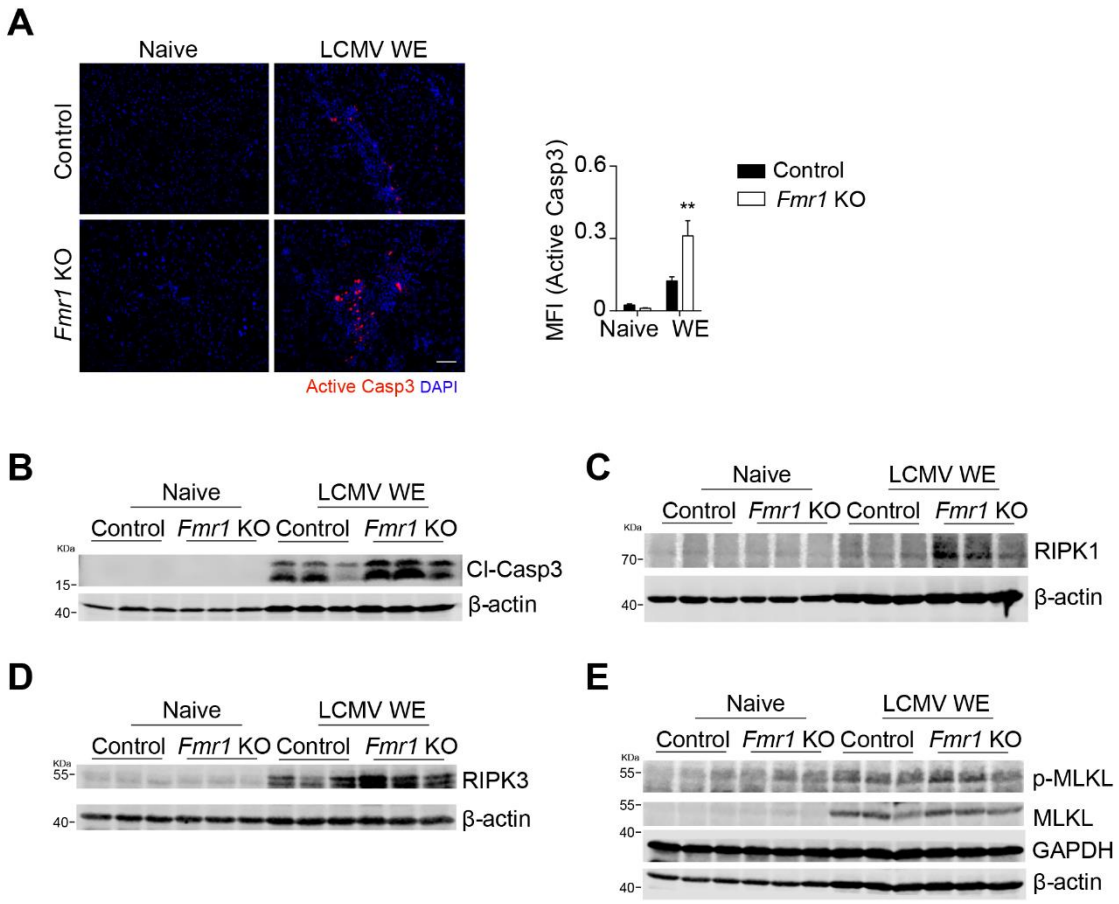

Supplemental Figure 9: Increased presence of cleaved-Casp3, RIPK1, RIPK3 and p-MLKL in *Fmr1*^{nul} mice following LCMV infection. (A-E) Control and *Fmr1*^{null} (*Fmr1* KO) mice were infected with 2x10^6 pfu of LCMV WE. **(A)** Sections of liver tissue from control and *Fmr1*^{null} (*Fmr1* KO) mice were stained for active caspase-3 after 12 days of infection (n=3, scale bar=100µm). Right panel indicates quantification. **(B-E)** Liver tissue homogenates from control and *Fmr1*^{null} mice 12 days after infection were assessed for expression of cleaved-caspase-3 (B), RIPK1 (C), RIPK3 (D) and p-MLKL and MLKL (E). Blots show n=3. Error bar in all graphs indicate SEM. $^{**}P < 0.01$.

2.2 B Cell-Mediated Maintenance of Cluster of Differentiation 169-Positive Cells Is Critical for Liver Regeneration

HEPATOLOGY

HEPATOLOGY, VOL. 68, NO. 6, 2018

LIVER INJURY/REGENERATION

B Cell-Mediated Maintenance of Cluster of Differentiation 169–Positive Cells Is Critical for Liver Regeneration

Kristina Behnke,[1*] Yuan Zhuang,[1*] Haifeng C. Xu,[1] Balamurugan Sundaram,[1] Maria Reich,[2] Prashant V. Shinde,[1] Jun Huang,[1] Nastaran Fazel Modares,[3] Alexei V. Tumanov,[4] Robin Polz,[3] Jürgen Scheller,[3] Carl F. Ware,[5] Klaus Pfeffer,[6] Verena Keitel,[2] Dieter Häussinger,[2] Aleksandra A. Pandyra,[1] Karl S. Lang,[7**] and Philipp A. Lang[1**]

The liver has an extraordinary capacity to regenerate through activation of key molecular pathways. However, central regulators controlling liver regeneration remain insufficiently studied. Here, we show that B cell–deficient animals failed to induce sufficient liver regeneration after partial hepatectomy (PHx). Consistently, adoptive transfer of B cells could rescue defective liver regeneration. B cell–mediated lymphotoxin beta production promoted recovery from PHx. Absence of B cells coincided with loss of splenic cluster of differentiation 169–positive ($CD169^+$) macrophages. Moreover, depletion of $CD169^+$ cells resulted in defective liver regeneration and decreased survival, which was associated with reduced hepatocyte proliferation. Mechanistically, $CD169^+$ cells contributed to liver regeneration by inducing hepatic interleukin-6 (IL-6) production and signal transducer and activator of transcription 3 activation. Accordingly, treatment of $CD169^+$ cell–depleted animals with IL-6/IL-6 receptor rescued liver regeneration and severe pathology following PHx. *Conclusion:* We identified $CD169^+$ cells to be a central trigger for liver regeneration, by inducing key signaling pathways important for liver regeneration. (HEPATOLOGY 2018;68:2348-2361).

Liver disease is a global health problem with millions of patients worldwide suffering from infections, toxic liver damage, and hepatocellular carcinoma. Liver tissue has an extraordinary potential to regenerate, an effect already described in Greek mythology. Since then, several key molecular pathways have been discovered to play important roles during liver regeneration, including nuclear factor kappa B, signal transducer and activator of transcription 3 (STAT3), and extracellular signal–regulated kinase (Erk).[1] Following 70% reduction of liver mass through partial hepatectomy (PHx), tumor necrosis factor (TNF) is rapidly produced, and TNF receptor 1 (TNFR1) signaling is required to induce liver regeneration.[2] Furthermore, the TNF superfamily members lymphotoxin (Lt) alpha and beta play a critical role during liver regeneration.[3,4] Consistently, mice deficient for both TNFRp55 and

Abbreviations: ALT, alanine aminotransferase; AST, aspartate aminotransferase; BAFFR, B cell–activating factor receptor; CD169, cluster of differentiation 169; ΔCt, Delta cycle threshold; DT, diphtheria toxin; DTR, DT receptor; EGFR, epidermal growth factor receptor; Erk, extracellular signal–regulated kinase; H&E, hematoxylin and eosin; IκBα, inhibitor of kappa B alpha; IL-6, interleukin 6; IL-6R, IL-6 receptor; Jh, joining heavy chain; Lt, lymphotoxin; LtβR, Ltβ receptor; PCNA, proliferating cell nuclear antigen; PHx, partial hepatectomy; phospho-H3, phospho-histone H3; Stat3, signal transducer and activator of transcription 3; TGFβ, transforming growth factor beta; TNFα, tumor necrosis factor alpha; TUNEL, terminal deoxynucleotidyl transferase–mediated deoxyuridine triphosphate nick-end labeling; WT, wild type.

Received September 25, 2017; accepted May 7, 2018.

Additional Supporting Information may be found at onlinelibrary.wiley.com/doi/10.1002/hep.30088/suppinfo.

**These authors contributed equally to this work.*

***These authors contributed equally to this work.*

Supported by the German Research Council (SFB974, KFO217, LA-2558/5-1), by the Jürgen Manchot Graduate School MOI III and by US NIH grant R01AI067890.

View this article online at wileyonlinelibrary.com.

DOI 10.1002/hep.30088

Potential conflict of interest: Nothing to report.

Ltβ receptor (LtβR) show delayed hepatocyte proliferation and impaired survival following PHx.[5] Furthermore, a marked increase in interleukin-6 (IL-6) concentrations in the serum can be detected following loss of liver mass, and IL-6-deficient mice show delayed liver regeneration following PHx.[6-8] Consistently, treatment with combined IL-6 and soluble IL-6 receptor (IL-6R) can improve liver regeneration and induce rapid hepatocyte proliferation.[6,9] Moreover, epidermal growth factor receptor (EGFR) ligands including transforming growth factor alpha (TGF-α) and amphiregulin are able to induce hepatocyte proliferation *in vitro*.[1,10] However, TGF-α-deficient animals exhibit normal recovery following PHx.[11] In turn, amphiregulin-deficient animals show delayed proliferation following loss of liver mass.[12] Consistently, specific deletion of EGFR in hepatocytes resulted in decreased liver regeneration following PHx.[13] Notably, TNF levels were strikingly increased in $EGFR^{\Delta HEP}$ animals following PHx, suggesting that factors important for liver regeneration can compensate for each other.[13] The central, key players during liver regeneration, however, remain insufficiently studied.

The spleen is tightly connected to the liver with important blood circuits. Receiving its blood from the splenic artery, it feeds through the splenic vein after joining of the arteria mesenteria inferior and superior into the portal vein. Hence, cytokines and chemokines produced in the spleen can act directly on the liver. The spleen itself is organized into red and white pulp, with the separating marginal zone including the marginal sinus in between.[14,15] B cells account for about 50% of all cells in the spleen and are located in the white pulp and the marginal zone.[14] B cells are critical for organization of the lymphoid tissue as B cell–deficient mice exhibit reduced presence of metallophilic cluster of differentiation 169–positive ($CD169^+$) macrophages.[16] $CD169^+$ cells are located along the marginal sinus and ideally situated to capture pathogens.[14,17] Interestingly, maintenance of $CD169^+$ cells depends on Ltα and Ltβ.[18-20] Specifically, B cell–specific and T cell–specific, Ltβ-deficient mice exhibit reduction of $CD169^+$ cells in the spleen.[18,19] Moreover, as spleen-resident macrophages, $CD169^+$ cells can contribute to cytokine production during inflammation and infection.[21-23] However, the contributions of B cells and $CD169^+$ cells during liver regeneration remain insufficiently characterized.

In this study, we identified B cells and $CD169^+$ cells as important players in liver regeneration following PHx. Specifically, genetic B-cell deficiency resulted in reduced signaling cascades required for hepatocyte proliferation and limited survival following PHx. B cell–deficient mice exhibited reduced presence of $CD169^+$ cells, which were critical for liver regeneration. Depletion of $CD169^+$ cells resulted in reduced IL-6 expression and reduced regeneration following PHx. Consistently, treatment of $CD169^+$ cell–depleted animals with IL-6/IL-6R could rescue the severe pathology we observed in our setting.

Materials and Methods

ANIMALS

This study was carried out in accordance with the German Animal Welfare Act and the guidelines of Shoochow University. The protocol was approved by

ARTICLE INFORMATION:

From the [1]Department of Molecular Medicine II, Medical Faculty; [2]Department of Gastroenterology, Hepatology, and Infectious Diseases and; [3]Institute of Biochemistry and Molecular Biology II, Medical Faculty, Heinrich Heine University, Düsseldorf, Germany; [4]Department of Microbiology, Immunology & Molecular Genetics, University of Texas Health Science Center, San Antonio, TX; [5]Infectious and Inflammatory Diseases Research Center, Sanford Burnham Prebys Medical Discovery Institute, La Jolla, CA; [6]Institute of Medical Microbiology and Hospital Hygiene, University Hospital, Heinrich Heine University, Düsseldorf, Germany; [7]Institute of Immunology, Medical Faculty, University of Duisburg-Essen, Essen, Germany.

ADDRESS CORRESPONDENCE AND REPRINT REQUESTS TO:

Philipp A. Lang, M.D., Ph.D.
Department of Molecular Medicine II, Medical Faculty
Heinrich Heine University
Universitätsstr. 1
40225 Düsseldorf, Germany
E-mail: langp@uni-duesseldorf.de
Tel: +49-2118113580

the local authorities. B cell–activating factor receptor–negative (*Baffr*$^{-/-}$), joining heavy chain–negative (*Jh*$^{-/-}$), *CD169-DTR* (diphtheria toxin [DT] receptor) mice have been described and were kept on a C57Bl/6 background.[18,24,25] Laparotomy was performed predominantly on male mice at 10-14 weeks of age using isoflurane inhalation narcosis, as described.[26] For PHx the left lateral and the left and right median liver lobes together with the gallbladder were excised subsequent to a one-step ligature using a 5-0 suture tie (Ethicon, Somerville, NJ).[5] Sham operations were performed in an identical manner without ligating and removing liver lobes. For splenectomy, the splenic artery and vein were ligated with a single-knot 5-0 suture at the same time as PHx or otherwise indicated in the figure legends. Next, connective tissue and spleen were removed. After irrigating the abdomen with 0.9% NaCl, both abdominal layers were closed with a running 5-0 suture (Ethicon).[26] Directly after surgery and 24 and 48 hours post-PHx mice received 5 mg/kg carprofen (Rimadyl; Pfizer, Würselen, Germany). As expected, splenectomized animals did not show any sign of pathology (Fig. 1A). Mice exhibiting severe disease symptoms were

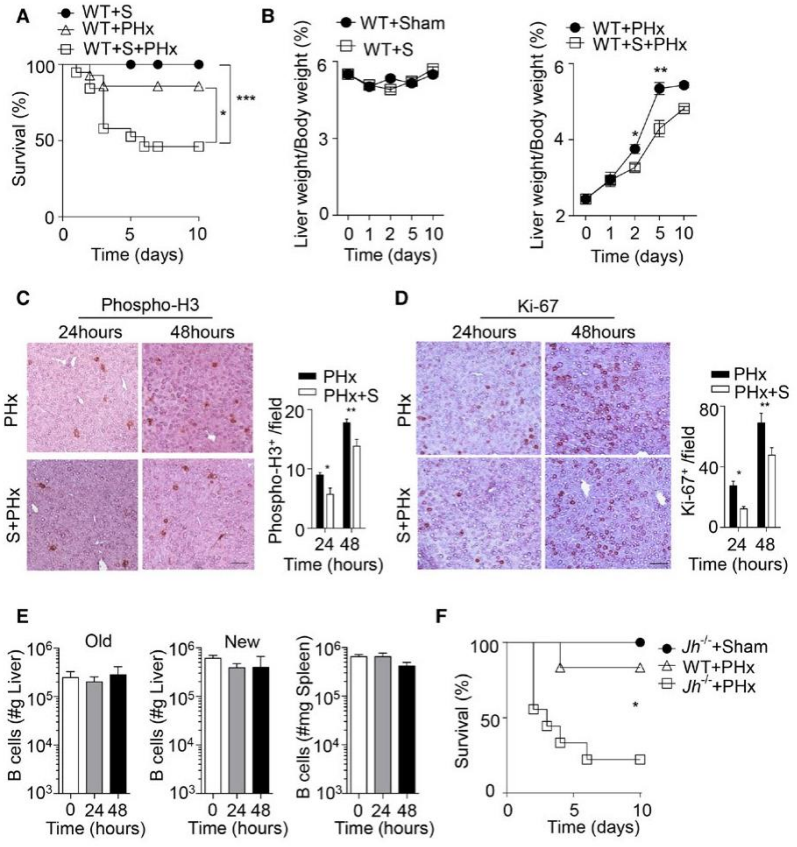

FIG. 1. Decreased liver regeneration in splenectomized and B cell–deficient mice following PHx. (A) Survival of splenectomized, 70% PHx, and splenectomized mice followed by PHx (PHx+S) was monitored (n = 14-19). (B) The liver weight/body weight ratio was determined at the indicated time points in WT sham-operated mice and splenectomized mice (left panel) and in PHx WT mice and splenectomized mice (PHx+S) (right panel) (n = 3-5). (C,D) Sections of snap-frozen liver tissue from 70% PHx and splenectomized mice followed by PHx (PHx+S) at the indicated time points were stained with (C) anti-phospho-H3 and (D) anti-Ki-67 antibodies. Representative sections for each time point are shown (n = 4; scale bar, 100 μm). Right panels indicate quantification. (E) B-cell numbers were determined by flow cytometry in the newly regenerated ("New," n = 7-8) and remaining ("Old," n = 3-4) liver lobes and spleen tissue (n = 7-8) at indicated time points after 70% PHx. Results were calculated according to the liver (grams) and spleen (milligrams) weights. (F) Survival of *Jh*$^{-/-}$ mice (n = 9) after 70% PHx compared to sham-operated *Jh*$^{-/-}$ mice (n = 3) and WT mice (n = 6). Error bars in all experiments represent SEM; $^{*}P < 0.05$, $^{**}P < 0.01$, $^{***}P < 0.001$. Abbreviation: S, splenectomy.

sacrificed and considered as dead. CD169$^+$ cells in the *CD169-DTR* animals were depleted by injecting two doses of 100 ng DT (Sigma) before the PHx. Wild-type (WT; C57Bl/6) mice were used as controls. Mice were 10-14 weeks old. For blood and tissue collection mice were anesthetized (100 mg/kg ketamine, 10 mg/kg xylazine; Vétoquinol GmbH, Ravensburg, Germany), weighed, and bled through the vena cava inferior; and serum was collected. The liver and spleen were removed, rinsed in phosphate-buffered saline (PBS), and weighed to calculate the liver weight to body weight ratio and the spleen weight. Liver and spleen samples were stored at −80 ˚C for histology and RNA and protein extraction.

LtβR ANTIBODY TREATMENT AND IL-6/IL-6R INJECTION

In order to induce LtβR signaling, mice were intraperitoneally injected with two doses of 200 μg LtβR antibody agonist (clone 4H8) 24 hours before and 24 hours after PHx.[27] DT-treated CD169-DTR mice were injected with two doses of 20 μg IL-6/IL-6R protein 24 hours before and immediately after PHx.

PURIFICATION OF B CELLS

For B-cell purification, single-cell suspensions of splenocytes were enriched following the manufacturer's instructions with a CD45R (B220) MicroBeads mouse kit (Miltenyi).

HISTOLOGY

Histological analysis on snap-frozen tissue (liver, spleen) was performed with hematoxylin and eosin (H&E) stain (Sigma-Aldrich, St. Louis, MO) and terminal deoxynucleotidyl transferase–mediated deoxyuridine triphosphate nick-end labeling (TUNEL; Roche). Snap-frozen tissue sections were stained with antibodies: CD169 (clone MOMA-1; ABD Serotec, Dusseldorf, Germany), B220 (eBioscience, San Diego, CA), Ki-67 (Abcam), phospho-histone H3 (phospho-H3; Millipore).

FLOW-CYTOMETRIC ANALYSIS

Different immune populations were identified in single-cell solutions from naive liver and spleen samples and spleen and liver samples newly regenerated (“new”) and remaining lobes (“old”) 24 and 48 hours after PHx using anti-B220, anti-CD21, anti-CD23, anti–progammed death ligand 1, anti-NK1.1, anti-CD3, anti-CD19, anti-CD11b, anti-Siglec-H, anti-CD8a, and anti-CD11c antibodies; anti–major histocompatibility complex class II; and anti-CD40, anti-CD80, anti-CD86, anti-F4/80, anti-Ly6C, anti-CD138, anti–immunoglobulin M, anti-CD38, anti-CD62L, anti-CD5, anti-IgD, anti-CD1d antibodies, and 7-amino-actinomycin D. All antibodies were obtained from eBioscience, except anti-CD169 (3D6.112), which was obtained from AbD Serotec. For quantification of cell populations, calibration beads were added to assess cell numbers (BD, San Diego, CA).

SERUM BIOCHEMISTRY

Aspartate aminotransferase (AST) and alanine aminotransferase (ALT) were measured using the automated biochemical analyzer Spotchem EZ SP-4430 (Arkray, Amstelveen, The Netherlands) and the Spotchem EZ Reagent Strips Liver-1.

QUANTITATIVE RT-PCR

RNA purification and RT-PCR analyses of liver and spleen were performed according to the manufacturer’s instructions (TRIzol reagent and iTaq Universal probes or SYBR Green One-Step Kit; BioRad). Expression of *Ltα*, *Ltβ*, *IL-6*, and *TNFα* was determined with fluorescein amidite probes (Applied Biosystems). Expression levels of other genes were tested using the following primer sequences: Egf_F, AGAAGGCTACGAAGGAGACG; Egf_R, AGAGTCAGGGCAACTCAGTC; Hbegf_F, GCAAATGCCTCCCTGGTTAC; Hbegf_R, GGACGACAGTACTACAGCCA; Areg_F, GCGAGGATGACAAGGACCTA; Areg_R, TCGTTTCCAAAGGTGCACTG; Tgfa_F, GCTCTGGAGAACAGCACATC; Tgfa_R, ACATGCTGGCTTCTCTTCCT; Tgfb1_F, TTGCTTCAGCTCCACAGAGA; Tgfb1_R, CAGAAGTTGGCATGGTAGCC; Hgf_F, CCAGAGGTACGCTACGAAGT; Hgf_R, CTGTGTGATCCATGGGACCT; Fgf1_F, CTCGCAGACACCAAATGAGG; Fgf1_R, CTTCTTGAGGCCCACAAACC; Vegfa_F, TTGAGA-

CCCTGGTGGACATC; Vegfa_R, GGGCTTCATCGTTACAGCAG; Vegfb_F, GCCACCAGAAGAAAGTGGTG; Vegfb_R, ATTGCCCATGAGTTCCATGC; Vegfc_F, AGGCAGCTAACAAGACATGTCCAAC; Vegfc_R, GGGTCCACAGACATCATGGAATC; Fgf2_F, GGACGGCTGCTGGCTTCTAA; Fgf2_R, CCAGTTCGTTTCAGTGCCACATAC; Pdgfb_F, ATGAAATGCTGAGCGACCAC; Pdgfb_R, CCCTCGAGATGAGCTTTCC. For analysis, the expression levels of all target genes were normalized to the β-actin expression or glyceraldehyde 3-phosphate dehydrogenase (Delta cycle threshold [ΔCt]). Gene expression values were calculated with the ΔΔCt method, with untreated WT mice as controls to which all other samples were normalized. Relative quantities (RQ) were determined with the equation $RQ = 2^{-\Delta\Delta Ct}$.

IMMUNOBLOTTING

Liver tissue was lysed in PBS containing 1% Triton X-100, protease inhibitors (Sigma), and PhosSTOP (1 tablet/10 mL). Immunoblots were probed with primary antibody: phospho-Stat3, Stat3, phospho-Erk1/2, Erk1/2, inhibitor of kappa B alpha (IκBα), IL-6, proliferating cell nuclear antigen (PCNA), and β-actin (Cell Signalling Technology), followed by secondary antibody and enhanced chemiluminescence detection or fluorescence secondary antibody and detected by a LI-COR imager.

STATISTICAL ANALYSES

Data are expressed as mean ± SEM. Statistically significant differences between two different groups were analyzed using the Student *t* test. Statistically significant differences between groups in experiments involving more than one time point were determined with two-way analysis of variance (repeated measurements). All quantifications were analyzed by ImageJ.

Results

B CELLS ARE IMPORTANT FOR LIVER REGENERATION

Based on previous data describing a beneficial role of the spleen during liver regeneration following PHx in mice,[28] we found that a proportion of splenectomized C57Bl/6 mice developed severe pathology (Fig. 1A; Supporting Fig. S1A). Consistently, the liver weight/body weight ratio following PHx was reduced in the absence of spleen tissue when compared to PHx controls (Fig. 1B).[28] Moreover, the activity of ALT and AST, indicators of liver damage, was markedly increased in the blood of splenectomized mice after PHx compared to PHx only or splenectomy controls (Supporting Fig. S1B). Although splenectomized mice exhibited histological changes in liver tissue, we did not observe a significant increase in TUNEL staining (Supporting Fig. S1C,D). However, staining for proliferation indicators such as Ki-67 and phospho-H3 was reduced in liver tissue of splenectomized animals (Fig. 1C,D; Supporting Fig. S1E). Next, we investigated, which splenic factors may be important for liver regeneration. B cells account for about 50% of all cells in the spleen and are located in the white pulp and the marginal zone.[14] However, we did not observe any difference in the presence of B-cell subsets following PHx in the spleen and liver (Fig. 1E; Supporting Fig. S2A-C), while T-cell numbers increased in the regenerating liver tissue following PHx, which is consistent with the literature (Supporting Fig. S2D).[4] Nevertheless, when we subjected B cell–deficient $Jh^{-/-}$ mice to PHx, we found reduced survival following PHx when compared to WT controls (Fig. 1F). This effect was not due to surgical complications or infection as sham-operated $Jh^{-/-}$ mice showed no signs of disease and survived after surgery (Fig. 1F). In contrast to splenectomized mice, B cell–deficient animals did not exhibit increased activity of liver transaminases when compared to WT controls (Fig. 2A). Consistently, we could not detect histological differences or increased TUNEL staining following PHx in $Jh^{-/-}$ mice compared to WT mice (Fig. 2B; Supporting Fig. S3A). Deficiency of B-cell survival promoting the B cell–activating factor of the TNF family (BAFF) results in B-cell lymphopenia in mice and humans.[25,29] Accordingly, $Baffr^{-/-}$ mice displayed severe disease symptoms following PHx compared to WT and sham-operated mice (Fig. 2C). In parallel to $Jh^{-/-}$ mice, $Baffr^{-/-}$ animals exhibited only slight increases in liver transaminases and, compared to control liver tissue, comparable histological appearance in H&E tissue sections (Fig. 2D; Supporting Fig. S3B). However, expression of phospho-H3 was reduced in B cell–deficient and BAFFR-deficient mice

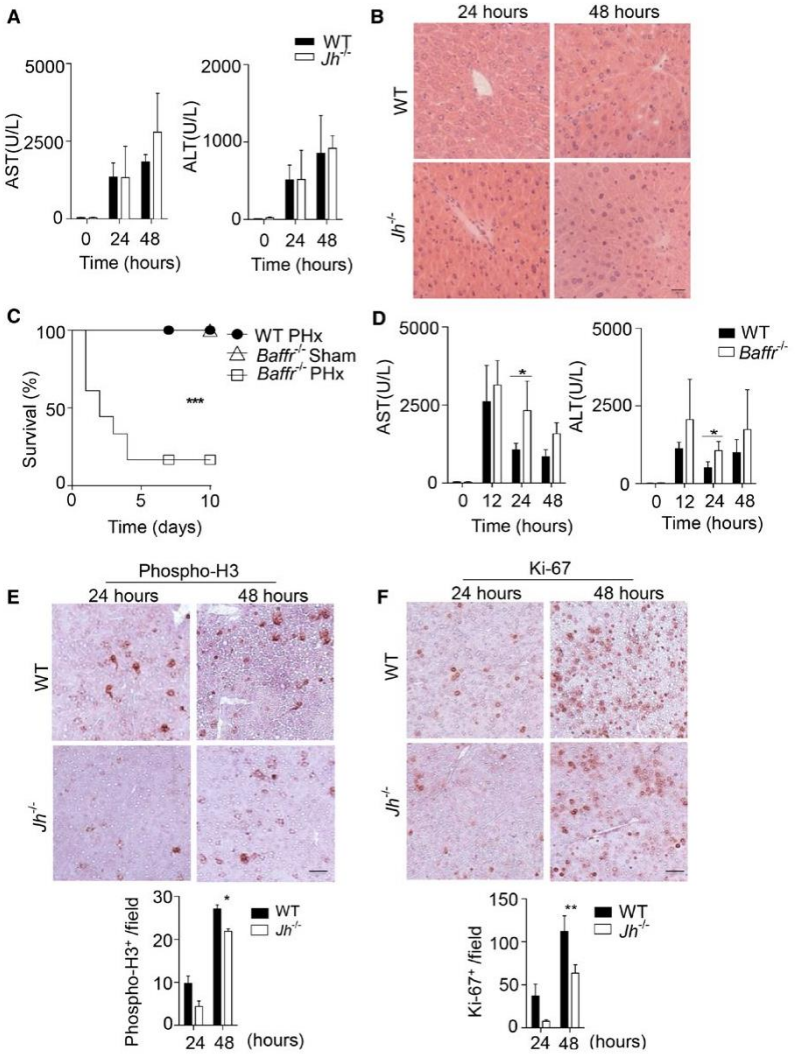

FIG. 2. B cells play a crucial role in liver regeneration after PHx. (A) The activity of AST and ALT was measured in serum of WT and $Jh^{-/-}$ mice following PHx at the indicated time points (n = 4-5). (B) Sections of snap-frozen liver tissue from WT and $Jh^{-/-}$ mice following PHx were stained with H&E. One representative set of n = 3 is shown (scale bar, 200 μm). (C) Survival of $Baffr^{-/-}$ mice (n = 18) after 70% PHx compared to sham-operated $Baffr^{-/-}$ mice (n = 4) and WT mice after 70% PHx (n = 7) was monitored. (D) The activity of AST and ALT was measured in serum of WT and $Baffr^{-/-}$ mice following PHx at the indicated time points (n = 4-5). (E,F) Sections of snap-frozen liver tissue from WT and $Jh^{-/-}$ mice following PHx were stained with (E) anti-phospho-H3 and (F) anti-Ki-67 antibodies. Representative sections for each time point are shown (n = 3; scale bar, 100 μm). Lower panels indicate quantification. Error bars in all experiments represent SEM; $^{*}P < 0.05$, $^{**}P < 0.01$, $^{***}P < 0.001$.

compared to WT controls following PHx (Fig. 2E; Supporting Fig. S3C,D). Furthermore, expression of Ki-67 was delayed in the absence of B cells or BAFFR (Fig. 2F; Supporting Fig. S3E,F). These data indicate that B cells provide important factors for hepatocyte proliferation and liver regeneration.

Next, we wondered which B cell–derived factors are important for liver regeneration. B cells express Ltα and Ltβ, which are critical for lymphoid tissue organization. We found decreased expression levels of *Ltβ* in $Jh^{-/-}$ mice compared to WT controls in both the spleen and liver after PHx and in naive mice

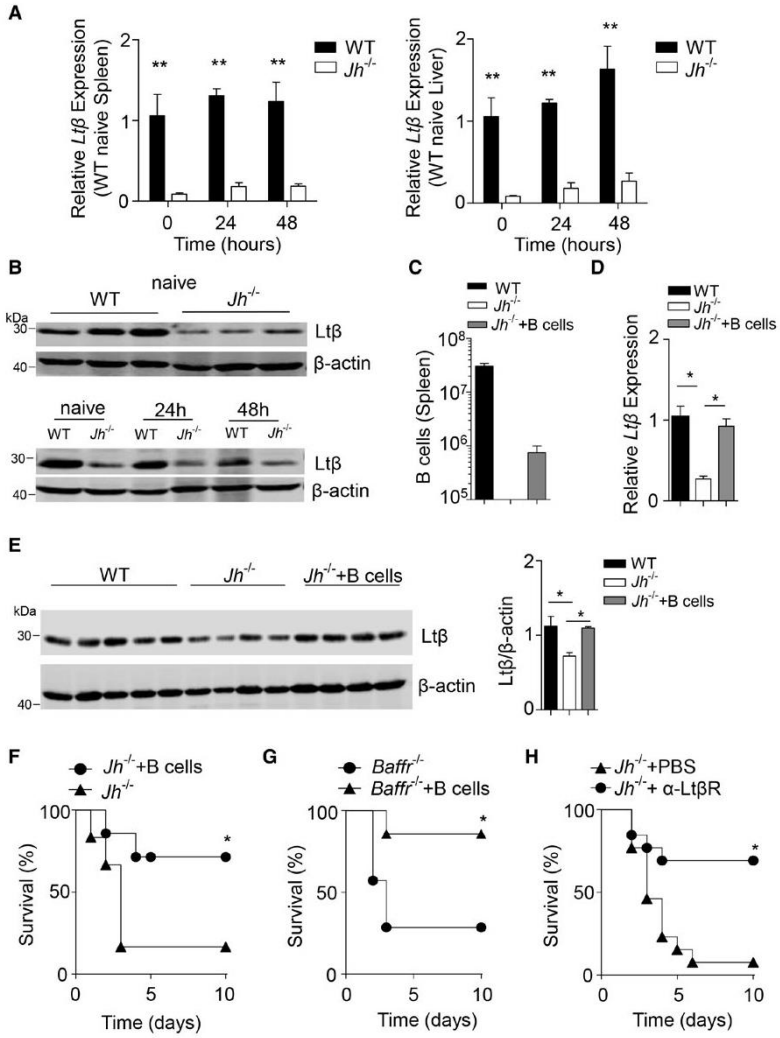

FIG. 3. B cell–derived Ltβ contributes to liver regeneration after PHx. (A) RNA expression of *Ltβ* was measured in spleen and liver tissue from WT and $Jh^{-/-}$ mice at the indicated time points post–70% PHx (n = 3-4). (B) Protein level of Ltβ was measured in liver tissue from naive WT and $Jh^{-/-}$ and from WT and $Jh^{-/-}$ mice at the indicated time points post–70% PHx. (C-E) Purified B cells (2×10^6) from WT mice were intravenously injected into $Jh^{-/-}$ mice. After 48 hours, (C) B-cell numbers were determined in the spleen by flow cytometry (n = 4-6). (D) RNA levels of *Ltβ* were measured in liver tissue (n = 3-5). (E) The protein level of Ltβ was measured in liver tissue. (F) Survival of $Jh^{-/-}$ mice without (n = 6) or after (n = 7) B-cell transfer was determined following 70% PHx. (G) Survival of $Baffr^{-/-}$ mice without (n = 7) or after (n = 7) B-cell transfer was determined following 70% PHx. (H) Survival of untreated (n = 13) and agonist LtβR antibody–treated (n = 13) $Jh^{-/-}$ mice was monitored after 70% PHx. Error bars in all experiments represent SEM; $^*P < 0.05$, $^{**}P < 0.01$.

(Fig. 3A,B), while the difference in Ltα expression was not significant after PHx in the liver in our setting (Supporting Fig. S4). This led us to speculate that Ltβ plays a major role in regulating B cell–mediated liver regeneration in our setting. To further validate that Ltβ is produced by B cells, we adoptively transferred B cells into $Jh^{-/-}$ mice (Fig. 3C), which rescued Ltβ expression levels in the liver (Fig. 3D,E). Consistently, when we adoptively transferred B cells into $Jh^{-/-}$ mice, we could rescue severe disease development following PHx (Fig. 3F). Furthermore, B-cell transfer into PHx $Baffr^{-/-}$ mice prevented severe disease (Fig. 3G).

Because lymphotoxins are known to be critical for liver regeneration,[30] we hypothesized that B cell–derived Ltβ expression may contribute to liver regeneration. Consistently, when we applied an agonistic anti-LtβR antibody prior to PHx, we observed protection of $Jh^{-/-}$ mice (Fig. 3H). Taken together, these data indicate that B cells are critical contributors to liver regeneration.

CD169$^+$ CELLS ARE CRITICAL FOR LIVER REGENERATION FOLLOWING PHx

Ltα and Ltβ are important cytokines for the maintenance of CD169$^+$ macrophages in the spleen.[18-20] B cells are critical for organization of the lymphoid tissue as B cell–deficient mice exhibit reduced presence of metallophilic CD169$^+$ macrophages (Fig. 4A,B).[15,23] Following adoptive transfer of B cells into $Jh^{-/-}$ mice, CD169$^+$ cells were restored (Fig. 4C). Therefore, we hypothesized that B cell–mediated maintenance of CD169$^+$ cells contributes to liver regeneration. Interestingly, we observed higher numbers of CD169$^+$ cells in the regenerating but also the remaining liver lobe using flow cytometry (Fig. 4D). Notably, following splenectomy the increase of CD169$^+$ cells was abolished (Supporting Fig. S5A). Furthermore, we observed a slight increase of CD169$^+$ cells in the spleen compared to unoperated mice (Fig. 4E). CD169$^+$ cells can be depleted by injection of DT into CD169-DTR mice.[24] To exclude effects of DT on other cell types, we administered DT to WT mice before and after PHx and observed no effects on liver regeneration and survival (Supporting Fig. S5B,C). Absence of CD169$^+$ cells resulted in slightly increased AST activity in the serum after PHx when compared to WT controls (Fig. 4F). Furthermore, DT-treated CD169-DTR mice succumbed after PHx compared to control mice (Fig. 4G). Taken together, we identified CD169$^+$ cells to be important for liver regeneration following PHx.

Consistent with the findings in B cell–deficient mice, we observed no histological differences in the absence or presence of CD169$^+$ cells in H&E tissue sections (Supporting Fig. S5D). Moreover, we could not detect increased TUNEL staining following PHx in DT-treated CD169-DTR mice compared to untreated controls (Supporting Fig. S5E). However, we observed delayed liver regeneration following PHx in DT-treated CD169-DTR mice in comparison to control animals as evident by a decreased liver/body weight ratio (Fig. 5A). Furthermore, we found reduced presence of phospho-H3 and reduced expression of Ki-67 cells in the liver tissue in DT-treated CD169-DTR mice in comparison to control animals (Fig. 5B,C; Supporting Fig. S5F). Consistently, expression of PCNA, which is involved in DNA repair and synthesis, was reduced in the liver as a result of CD169$^+$ cell depletion compared to WT mice following PHx (Fig. 5D). We next analyzed the liver morphology in DT-treated CD169-DTR mice at later time points such as 13 days after PHx. We observed a slight but significant reduction in liver weight in DT-treated mice compared to untreated controls (Fig. 5E). Together these data suggest that CD169$^+$ cells promote proliferation following PHx and therefore contribute to liver regeneration.

CD169$^+$ CELLS PROMOTE IL-6 PRODUCTION DURING LIVER REGENERATION

To define how CD169$^+$ cells contribute to liver regeneration, we analyzed RNA expression levels of genes encoding for cytokines important for liver regeneration (Fig. 6A). We found decreased IL-6 expression in B cell–deficient mice in the liver when compared to control animals in our setting (Fig. 6A,B). Transfer of B cells into $Jh^{-/-}$ mice could restore *IL-6* expression levels in the liver (Fig. 6C). Because IL-6-deficient mice show delayed liver regeneration,[6-8] we speculated that CD169$^+$ cells might trigger liver regeneration by inducing expression of IL-6. In line with that, DT-treated CD169-DTR mice showed reduced RNA expression levels of *Il-6* in liver tissue compared to control animals 6 and 48 hours after PHx (Fig. 6D,E). Moreover, IL-6 expression was reduced on a protein level 48 hours following PHx in the absence of CD169$^+$ cells (Fig. 6F). Notably, we also observed an early increase in *Il-6* expression levels in the absence of CD169$^+$ cells and, accordingly, STAT3 phosphorylation 12 hours after PHx (Fig. 6D,G). However, consistent with the reduced expression of IL-6, we observed lower expression of phospho-STAT3 in liver tissue harvested from CD169$^+$ cell–deficient mice compared to CD169$^+$ cell–competent mice 24 and 48 hours after PHx (Fig. 6G; Supporting Fig. S6). Notably, we observed similar induction of phospho-Erk and a similar decrease of IκBα, indicating

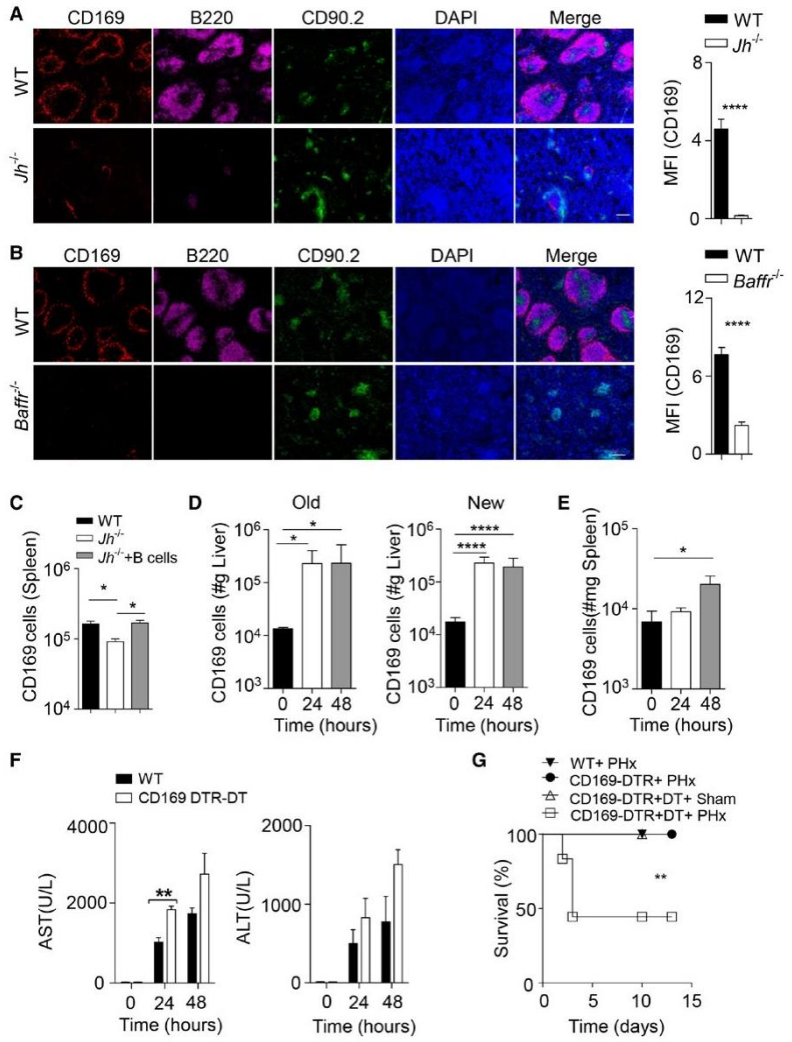

FIG. 4. CD169$^+$ cells contribute to liver regeneration. (A) Sections of snap-frozen spleen tissue from WT and *Jh*$^{-/-}$ mice were stained with anti-CD169, anti-B220, and anti-CD90.2 antibodies. Representative sections are shown (n = 4-5; scale bar, 100 μm). Right panel indicates average and SEM of mean fluorescence intensities of CD169 staining. (B) Sections from snap-frozen spleen tissue from WT and *Baffr*$^{-/-}$ mice were stained with anti-CD169 anti-B220 and anti-CD90.2 antibodies. Representative sections are shown (n = 4-5; scale bar, 100 μm). Right panel indicates average and SEM of mean fluorescence intensities of CD169 staining. (C) Purified B cells (2×10^6) from WT mice were adoptively transferred into *Jh*$^{-/-}$ mice. After 48 hours, CD169-cell numbers were determined in the spleen by flow cytometry (n = 4-6). (D,E) CD169$^+$ cells were measured by flow cytometry in the newly regenerated (n = 7-8) and remaining ("Old") (n = 3-4) liver lobes (D) and spleen tissue (n = 7-8) (E) at the indicated time points after 70% PHx. Results were calculated according to liver (grams) and spleen (milligrams) weights. (F) The activity of AST and ALT was measured in serum of WT and DT-treated CD169-DTR mice following PHx at the indicated time points (n = 3). (G) Survival of DT-treated CD169-DTR mice after PHx (n = 12) compared to WT mice (n = 8) after PHx, CD169-DTR mice (n = 5) after PHx, and sham-operated, DT-treated CD169-DTR mice (n = 4) was monitored. Error bars in all experiments represent SEM; *$P < 0.05$, **$P < 0.01$, ****$P < 0.0001$. Abbreviations: DAPI, 4′,6-diamidino-2-phenylindole; MFI, mean fluorescence intensity.

that other signaling pathways participating in liver regeneration remain intact in the absence of CD169$^+$ cells in our setting (Fig. 6G; Supporting Fig. S6).

To explore whether IL-6R signaling can compensate for CD169$^+$ cells, we administered IL-6/IL-6R protein before and after PHx in DT-treated

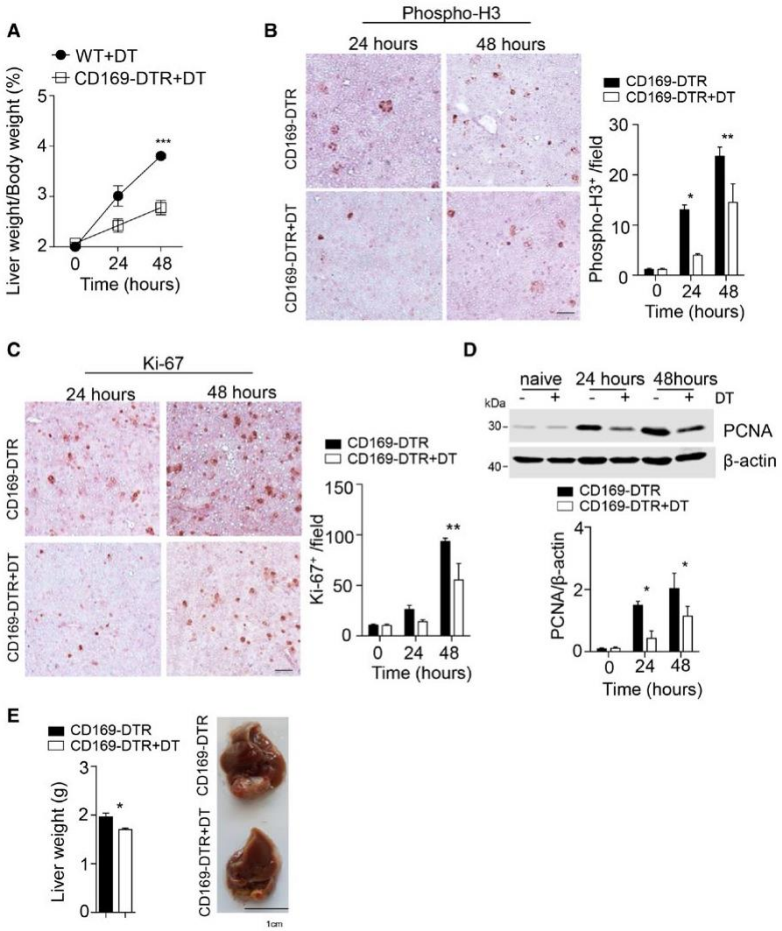

FIG. 5. CD169$^+$ cells promote the presence of hepatic proliferation markers after PHx. (A) The liver weight/body weight ratio was determined after 70% PHx in DT-treated WT mice and DT-treated CD169-DTR mice followed by PHx (n = 3). (B,C) Sections of snap-frozen liver tissue from CD169-DTR and DT-treated CD169-DTR mice at the indicated time points after 70% PHx were stained with anti-phospho-H3 (B) and anti-Ki-67 (C) antibodies. Representative sections for each time point are shown (n = 3; scale bar, 100 μm). Right panels indicate quantification. (D) Protein level of PCNA was measured at the indicated time points after 70% PHx in DT-treated CD169-DTR and CD169-DTR mice (n = 4). Lower panel indicates quantification. (E) Liver weight (left panel) and liver morphology (right panel) were determined at day 13 after 70% PHx of DT-treated CD169-DTR and CD169-DTR mice (n = 3-5). Error bars in all experiments represent SEM; $^*P < 0.05$, $^{**}P < 0.01$, $^{***}P < 0.001$.

CD169-DTR mice.[6] As expected, we found increased STAT3 phosphorylation following injection with IL-6/IL-6R in both CD169$^+$ cell–competent and CD169$^+$ cell–depleted animals (Fig. 7A). Notably, the liver weight/body weight ratio in CD169-DTR DT-treated animals after PHx following treatment with IL-6/IL-6R was comparable to that in untreated CD169-DTR mice following PHx (Fig. 7B), indicating that injection of IL-6/IL-6R could restore liver regeneration in CD169$^+$ cell–depleted mice. Consistently, we found increased expression of phospho-H3 and Ki-67 following treatment with IL-6/IL-6R of CD169-DTR mice when compared to CD169-DTR controls (Fig. 7C). Moreover, PCNA expression was increased after IL-6/IL-6R treatment in the absence of CD169$^+$ cells after PHx (Fig. 7D). Furthermore, we found that IL-6/IL-6R protein significantly rescued the pathology following PHx in CD169-DTR animals (Fig. 7E). In conclusion, we identified that B cell–mediated maintenance of CD169$^+$ cells contributes to IL-6 production and liver regeneration.

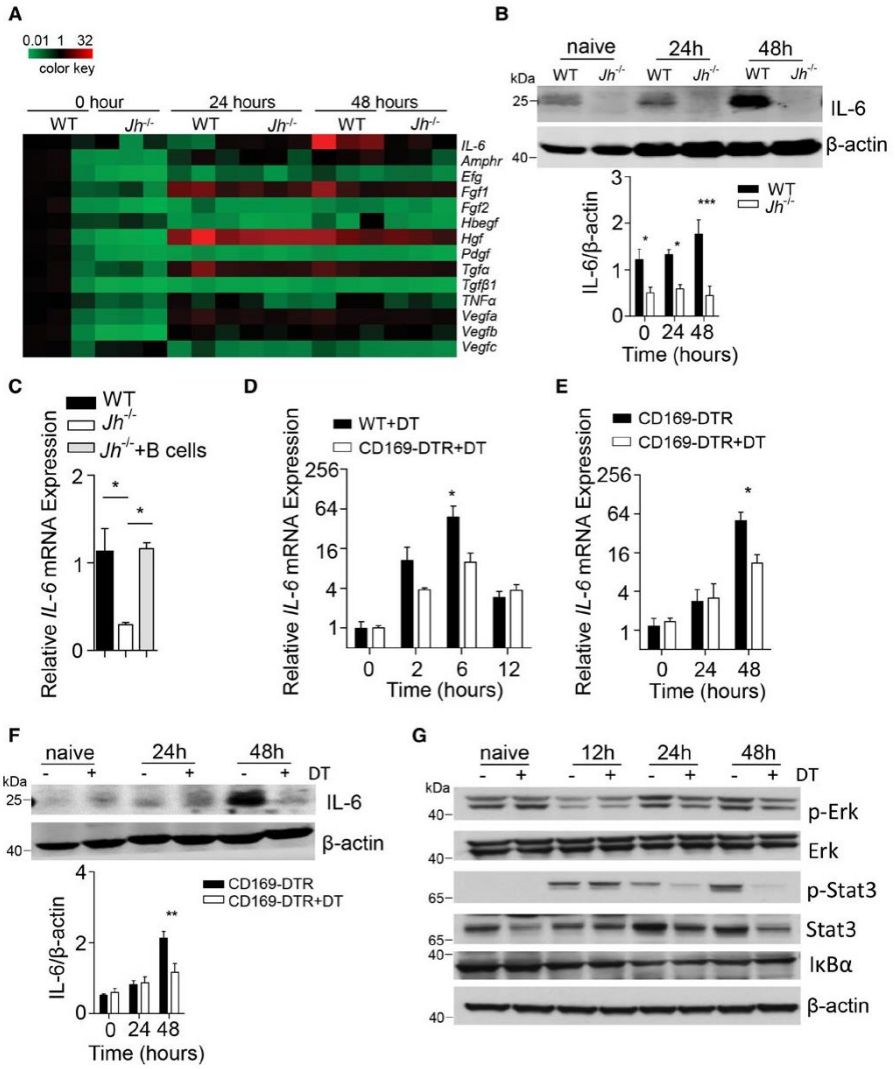

FIG. 6. Defective activation of IL-6 signaling in the absence of CD169$^+$ cells. (A) RNA expression level of cytokines important for liver regeneration was determined in the liver tissue from WT and $Jh^{-/-}$ mice at the indicated time points post–70% PHx (n = 3). (B) Protein expression of IL-6 was determined in liver tissue from WT and $Jh^{-/-}$ mice at the indicated time points after 70% PHx (n = 3). Lower panel indicates quantification. (C) RNA expression levels of *IL-6* was measured in the liver tissue of WT and $Jh^{-/-}$ mice without or with purified B cells (n = 3-5). (D,E) RNA expression levels of *Il-6* were determined in liver tissue from DT-treated WT, CD169-DTR, and DT-treated CD169-DTR mice as labeled at the indicated time points after 70% PHx (n = 3-5). (F) Protein expression of IL-6 was determined in liver tissue from CD169-DTR and DT-treated CD169-DTR mice at the indicated time points after 70% PHx (n = 3). Lower panel indicates quantification. (G) Protein lysates of liver tissue from CD169-DTR mice and DT-treated CD169-DTR mice at the indicated time points after PHx were blotted and stained with anti-phospho-Erk, anti-Erk, anti-phospho-STAT3, anti-STAT3, anti-IκBα, and anti-β-actin antibodies (one representative of n = 3 blots is shown). Error bars in all experiments represent SEM; $^*P < 0.05$, $^{**}P < 0.01$, $^{***}P < 0.001$. Abbreviations: Amphr, amphiregulin; Hbegf, heparin-binding EGF-like growth factor; Hgf, hepatocyte growth factor; Fgf, fibroblast growth factor; Pdgf, platelet-derived growth factor; Vegf, vascular endothelial growth factor.

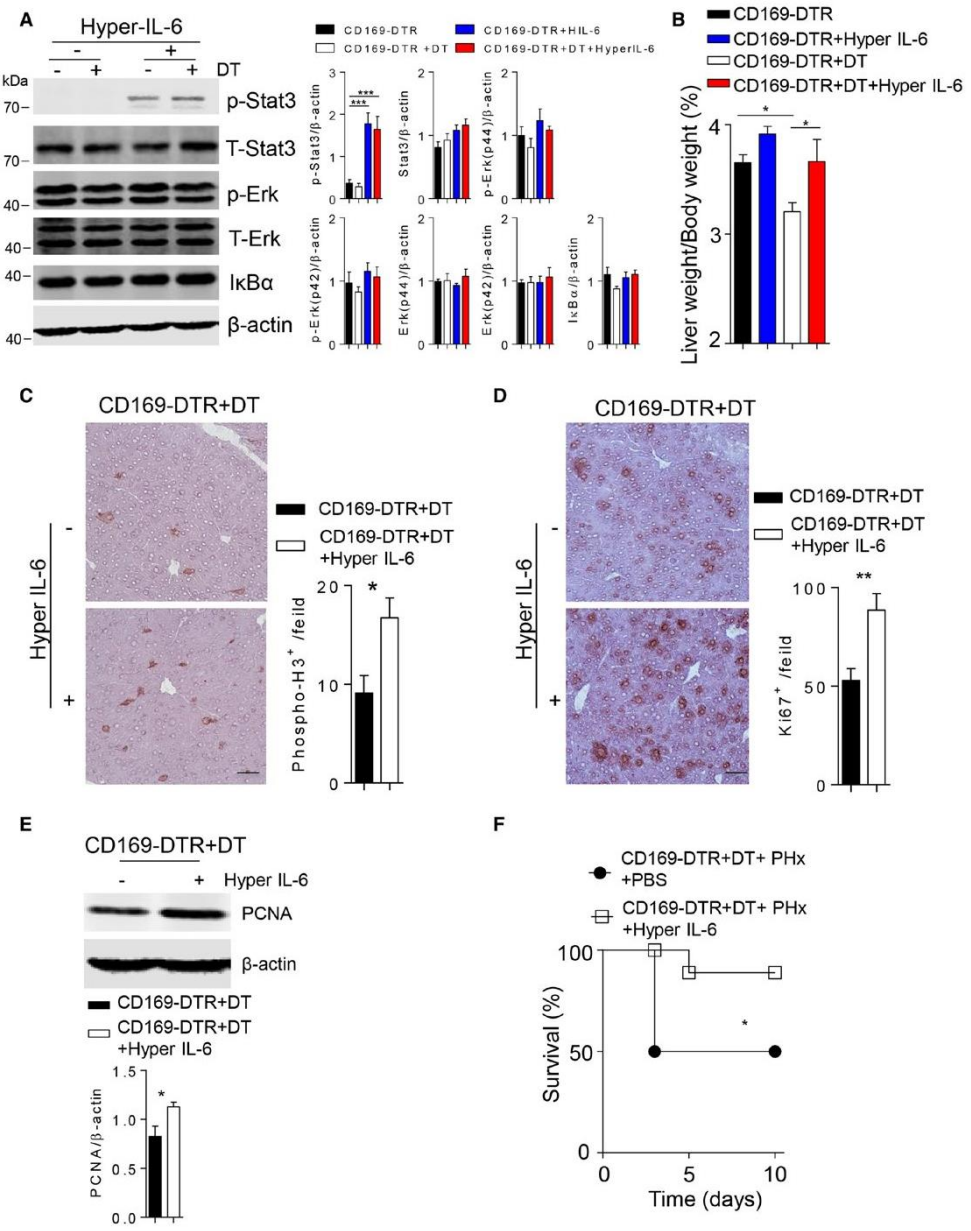

FIG. 7. IL-6/IL-6R treatment can rescue liver regeneration in the absence of CD169$^+$ cells. (A) Protein lysates of liver tissue from CD169-DTR mice or DT-treated CD169-DTR mice following IL-6/IL-6R treatment were blotted and stained with anti-phospho-Erk, anti-Erk, anti-phospho-STAT3, anti-STAT3, anti-IκBα, and anti-β-actin antibodies. One representative of n = 6 blots is shown. Right panels indicate quantification. (B) The liver weight/body weight ratio was determined at 48 hours after 70% PHx in CD169-DTR mice and DT-treated CD169-DTR mice and following IL-6/IL-6R treatment (n = 3-5). (C,D) Sections of snap-frozen liver tissue from DT-treated CD169-DTR mice without or after IL-6/IL-6R treatment at 48 hours after 70% PHx were stained with (C) anti-phospho-H3 and (D) anti-Ki-67 antibodies. Representative sections for each time point are shown (n = 3-5; scale bars, [C] 50 μm, [D], 100 μm). Right panels indicate quantification. (E) Protein level of PCNA was measured in DT-treated CD169-DTR mice in the absence and presence of IL-6/IL-6R treatment at 48 hours after 70% PHx (n = 5). Lower panel indicates quantification. (F) Survival of DT-treated CD169-DTR mice without or after IL-6/IL-6R treatment was monitored (n = 8-9). Error bars in all experiments represent SEM; $^*P < 0.05$, $^{**}P < 0.01$, $^{***}P < 0.001$.

Discussion

In this study, we identify that B cells promoted maintenance of CD169$^+$ cells, which are critical for liver regeneration. Consistently, depletion of CD169$^+$ cells resulted in reduced IL-6 expression following PHx and consequently reduced activation of STAT3 signaling pathways. Application of IL-6/IL-6R could rescue defective liver regeneration in the absence of CD169$^+$ cells.

Liver regeneration is triggered by key signaling pathways, which are regulated through several cytokines. Specifically, the TNF superfamily members TNF, Ltα, and Ltβ have been shown to be important for liver regeneration. Ltα and Ltβ production by T cells play an important role during liver regeneration. Notably, B cell–specific and T cell–specific Ltα-deficient and Ltβ-deficient mice display also reduced presence of CD169$^+$ cells.[19] Hence, Lt could exhibit effects not only on hepatocytes but also on CD169$^+$ cells and thereby affect IL-6-mediated signaling. Specifically, we observed reduced IL-6 expression in liver tissue from DT-treated CD169-DTR mice compared to control animals. Consistently, defective IL-6 signaling results in impaired liver regeneration, a transient effect which can result in altering the severity of the phenotype.[6,7] Similarly, we observed severe pathology in a proportion of animals following splenectomy and PHx, although other studies, which also reported a supporting role of the spleen during liver regeneration in mice, did not indicate a severe pathology.[28] Because at later time points we observed only slight but significant decreases in liver mass in the absence of CD169$^+$ cells, the effects described here might be also transient. We speculated that underlying mechanisms following defective liver regeneration in B cell–deficient and CD169$^+$ cell–deficient animals likely preceded the development of disease symptoms and therefore analyzed early time points following PHx. Consistently, we found reduced presence of proliferation markers and reduced liver weight/body weight ratios during these time points. However, treatment with IL-6/IL-6R improved expression of hepatic proliferation markers, liver weight/body weight ratio, and observed pathology in the absence of CD169$^+$ cells.[6]

The spleen is ideally situated to trigger liver regeneration. The blood from spleen tissue directly feeds into the portal vein circulation. Accordingly, cytokines and chemokines produced in the spleen are able to trigger their effects in the liver. As discussed above, several immune factors contribute to or regulate liver regeneration. Splenectomy has been shown to be beneficial in clinical settings of liver cirrhosis and portal hypertension or hypersplenism.[31,32] These beneficial effects have been attributed to reduction of the portal circulation.[33] Furthermore, experiments using rats have shown that splenectomy can result in reduced concentrations of TGFβ and consequently reduced inhibitory effects on liver regeneration.[34,35] Interestingly, these effects increase with the amount of liver mass removed.[35] In mice, splenectomy results in delayed liver regeneration following PHx.[28] The role of B cells in the regulation of liver functions during acute and chronic liver disease remains controversial.[36,37] In our settings, splenectomy, B-cell deficiency, and deletion of CD169$^+$ cells resulted in impaired liver regeneration following PHx. One explanation could be that in rats CD169$^+$ cells from other lymphoid tissue compensate for loss of splenic CD169$^+$ cells. Furthermore, increased IL-6/IL-6R signaling might compensate for the splenic loss of CD169$^+$ cells. In our setting, treatment with IL-6/IL-6R could prevent severe pathology in the absence of CD169$^+$ cells. Future studies could compare the activation of B cells and CD169$^+$ cells during chronic liver disease and liver pathology.

In conclusion, we identified in our model systems that B cell–mediated maintenance of CD169$^+$ cells contributes to liver regeneration.

REFERENCES

1) Michalopoulos GK. Liver regeneration after partial hepatectomy: critical analysis of mechanistic dilemmas. Am J Pathol 2010;176:2-13.
2) Yamada Y, Kirillova I, Peschon JJ, Fausto N. Initiation of liver growth by tumor necrosis factor: deficient liver regeneration in mice lacking type I tumor necrosis factor receptor. Proc Natl Acad Sci USA 1997;94:1441-1446.
3) Anders RA, Subudhi SK, Wang J, Pfeffer K, Fu YX. Contribution of the lymphotoxin beta receptor to liver regeneration. J Immunol 2005;175:1295-1300.
4) Tumanov AV, Koroleva EP, Christiansen PA, Khan MA, Ruddy MJ, Burnette B, et al. T cell-derived lymphotoxin regulates liver regeneration. Gastroenterology 2009;136:694-704.
5) **Sorg UR**, **Behnke K**, Degrandi D, Reich M, Keitel V, Herebian D, et al. Cooperative role of lymphotoxin beta receptor and tumor necrosis factor receptor p55 in murine liver regeneration. J Hepatol 2016;64:1108-1117.
6) Schmidt-Arras D, Rose-John S. IL-6 pathway in the liver: from physiopathology to therapy. J Hepatol 2016;64:1403-1415.

7) Cressman DE, Greenbaum LE, DeAngelis RA, Ciliberto G, Furth EE, Poli V, et al. Liver failure and defective hepatocyte regeneration in interleukin-6-deficient mice. Science 1996;274:1379-1383.
8) Sakamoto T, Liu Z, Murase N, Ezure T, Yokomuro S, Poli V, et al. Mitosis and apoptosis in the liver of interleukin-6-deficient mice after partial hepatectomy. Hepatology 1999;29:403-411.
9) Peters M, Blinn G, Jostock T, Schirmacher P, Zum Buschenfelde KHM, Galle PR, et al. Combined interleukin 6 and soluble interleukin 6 receptor accelerates murine liver regeneration. Gastroenterology 2000;119:1663-1671.
10) Block GD, Locker J, Bowen WC, Petersen BE, Katyal S, Strom SC, et al. Population expansion, clonal growth, and specific differentiation patterns in primary cultures of hepatocytes induced by HGF/SF, EGF and TGF alpha in a chemically defined (HGM) medium. J Cell Biol 1996;132:1133-1149.
11) Russell WE, Kaufmann WK, Sitaric S, Luetteke NC, Lee DC. Liver regeneration and hepatocarcinogenesis in transforming growth factor-alpha-targeted mice. Mol Carcinog 1996;15:183-189.
12) Berasain C, Garcia-Trevijano ER, Castillo J, Erroba E, Lee DC, Prieto J, et al. Amphiregulin: an early trigger of liver regeneration in mice. Gastroenterology 2005;128:424-432.
13) Natarajan A, Wagner B, Sibilia M. The EGF receptor is required for efficient liver regeneration. Proc Natl Acad Sci USA 2007;104:17081-17086.
14) Junt T, Scandella E, Ludewig B. Form follows function: lymphoid tissue microarchitecture in antimicrobial immune defence. Nat Rev Immunol 2008;8:764-775.
15) Davies LC, Jenkins SJ, Allen JE, Taylor PR. Tissue-resident macrophages. Nat Immunol 2013;14:986-995.
16) Nolte MA, Arens R, Kraus M, van Oers MH, Kraal G, van Lier RA, et al. B cells are crucial for both development and maintenance of the splenic marginal zone. J Immunol 2004;172:3620-3627.
17) Honke N, Shaabani N, Cadeddu G, Sorg UR, Zhang DE, Trilling M, et al. Enforced viral replication activates adaptive immunity and is essential for the control of a cytopathic virus. Nat Immunol 2012;13:51-57.
18) Tumanov A, Kuprash D, Lagarkova M, Grivennikov S, Abe K, Shakhov A, et al. Distinct role of surface lymphotoxin expressed by B cells in the organization of secondary lymphoid tissues. Immunity 2002;17:239-250.
19) Tumanov AV, Grivennikov SI, Shakhov AN, Rybtsov SA, Koroleva EP, Takeda J, et al. Dissecting the role of lymphotoxin in lymphoid organs by conditional targeting. Immunol Rev 2003;195:106-116.
20) Futterer A, Mink K, Luz A, Kosco-Vilbois MH, Pfeffer K. The lymphotoxin beta receptor controls organogenesis and affinity maturation in peripheral lymphoid tissues. Immunity 1998;9:59-70.
21) Asano K, Takahashi N, Ushiki M, Monya M, Aihara F, Kuboki E, et al. Intestinal CD169$^+$ macrophages initiate mucosal inflammation by secreting CCL8 that recruits inflammatory monocytes. Nat Commun 2015;6:7802.
22) Moseman EA, Iannacone M, Bosurgi L, Tonti E, Chevrier N, Tumanov A, et al. B cell maintenance of subcapsular sinus macrophages protects against a fatal viral infection independent of adaptive immunity. Immunity 2012;36:415-426.
23) **Xu HC**, **Huang J**, Khairnar V, Duhan V, Pandyra AA, Grusdat M, et al. BAFFR deficiency results in limited CD169$^+$ macrophage function during viral infection. J Virol 2015;89:4748-4759.
24) Asano K, Nabeyama A, Miyake Y, Qiu CH, Kurita A, Tomura M, et al. CD169-positive macrophages dominate antitumor immunity by crosspresenting dead cell-associated antigens. Immunity 2011;34:85-95.
25) Sasaki Y, Casola S, Kutok JL, Rajewsky K, Schmidt-Supprian M. TNF family member B cell–activating factor (BAFF) receptor–dependent and –independent roles for BAFF in B cell physiology. J Immunol 2004;173:2245-2252.
26) Greene AK, Puder M. Partial hepatectomy in the mouse: technique and perioperative management. J Invest Surg 2003;16:99-102.
27) Dejardin E, Droin NM, Delhase M, Haas E, Cao Y, Makris C, et al. The lymphotoxin-beta receptor induces different patterns of gene expression via two NF-kappaB pathways. Immunity 2002;17:525-535.
28) Furuya S, Kono H, Hara M, Hirayama K, Tsuchiya M, Fujii H. Interleukin-17A plays a pivotal role after partial hepatectomy in mice. J Surg Res 2013;184:838-846.
29) **Warnatz K**, **Salzer U**, Rizzi M, Fischer B, Gutenberger S, Bohm J, et al. B-cell activating factor receptor deficiency is associated with an adult-onset antibody deficiency syndrome in humans. Proc Natl Acad Sci USA 2009;106:13945-13950.
30) Tumanov AV, Koroleva EP, Christiansen PA, Khan MA, Ruddy MJ, Burnette B, et al. T cell–derived lymphotoxin regulates liver regeneration. Gastroenterology 2009;136:694-704.
31) Kawanaka H, Akahoshi T, Kinjo N, Harimoto N, Itoh S, Tsutsumi N, et al. Laparoscopic splenectomy with technical standardization and selection criteria for standard or hand-assisted approach in 390 patients with liver cirrhosis and portal hypertension. J Am Coll Surg 2015;221:354-366.
32) Tomikawa M, Akahoshi T, Sugimachi K, Ikeda Y, Yoshida K, Tanabe Y, et al. Laparoscopic splenectomy may be a superior supportive intervention for cirrhotic patients with hypersplenism. J Gastroenterol Hepatol 2010;25:397-402.
33) Eipel C, Abshagen K, Ritter J, Cantre D, Menger MD, Vollmar B. Splenectomy improves survival by increasing arterial blood supply in a rat model of reduced-size liver. Transpl Int 2010;23:998-1007.
34) Lee SC, Jeong HJ, Choi BJ, Kim SJ. Role of the spleen in liver regeneration in relation to transforming growth factor-beta 1 and hepatocyte growth factor. J Surg Res 2015;196:270-277.
35) Kim J, Kim CJ, Ko IG, Joo SH, Ahn HJ. Splenectomy affects the balance between hepatic growth factor and transforming growth factor-beta and its effect on liver regeneration is dependent on the amount of liver resection in rats. J Korean Surg Soc 2012;82:238-245.
36) Novobrantseva TI, Majeau GR, Amatucci A, Kogan S, Brenner I, Casola S, et al. Attenuated liver fibrosis in the absence of B cells. J Clin Invest 2005;115:3072-3082.
37) Richards JA, Bucsaiova M, Hesketh EE, Ventre C, Henderson NC, Simpson K, et al. Acute liver injury is independent of B cells or immunoglobulin M. PLoS One 2015;10:e0138688.

Author names in bold designate shared co-first authorship.

Supporting Information

Additional Supporting Information may be found at onlinelibrary.wiley.com/doi/10.1002/hep.30088/suppinfo.

Supplemental Figure 1

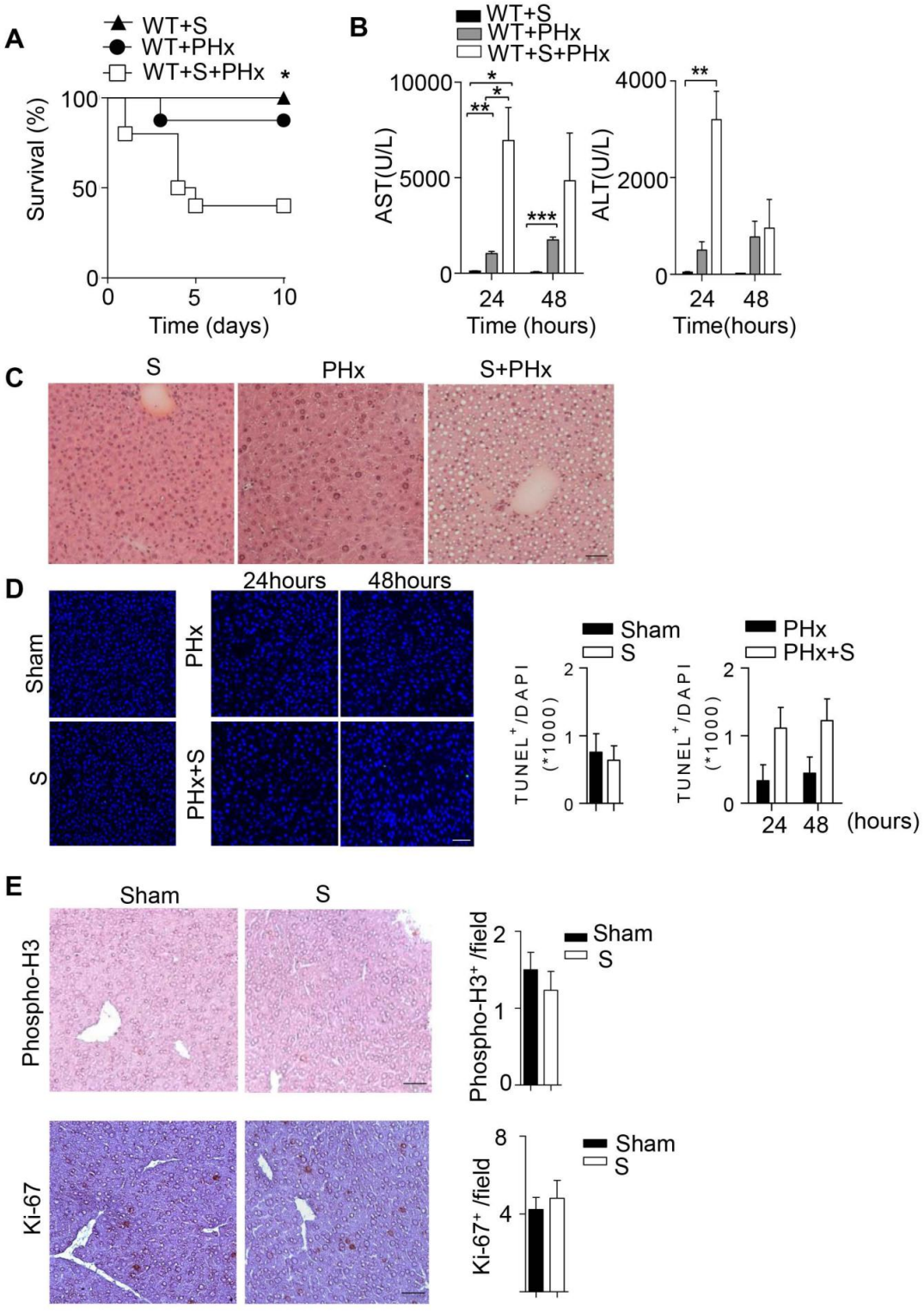

Supplemental Figure 1: Splenectomy results in fatal disease after PHX in otherwise healthy mice. (A) WT mice were splenectomized and were kept under observation for 10 days. After 10 days PHx was performed (n=10) along with control groups of only splenectomized (n=7) or only with PHx (n=8). **(B)** The activity of aspartate aminotransferase (AST) and alanine aminotransferase (ALT) was measured in serum of splenectomized (S), 70 % PHx, and splenectomized mice following PHx (PHx+S) (n=6). **(C)** Section of snap-frozen liver tissue from splenectomized (S), PHx and splenectomized mice following PHx (PHx+S) at 24 hours after PHx were stained with H&E. One representative set of n=3 is shown (Scale bar = 100µm). **(D)** Section of snap-frozen liver tissue from sham operated, splenectomized (S), PHx and splenectomized mice following PHx (S+PHx) at indicated time points were stained with TUNEL. One representative set of n=3-4 is shown (Scale bar = 200µm). Right panels indicate quantification. **(E)** Sections of snap-frozen liver tissue from sham operated WT mice and splenectomized WT mice were stained with anti-phospho-H3 (upper panels) and anti-Ki-67 (lower panels) antibodies. Representative sections for each time point are shown (n=4, scale bar upper panels = 50µm, lower panels =100 µm). Right panels indicate quantification. Error bar in the all the above experiments represent SEM, *$P < 0.05$, **$P < 0.01$, ***<0.001.

Supplemental Figure 2

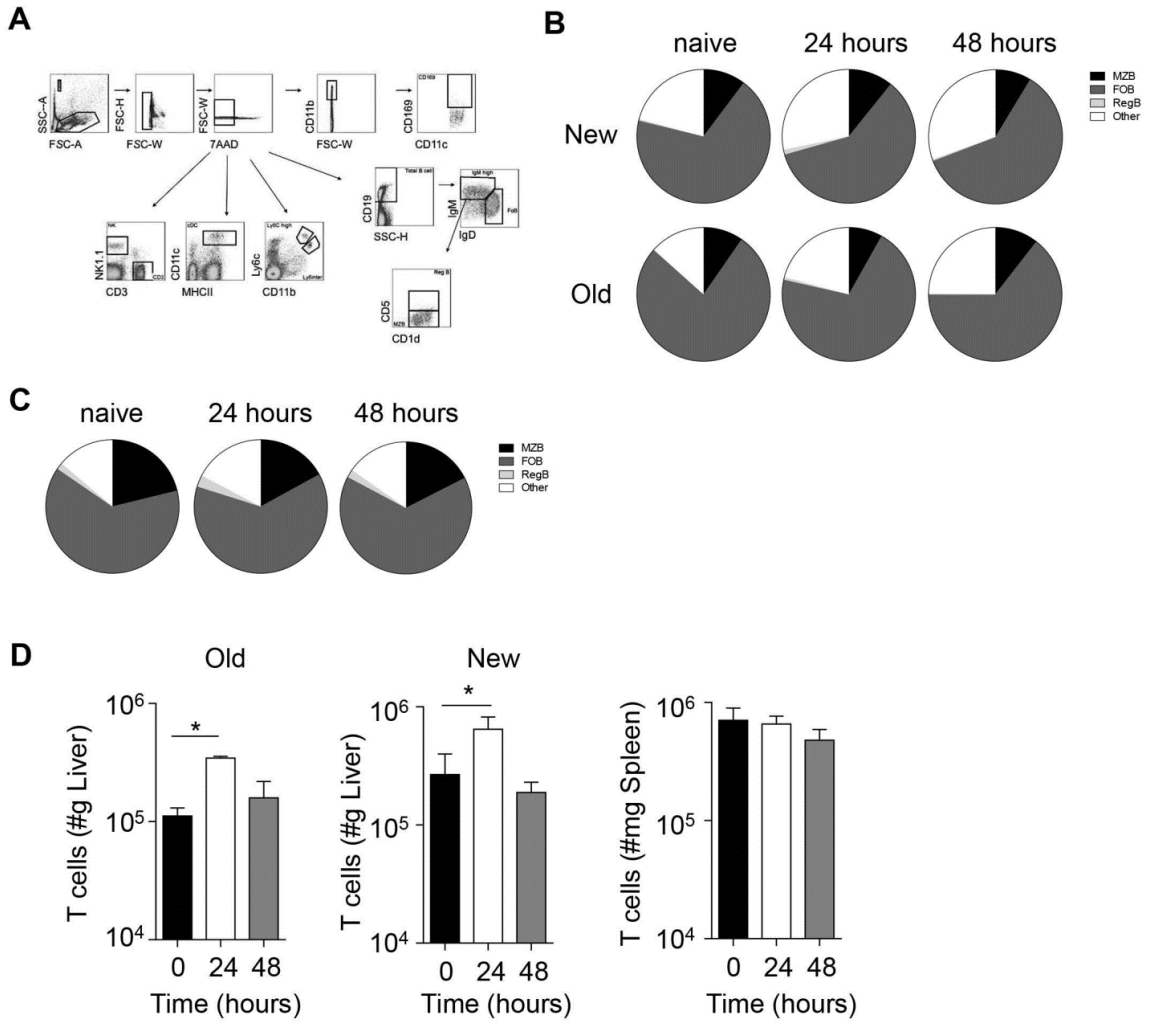

Supplemental Figure 2: B cell subsets and T cell response following PHx. (A) Gating strategy of the flow cytometric analysis. **(B)** Pie graph of B cell subsets in the newly regenerated liver lobes (n=7-8) and the remaining (old) lobes (n=3-4) after 70% PHx. **(C)** Pie graph of B cell subsets in the spleen after 70% PHx (n= 7-8). **(D)** T cell counts in the liver were as assessed by flow cytometric analysis in the (newly regenerated (New) (n=7-8), the remaining lobes (Old) (n=3-4) and the spleen (n= 7-8) at indicated time points after 70% PHx. Results were calculated according to the liver (g) and spleen weight (mg). Error bar in the all the above experiments represent SEM, $*P < 0.05$.

Supplemental Figure 3

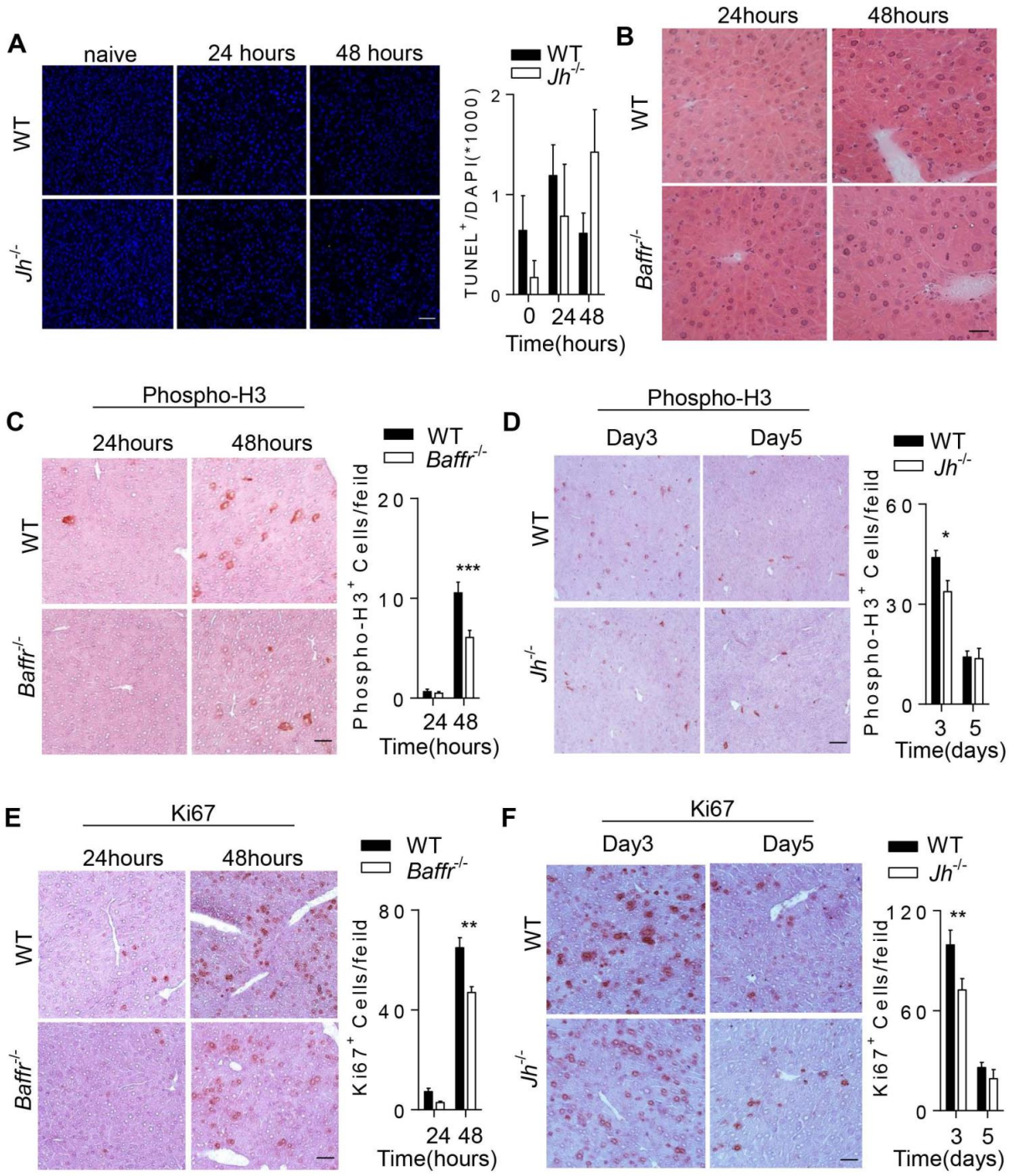

Supplemental Figure 3: B cells contribute to expression of hepatic proliferation markers. **(A)** Sections of snap-frozen liver tissue from WT and *Jh*$^{-/-}$ mice at indicated time points following PHx were stained with TUNEL. One representative set of n=3 is shown. (Scale bar = 200µm). Right panel indicates quantification. **(B)** Sections of snap-frozen liver tissue from WT and *Baffr*$^{-/-}$ mice following PHx were stained with H&E. One representative set of n=3-4 is shown (Scale bar = 200µm). **(C-D)** Sections of snap-frozen liver tissue from **(C)** WT and *Baffr*$^{-/-}$ mice and **(D)** WT and *Jh*$^{-/-}$ mice at indicated time points after PHx were stained with anti-phospho-H3 antibodies. Representative sections for each time point are shown (n=3-4, scale bar = 50µm). Right panels indicate quantification. **(E-F)** Sections of snap-frozen liver tissue from **(E)** WT and *Baffr*$^{-/-}$ mice and **(F)** WT and *Jh*$^{-/-}$ mice at indicated time points after PHx were stained with anti-Ki-67 antibodies. Representative sections for each time point are shown (n=3-4, scale bar = 100µm). Right panels indicate quantification. Right panel indicates quantification. Error bar in the all the above experiments represent SEM, *$P < 0.05$, **$P < 0.01$, ***<0.001.

Supplemental Figure 4

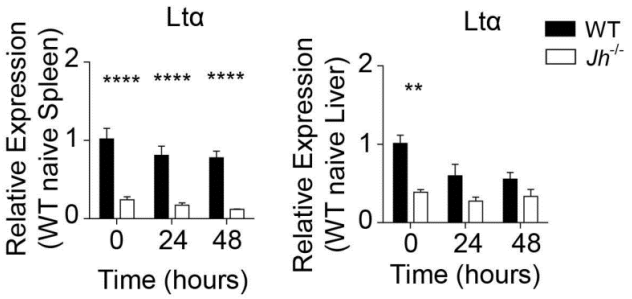

Supplemental Figure 4: RNA expression level of *Ltα* in the spleen (left panel) and liver tissue (right panel) of WT and *Jh*$^{-/-}$ mice before and at indicated time points after PHx (n=3). Error bar in the all the above experiments represent SEM, $^{**}P < 0.01$, ***<0.001.

Supplemental Figure 5

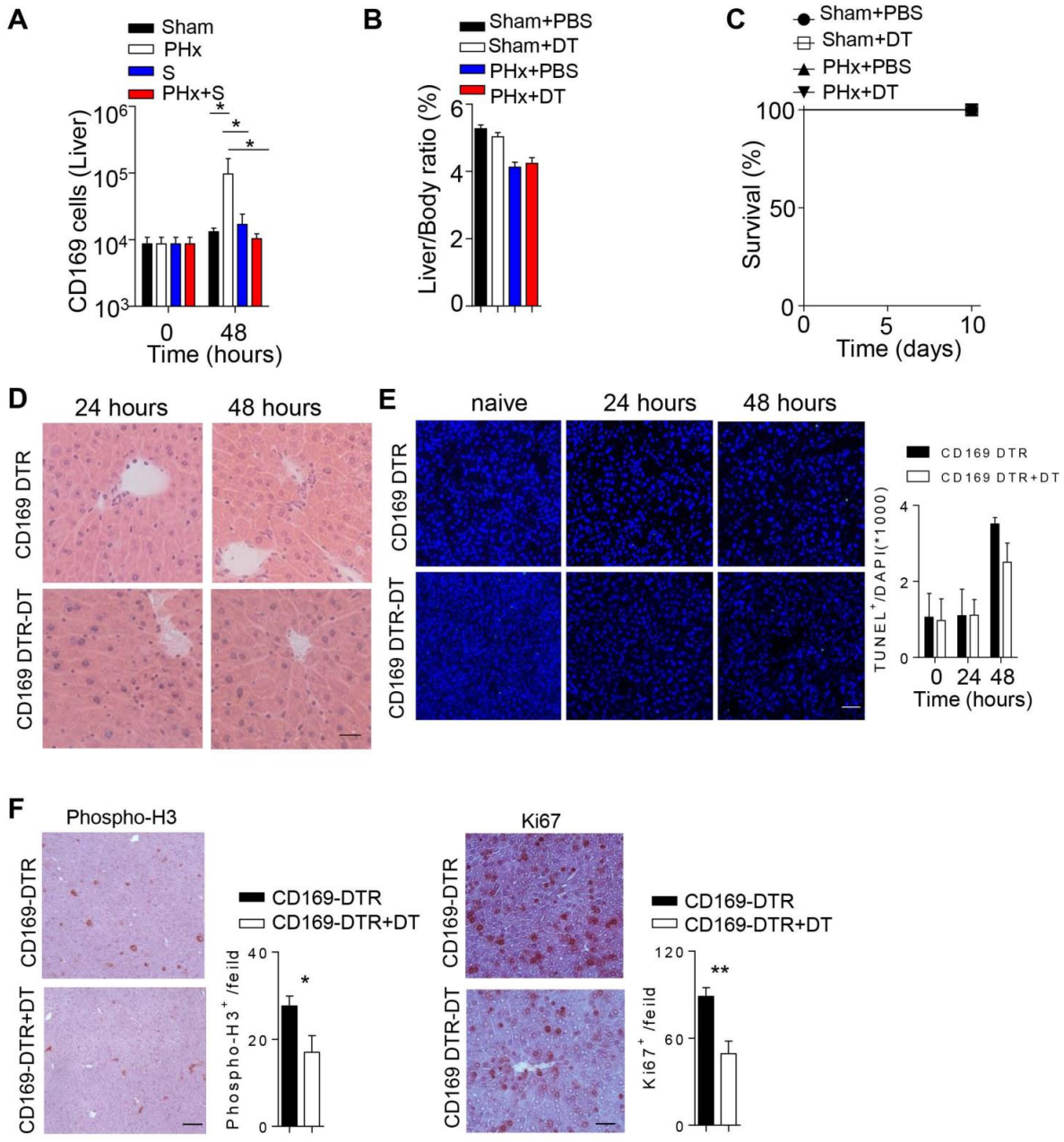

Supplemental Figure 5: CD169$^+$ cells promote expression of hepatic proliferation markers during liver regeneration. (A) CD169$^+$ cell numbers were determined in the liver from sham operated WT mice, splenectomized WT mice, PHx and splenectomized mice followed by PHx (PHx+S) 48 hours after operation (n=3-4). **(B)** Liver weight / body weight ratio was measured of Sham operated WT mice, Sham operated DT treated WT mice, PHx WT mice, and PHx DT treated WT miceat day 10 after PHx (n=4-6). **(C)** Survival of Sham operated WT mice, Sham operated DT treated WT mice, PHx WT mice, and PHx DT treated WT mice was monitored (n=4-6). **(D-E)** Sections of snap-frozen liver tissue from CD169 DTR and DT treated CD169 DTR mice after PHx at indicated time were stained with **(D)** H&E and **(E)**TUNEL. One representative set of n=3 is shown (Scale bar D= 200µm, E= 100µm). Right panel indicates quantification. **(F)** Sections of snap-frozen liver tissue from CD169-DTR and DT treated CD169-DTR mice at day 3 following PHx were stained with anti-Phospho-H3 (left panels) and anti-Ki-67 (right panels) antibodies. One representative set of n=3 is shown (Scale bar left panel= 50µm, panel right=100 µm) Right panel indicates quantification. Error bar in the all the above experiments represent SEM; *$P < 0.05$, **$P < 0.01$.

Supplemental Figure 6

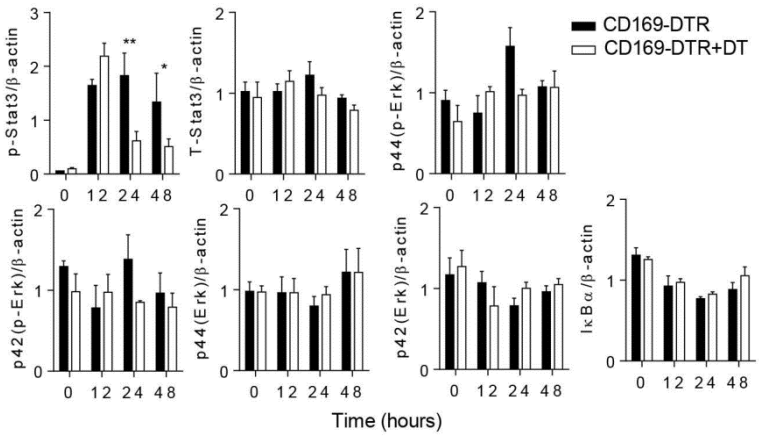

Supplemental Figure 6: CD169$^+$ cells trigger hepatic STAT3 phosphorylation.
Quantifications of Western blots shown in Fig. 6G are presented as indicated. Protein lysates of liver tissue from CD169-DTR mice and DT treated CD169-DTR mice at indicated time points after PHx were blotted and stained with anti-phospho-Erk, anti-Erk, anti-phospho-STAT3, anti-STAT3, anti-IκBα and anti-β-actin antibodies (n=3). Error bar in the all the above experiments represent SEM; *$P < 0.05$, **$P < 0.01$.

3. Discussion

In our study, we identified a novel role of FMRP in inhibiting TNF induced cell death in the liver. Loss of FMRP in the mice resulted in increased virus hepatitis, TNF-mediated liver damage as well as liver pathology following cholestasis. All these liver pathology models point to an important role of FMRP in the liver. Mechanistically, absence of FMRP prolongs RIPK1 expression and promotes RIPK1 phosphorylation, leading to TNF-TNFR1 mediated cell death. In addition, administration of Nec-1s, a RIPK1 kinase inhibitor, could alleviate liver damage following TNF/D-Gal treatment or pathology induced by cholestasis in *Fmr1*^{null} mice. Although the full implications of these findings in human health are still not evident, it would require more in depth studies in patients carrying FMR1 mutations.

Maintaining synaptic plasticity and regulating neuron development by translational regulation is a classical function of FMRP (32). FMRP is more studied during neuronal development rather than its function in other organs. However, within the past 10 years, functions of FMRP outside of the brain have been identified. Testes and ovaries are affected by FMRP deficiency. *Fmr1*^{null} mice have increased ovarian weight, premature follicular ovary development as well as impaired spermatogenesis, which have been observed in human fragile X patients also (51, 52). *Fmr1* mutants of drosophila show developmental defects in the intestine via increased insulin signaling (237). Developmental defects of the liver with FMRP deficiency have not been discussed. Considering our data, we found a pro-survival role of FMRP in regulating cell death, specifically in hepatocytes. Our observations are consistent with published findings, absence of *Fmr1* reduces the DNA damage repair, as well as increased cell death after aphidicolin (replication stress inducer) treatment (46).

We found high upregulation of FMRP expression after BDL compared to sham operated control mice. Moreover, in hepatocellular carcinoma tissue, it has been shown that FMR1 expression levels were increased when compared with tumor-free tissue. FMRP has been characterized to regulate influenza A virus and Zika virus replication (42, 43). Consistently, we found upregulation of *Fmr1* expression after LCMV infection. All these observations inspired us to explore whether FMRP plays a role during LCMV infection. We did not find significant differences in virus replication as well as $CD8^+$ T cell response in *Fmr1*^{null} and control mice.

Surprisingly we saw more liver damage and cell death in *Fmr1*^{nul} mice after LCMV infection. During infection, CD8+ cytotoxic T cells produce several cytokines such as Fas

ligand, TNF and IFNγ, which can bind to their receptors on target cells and promote cell death (171, 238). This is consistent with our finding that $CD8^+$ T cells depletion reduced liver damage after infection. We then identified that *Fmr1*^{nul} mice are more susceptible to TNF induced liver damage but not towards Fas.

However, we did not check the effects of IFNγ on liver disease in *Fmr1*^{nul} and control mice. To further explore this, neutralizing antibodies could be used to block IFN γ signaling, following by monitoring the liver damage after LCMV infection (239).

TNF/D-Gal treatment is widely used model to study septic shock and liver damage (72, 240). In this model, we found that absence of FMRP triggers TNF-mediated apoptosis and necroptosis in the liver tissue. A hall mark of TNF-mediated apoptosis is activation of caspase-8 and a hall marker of necroptosis is the phosphorylation of RIPK1, RIPK3 and MLKL. All of these cell deaths are dependent on deubiquitinated-RIPK1. However there is also RIPK1 independent apoptosis wherein FADD can directly bind to caspase-8 (241). Moreover, necroptosis ensues in cells lacking FADD or caspase-8, suggesting on inhibitory role of FADD-procaspase-8-cFLIPL complex (241). With the help of caspase inhibitors, necroptosis can be studied further (76).

Considering this phenomenon, we were curious how RIPK1 is involved in regulating cell death in the liver. Since RIPK1 plays two roles in deciding between cell survival or death, it promotes cell survival through its scaffold properties and cell death through its kinase activity (242). It has been shown that mice lacking RIPK1 die at embryonic stage, however, kinase-inactive mutants of RIPK1 mice are viable and show resistance to TNF-induced cell death (243-246).

Moreover, naïve mice with liver parenchymal cell (LPC)-specific deletion of RIPK1 do not exhibit substantial liver damage. Hence, RIPK1 is dispensable for liver development. However, liver parenchymal cell (LPC)-specific deletion of NEMO ($NEMO^{LPC}$) mice develop massive liver pathology (247). Kinase-inactive $RIPK1^{D138N}$ mutant introduced in hepatocytes of $NEMO^{LPC}$ mice significantly reduced liver pathology. Mechanistically, NEMO prevents the formation of Complex IIb and reduces hepatocellular death (247). Additionally, Nec-1 administration or kinase-inactive RIPK1 knock-in mice showed significantly decreased liver damage following acetaminophen (APAP) and Concanavalin A (ConA) injection (248-251). All these studies suggest that RIPK1 kinase activity drives hepatocellular death (252). In our study, we detected severe apoptosis in liver tissue of *Fmr1*^{null} mice by showing higher activation of caspase 8 even at 3 hours after TNF/D-Gal treatment. Surprisingly, necroptosis was also induced in *Fmr1*^{null} mice. This is could be explained by prolonged presence of RIPK1

and increased phosphorylation of RIPK1 in *Fmr1*^{null} mice, which facilitates both apoptosis and necroptosis.

LCMV infection leads to cytotoxic CD8^{+} T cell mediated hepatocyte death. Our data clearly shows that both control and *Fmr1* KO mice exhibit hepatocytes apoptosis. Histologically, significant number of hepatocytes were positive for TUNEL signal in *Fmr1*^{null} mice. However, an increased presence of RIPK1, RIPK3 and p-MLKL in *Fmr1*^{null} mice was detected following LCMV infection suggesting additional necroptosis in the absence of FMR1. Unlike during TNF/D-Gal treatment and LCMV induced liver damage, we detected only change in markers of necroptosis but not apoptosis following BDL. We failed to detect any evidence suggesting dysregulation of apoptosis in *Fmr1*^{null} in our settings. Hence, we speculate that hepatocyte death in *Fmr1*^{null} mice was also induced by necroptosis.

It has been shown that necroptosis is involved in several liver disease models including hepatitis B and C virus infection, alcoholic liver disease, nonalcoholic steatohepatitis, drug-induced liver injury and autoimmune hepatitis (249, 253-256). Furthermore, *Afonso et al.,* identified that necroptosis is activated in liver tissue of human patients diagnosed with primary biliary cholangitis (253). Activation of necroptosis was detectable in BDL-operated mice, which was confirmed by reduced necroptosis in *RIPK3* KO mice (253). Consistently, treatment with Nec-1s can alleviate pathology during TNF/D-Gal stimulation and BDL in *Fmr1*^{null} mice.

Taken together, we can conclude that loss of FMRP triggers apoptosis as well as necroptosis.

Since degradation of IkBα and nuclear translocation of p65 were identified in both *Fmr1*^{null} and control mice, we conclude that the NF-kB pathway was activated in both groups. We did not detect a significant difference at early time points, but at later time points we observed a slightly but significantly increased expression of Il2, Ccl2, Cxcl10 and Cxcl12 in *Fmr1*^{null} liver tissue when compared with controls. These results suggested that TNF-mediated NF-κB activation is only marginally affected in *Fmr1*^{null} mice. This possibility can be supported by finding of *Xu et al.,* who identified that lack of TBK1 induces massive cell death after TNF treatment, while NF-κB activation was not significantly affected (257).

It has been shown that the *Fmr1* mutant drosophila showed dysregulation of metabolism (258). *Leboucher et al.,* characterized the liver proteome of *Fmr1*^{null} and WT littermate mice by using quantitative mass spectrometry. They found dysregulated proteins related with oxidation-reduction processes, lipid metabolic processes, cholesterol metabolism processes and bile acid biosynthetic processes (259). There are no reports available showing severe liver pathology in Fragile X syndrome patients. However, after analyzing Fragile X

Syndrome patient serum samples, reduced glucose and insulin levels and increased circulating free fatty acids have been found (259). Consistently, there are significant differences in obesity rates in young fragile X males (31%) compared to age matched controls (18%) (260).

Necroptosis and activation of RIPK1 are associated with a variety of neurological diseases including Alzheimer's disease, amyotrophic lateral sclerosis (ALS) and multiple sclerosis. Hence, TNFR1-deficient mice exhibit reduced amyloid β generation and disease symptoms during Alzheimer model systems. Notably, it has been shown that FMRP is crucial for regulating local protein synthesis at developing synapses (261, 262).

Meanwhile, TNF has been shown to regulate synaptic plasticity, including the Hebbian synaptic plasticity and the synaptic scaling, in different brain areas such as the cortex, striatum and hippocampus. It is also an important cytokine, which plays a role in inflammation, proliferation, and development of neurons (263). Activation of TNFR1 has been found to affect synaptic scaling (264, 265).

Moreover, TNF promotes neurotoxic effects during liver disease and acute ammonia intoxication (266). According to our data, both FMRP mRNA and protein expression were upregulated after TNF treatment, suggesting that FMRP is involved in regulating TNF signaling. Additionally, when TNFR2-Fc fusion protein (Etanercept) as TNF inhibitor was administered, we found reduced presence of liver enzymes including ALT, AST and lactate dehydrogenase in the sera of LCMV infected *Fmr1*^{null} mice when compared with untreated *Fmr1*^{null} animals. TNF-mediated cell death blockage could rescue the severe liver pathology in the absence of FMRP.

In summary, we identified a protective role of FMRP in TNF-mediated liver damage.

In study of immune cells in liver regeneration, we have identified that $CD169^+$ macrophages are critical for liver regeneration after partial hepatectomy (PHx). Mice that lack $CD169^+$ macrophages display impaired liver regeneration after partial hepatectomy (PHx) and show severe disease symptom. Mechanistically, depletion of $CD169^+$ macrophages resulted in reduced IL-6 expression following PHx and consequently reduced activation of STAT3 signaling pathways. STAT3 activation is a paramount event in the healing and regeneration of liver tissue, which is activated by secretion of IL-6 (207). Administration of recombinant IL-6/IL-6R could rescue defective liver regeneration after PHx in the absence of $CD169^+$ macrophages. Hepatocytes have the distinctive capacity to replicate and contribute to the rapid restoration of liver function after PHx, liver transplant or toxic injury (267). PHx is a widely used model to study liver regeneration. The model we used in our study was 70% partial hepatectomy, in which the two biggest lobes of the liver are surgically removed. Quiescent cells in the remaining liver rapidly proliferate and restore the liver mass within a few days. In previous studies, multiple cytokines have been characterized to contribute to liver regeneration (198, 202). IL-6 is one critical cytokine to promote liver regeneration. *Cressman et al.,* first identified that IL-6 deficient mice displayed decreased hepatocellular proliferation, increased necrosis, reduced liver regeneration (207).

Additionally, *Modares et al.,* recently characterized that IL-6 trans-signaling, not classic signaling, regulates liver regeneration after PHx (208). It has been reported that Kupffer cells are one source of IL-6 (268). After PHx, gut-derived factors such as lipopolysaccharide (LPS) reaches the liver through the portal vein and activate liver-resident Kupffer cells to produce IL-6 (197). Furthermore, depletion of Kupffer cells results in decreased liver regeneration and increases the mortality after PHx (269).

It has been reported that macrophage colony stimulating factor (M-CSF) deficiency results in impaired liver regeneration as well (270). Furthermore, macrophage depleted mice show reduced liver regeneration and succumbed after PHx (269). However, traditional depletion of macrophages is unspecific and leads to global macrophage depletion. The liver has heterogeneous macrophage populations (269). $CD169^+$ macrophages are one of the subpopulations of macrophages. $CD169^+$ macrophages can be depleted specifically using transgenic mice expressing human diphtheria toxin receptor under CD169 promoter (CD169-DTR) (134). Diphtheria toxin (DT) is usually nontoxic to mice since they do not express the DT receptor. The $CD169^+$ macrophages in these transgenic mice express the DT receptor. Once

these mice are injected with DT, only CD169$^+$ macrophages undergo apoptosis, hence it serves as a great tool to study CD169$^+$ macrophages (134).

We observed reduced RNA and protein expression levels of IL-6 in the liver tissue harvested from DT-treated CD169-DTR mice compared to control animals. Hence, we conclude that one particular cell population of macrophages (CD169$^+$ macrophages) contributes to IL-6 production following PHx. It has been reported that CD169$^+$ macrophages regulate cytokine production such as IFN-I in response to vesicular stomatitis virus (VSV) infection, as well as lymphocytic choriomeningitis virus (LCMV) infection (271, 272).

To further characterize the effects of IL-6 signaling in CD169$^+$ cells following PHx, we administered Hyper IL-6 to DT-treated CD169-DTR mice. The liver weight/body weight ratio in CD169-DTR DT-treated animals after PHx following treatment with Hyper IL-6 was comparable to that in untreated CD169-DTR mice following PHx, indicating that injection of Hyper IL-6 could restore liver regeneration in CD169$^+$ macrophage depleted mice. *Peters et al.,* showed that Hyper-IL-6 directly stimulates gp130 even in the absence of membrane-bound IL-6R to facilitate liver regeneration through the activation of STAT3 (273). We also observed that increased activation of STAT3, while we did not find significant differences in either ERK or NF-κB activation following injection with Hyper IL-6. Consistently, only phosphorylation of STAT3 was reduced in the absence of CD169$^+$ cells, in contrast to expression of IκBα and phosphorylation of ERK. Hence, it is highly possible that CD169$^+$ macrophages promote liver regeneration through IL-6/STAT3 signaling. To explore whether IL-6 is produced by CD169$^+$ cells, further studies such as fluorescence in situ hybridization (FISH) assay can be used.

It still remains to be answered how these findings can be transferred to liver regeneration in humans. It has been shown that human macrophages can express CD169 (274). Considering our data, we observed higher numbers of CD169$^+$ macrophages in the regenerating liver lobe by using flow cytometry. Although these results suggest a direct link of CD169$^+$ macrophages in secreting IL-6 after PHx, the implications in human health need to be determined.

Whether these increased cell populations can be detected in the human regenerating liver, or, whether these cell populations similarly contribute to induction of IL-6 expression during liver regeneration remains unknown. If CD169$^+$ macrophages could be a major contributor of IL-6 production, CD169$^+$ macrophages could be used as potential biomarker for patients to evaluate the capacity of liver regeneration.

Our study shows that B cells display similar effects on liver regeneration as $CD169^+$ macrophages. A previous study showed attenuated liver fibrosis in absence of B cells after Carbon tetrachloride (CCl4) treatment, but the role in the liver regeneration was not shown (275). According to our data, we observed impaired liver regeneration in B-cell deficient mice following PHx. In line with this we also observed reduced liver regeneration and slight but significant increased liver pathology in B cell-activating factor receptor (*Baffr*) KO mice following PHx.

It has been well characterized that BAFFR is critical for B cell development (276). We detected reduced B cells numbers in the spleen of *Baffr* KO mice compared to control mice. Additionally, B cells are critical for organization of the lymphoid tissue as B cell–deficient mice exhibit reduced presence of metallophilic $CD169^+$ macrophages in the spleen (138, 277). Interestingly, when purified B cells from WT mice were adoptively transferred into B cell deficient mice, we observed that $CD169^+$ macrophages were restored. Taken together, we conclude that lack of B cells was associated with the reduced presence of $CD169^+$ macrophages, which results in impaired liver regeneration in B cell deficient mice following PHx. As expected, our data showed reduced IL-6 expression in B cell deficient mice following PHx.

In summary, we found that B cell–mediated maintenance of $CD169^+$ macrophages contributes to IL-6 production and liver regeneration.

4. References

1. Abdel-Misih SR, Bloomston M. 2010. Liver anatomy. Surg Clin North Am 90:643-53.
2. Nykonenko A, Vavra P, Zonca P. 2017. Anatomic Peculiarities of Pig and Human Liver. Exp Clin Transplant 15:21-26.
3. Trefts E, Gannon M, Wasserman DH. 2017. The liver. Curr Biol 27:R1147-R1151.
4. Bismuth H. 1982. Surgical anatomy and anatomical surgery of the liver. World J Surg 6:3-9.
5. Eipel C, Abshagen K, Vollmar B. 2010. Regulation of hepatic blood flow: the hepatic arterial buffer response revisited. World J Gastroenterol 16:6046-57.
6. Vollmar B, Menger MD. 2009. The hepatic microcirculation: mechanistic contributions and therapeutic targets in liver injury and repair. Physiol Rev 89:1269-339.
7. Kelley WN. 1989. Textbook of internal medicine. Lippincott, Philadelphia.
8. Kmiec Z. 2001. Cooperation of liver cells in health and disease. Adv Anat Embryol Cell Biol 161:III-XIII, 1-151.
9. Rowe IA. 2017. Lessons from Epidemiology: The Burden of Liver Disease. Dig Dis 35:304-309.
10. Talwani R, Gilliam BL, Howell C. 2011. Infectious diseases and the liver. Clin Liver Dis 15:111-30.
11. Luedde T, Kaplowitz N, Schwabe RF. 2014. Cell death and cell death responses in liver disease: mechanisms and clinical relevance. Gastroenterology 147:765-783 e4.
12. Iredale JP, Benyon RC, Pickering J, McCullen M, Northrop M, Pawley S, Hovell C, Arthur MJ. 1998. Mechanisms of spontaneous resolution of rat liver fibrosis. Hepatic stellate cell apoptosis and reduced hepatic expression of metalloproteinase inhibitors. J Clin Invest 102:538-49.
13. Rehermann B. 2013. Pathogenesis of chronic viral hepatitis: differential roles of T cells and NK cells. Nat Med 19:859-68.
14. Knolle PA, Thimme R. 2014. Hepatic immune regulation and its involvement in viral hepatitis infection. Gastroenterology 146:1193-207.
15. Wang H, Sun L, Su L, Rizo J, Liu L, Wang LF, Wang FS, Wang X. 2014. Mixed lineage kinase domain-like protein MLKL causes necrotic membrane disruption upon phosphorylation by RIP3. Mol Cell 54:133-146.

16. Nanji AA, Hiller-Sturmhofel S. 1997. Apoptosis and necrosis: two types of cell death in alcoholic liver disease. Alcohol Health Res World 21:325-30.
17. Feldstein AE, Canbay A, Angulo P, Taniai M, Burgart LJ, Lindor KD, Gores GJ. 2003. Hepatocyte apoptosis and fas expression are prominent features of human nonalcoholic steatohepatitis. Gastroenterology 125:437-43.
18. Ziol M, Tepper M, Lohez M, Arcangeli G, Ganne N, Christidis C, Trinchet JC, Beaugrand M, Guillet JG, Guettier C. 2001. Clinical and biological relevance of hepatocyte apoptosis in alcoholic hepatitis. J Hepatol 34:254-60.
19. Kazdoba TM, Leach PT, Silverman JL, Crawley JN. 2014. Modeling fragile X syndrome in the Fmr1 knockout mouse. Intractable Rare Dis Res 3:118-33.
20. Martin JP, Bell J. 1943. A Pedigree of Mental Defect Showing Sex-Linkage. J Neurol Psychiatry 6:154-7.
21. Lubs HA. 1969. A marker X chromosome. Am J Hum Genet 21:231-44.
22. Sutherland GR. 1977. Fragile sites on human chromosomes: demonstration of their dependence on the type of tissue culture medium. Science 197:265-6.
23. Verkerk AJ, Pieretti M, Sutcliffe JS, Fu YH, Kuhl DP, Pizzuti A, Reiner O, Richards S, Victoria MF, Zhang FP, et al. 1991. Identification of a gene (FMR-1) containing a CGG repeat coincident with a breakpoint cluster region exhibiting length variation in fragile X syndrome. Cell 65:905-14.
24. Pieretti M, Zhang FP, Fu YH, Warren ST, Oostra BA, Caskey CT, Nelson DL. 1991. Absence of expression of the FMR-1 gene in fragile X syndrome. Cell 66:817-22.
25. Siomi H, Choi M, Siomi MC, Nussbaum RL, Dreyfuss G. 1994. Essential role for KH domains in RNA binding: impaired RNA binding by a mutation in the KH domain of FMR1 that causes fragile X syndrome. Cell 77:33-9.
26. Saldarriaga W, Tassone F, Gonzalez-Teshima LY, Forero-Forero JV, Ayala-Zapata S, Hagerman R. 2014. Fragile X syndrome. Colomb Med (Cali) 45:190-8.
27. Willemsen R, Levenga J, Oostra BA. 2011. CGG repeat in the FMR1 gene: size matters. Clin Genet 80:214-25.
28. Ciaccio C, Fontana L, Milani D, Tabano S, Miozzo M, Esposito S. 2017. Fragile X syndrome: a review of clinical and molecular diagnoses. Ital J Pediatr 43:39.
29. Siomi MC, Higashijima K, Ishizuka A, Siomi H. 2002. Casein kinase II phosphorylates the fragile X mental retardation protein and modulates its biological properties. Mol Cell Biol 22:8438-47.

30. Ishizuka A, Siomi MC, Siomi H. 2002. A Drosophila fragile X protein interacts with components of RNAi and ribosomal proteins. Genes Dev 16:2497-508.
31. Anonymous. 1994. Fmr1 knockout mice: a model to study fragile X mental retardation. The Dutch-Belgian Fragile X Consortium. Cell 78:23-33.
32. Luo Y, Shan G, Guo W, Smrt RD, Johnson EB, Li X, Pfeiffer RL, Szulwach KE, Duan R, Barkho BZ, Li W, Liu C, Jin P, Zhao X. 2010. Fragile x mental retardation protein regulates proliferation and differentiation of adult neural stem/progenitor cells. PLoS Genet 6:e1000898.
33. Shen M, Wang F, Li M, Sah N, Stockton ME, Tidei JJ, Gao Y, Korabelnikov T, Kannan S, Vevea JD, Chapman ER, Bhattacharyya A, van Praag H, Zhao X. 2019. Reduced mitochondrial fusion and Huntingtin levels contribute to impaired dendritic maturation and behavioral deficits in Fmr1-mutant mice. Nat Neurosci 22:386-400.
34. Carmo C, Naia L, Lopes C, Rego AC. 2018. Mitochondrial Dysfunction in Huntington's Disease. Adv Exp Med Biol 1049:59-83.
35. Dolen G, Osterweil E, Rao BS, Smith GB, Auerbach BD, Chattarji S, Bear MF. 2007. Correction of fragile X syndrome in mice. Neuron 56:955-62.
36. Levenga J, Hayashi S, de Vrij FM, Koekkoek SK, van der Linde HC, Nieuwenhuizen I, Song C, Buijsen RA, Pop AS, Gomezmancilla B, Nelson DL, Willemsen R, Gasparini F, Oostra BA. 2011. AFQ056, a new mGluR5 antagonist for treatment of fragile X syndrome. Neurobiol Dis 42:311-7.
37. Sourial M, Cheng C, Doering LC. 2013. Progress toward therapeutic potential for AFQ056 in Fragile X syndrome. J Exp Pharmacol 5:45-54.
38. Jacquemont S, Berry-Kravis E, Hagerman R, von Raison F, Gasparini F, Apostol G, Ufer M, Des Portes V, Gomez-Mancilla B. 2014. The challenges of clinical trials in fragile X syndrome. Psychopharmacology (Berl) 231:1237-50.
39. Scharf SH, Jaeschke G, Wettstein JG, Lindemann L. 2015. Metabotropic glutamate receptor 5 as drug target for Fragile X syndrome. Curr Opin Pharmacol 20:124-34.
40. Jacquemont S, Curie A, des Portes V, Torrioli MG, Berry-Kravis E, Hagerman RJ, Ramos FJ, Cornish K, He Y, Paulding C, Neri G, Chen F, Hadjikhani N, Martinet D, Meyer J, Beckmann JS, Delange K, Brun A, Bussy G, Gasparini F, Hilse T, Floesser A, Branson J, Bilbe G, Johns D, Gomez-Mancilla B. 2011. Epigenetic modification of the FMR1 gene in fragile X syndrome is associated with differential response to the mGluR5 antagonist AFQ056. Sci Transl Med 3:64ra1.

41. O'Connor RM, Stone EF, Wayne CR, Marcinkevicius EV, Ulgherait M, Delventhal R, Pantalia MM, Hill VM, Zhou CG, McAllister S, Chen A, Ziegenfuss JS, Grueber WB, Canman JC, Shirasu-Hiza MM. 2017. A Drosophila model of Fragile X syndrome exhibits defects in phagocytosis by innate immune cells. J Cell Biol 216:595-605.
42. Zhou Z, Cao M, Guo Y, Zhao L, Wang J, Jia X, Li J, Wang C, Gabriel G, Xue Q, Yi Y, Cui S, Jin Q, Wang J, Deng T. 2014. Fragile X mental retardation protein stimulates ribonucleoprotein assembly of influenza A virus. Nat Commun 5:3259.
43. Soto-Acosta R, Xie X, Shan C, Baker CK, Shi PY, Rossi SL, Garcia-Blanco MA, Bradrick S. 2018. Fragile X mental retardation protein is a Zika virus restriction factor that is antagonized by subgenomic flaviviral RNA. Elife 7.
44. Feng Y, Gutekunst CA, Eberhart DE, Yi H, Warren ST, Hersch SM. 1997. Fragile X mental retardation protein: nucleocytoplasmic shuttling and association with somatodendritic ribosomes. J Neurosci 17:1539-47.
45. Xu H, Rosales-Reynoso MA, Barros-Nunez P, Peprah E. 2013. DNA repair/replication transcripts are down regulated in patients with Fragile X Syndrome. BMC Res Notes 6:90.
46. Alpatov R, Lesch BJ, Nakamoto-Kinoshita M, Blanco A, Chen S, Stutzer A, Armache KJ, Simon MD, Xu C, Ali M, Murn J, Prisic S, Kutateladze TG, Vakoc CR, Min J, Kingston RE, Fischle W, Warren ST, Page DC, Shi Y. 2014. A chromatin-dependent role of the fragile X mental retardation protein FMRP in the DNA damage response. Cell 157:869-81.
47. Isabelle M, Moreel X, Gagne JP, Rouleau M, Ethier C, Gagne P, Hendzel MJ, Poirier GG. 2010. Investigation of PARP-1, PARP-2, and PARG interactomes by affinity-purification mass spectrometry. Proteome Sci 8:22.
48. Jenkins EC, Tassone F, Ye L, Gu H, Xi M, Velinov M, Brown WT, Hagerman RJ, Hagerman PJ. 2008. Reduced telomere length in older men with premutation alleles of the fragile X mental retardation 1 gene. Am J Med Genet A 146A:1543-6.
49. Tian H, Cao YX, Zhang XS, Liao WP, Yi YH, Lian J, Liu L, Huang HL, Liu WJ, Yin MM, Liang M, Shan G, Sun F. 2013. The targeting and functions of miRNA-383 are mediated by FMRP during spermatogenesis. Cell Death Dis 4:e617.
50. Jeon SJ, Seo JE, Yang SI, Choi JW, Wells D, Shin CY, Ko KH. 2011. Cellular stress-induced up-regulation of FMRP promotes cell survival by modulating PI3K-Akt phosphorylation cascades. J Biomed Sci 18:17.

51. Ascano M, Jr., Mukherjee N, Bandaru P, Miller JB, Nusbaum JD, Corcoran DL, Langlois C, Munschauer M, Dewell S, Hafner M, Williams Z, Ohler U, Tuschl T. 2012. FMRP targets distinct mRNA sequence elements to regulate protein expression. Nature 492:382-6.
52. Johannisson R, Rehder H, Wendt V, Schwinger E. 1987. Spermatogenesis in two patients with the fragile X syndrome. I. Histology: light and electron microscopy. Hum Genet 76:141-7.
53. Old LJ. 1985. Tumor necrosis factor (TNF). Science 230:630-2.
54. Algire GH, Legallais FY, Anderson BF. 1952. Vascular reactions of normal and malignant tissues in vivo. V. The role of hypotension in the action of a bacterial polysaccharide on tumors. J Natl Cancer Inst 12:1279-95.
55. Carswell EA, Old LJ, Kassel RL, Green S, Fiore N, Williamson B. 1975. An endotoxin-induced serum factor that causes necrosis of tumors. Proc Natl Acad Sci U S A 72:3666-70.
56. Aggarwal BB, Kohr WJ, Hass PE, Moffat B, Spencer SA, Henzel WJ, Bringman TS, Nedwin GE, Goeddel DV, Harkins RN. 1985. Human tumor necrosis factor. Production, purification, and characterization. J Biol Chem 260:2345-54.
57. Matthews N, Watkins JF. 1978. Tumour-necrosis factor from the rabbit. I. Mode of action, specificity and physicochemical properties. Br J Cancer 38:302-9.
58. Ruff MR, Gifford GE. 1981. Rabbit tumor necrosis factor: mechanism of action. Infect Immun 31:380-5.
59. Mannel DN, Moore RN, Mergenhagen SE. 1980. Macrophages as a source of tumoricidal activity (tumor-necrotizing factor). Infect Immun 30:523-30.
60. Aggarwal BB, Gupta SC, Kim JH. 2012. Historical perspectives on tumor necrosis factor and its superfamily: 25 years later, a golden journey. Blood 119:651-65.
61. Aggarwal BB. 2003. Signalling pathways of the TNF superfamily: a double-edged sword. Nat Rev Immunol 3:745-56.
62. Locksley RM, Killeen N, Lenardo MJ. 2001. The TNF and TNF receptor superfamilies: integrating mammalian biology. Cell 104:487-501.
63. French LE, Tschopp J. 2003. Protein-based therapeutic approaches targeting death receptors. Cell Death Differ 10:117-23.
64. Lavrik I, Golks A, Krammer PH. 2005. Death receptor signaling. J Cell Sci 118:265-7.
65. Li J, Yin Q, Wu H. 2013. Structural basis of signal transduction in the TNF receptor superfamily. Adv Immunol 119:135-53.

66. Mukai Y, Nakamura T, Yoshikawa M, Yoshioka Y, Tsunoda S, Nakagawa S, Yamagata Y, Tsutsumi Y. 2010. Solution of the structure of the TNF-TNFR2 complex. Sci Signal 3:ra83.

67. Mukai Y, Shibata H, Nakamura T, Yoshioka Y, Abe Y, Nomura T, Taniai M, Ohta T, Ikemizu S, Nakagawa S, Tsunoda S, Kamada H, Yamagata Y, Tsutsumi Y. 2009. Structure-function relationship of tumor necrosis factor (TNF) and its receptor interaction based on 3D structural analysis of a fully active TNFR1-selective TNF mutant. J Mol Biol 385:1221-9.

68. Horiuchi T, Mitoma H, Harashima S, Tsukamoto H, Shimoda T. 2010. Transmembrane TNF-alpha: structure, function and interaction with anti-TNF agents. Rheumatology (Oxford) 49:1215-28.

69. Kriegler M, Perez C, DeFay K, Albert I, Lu SD. 1988. A novel form of TNF/cachectin is a cell surface cytotoxic transmembrane protein: ramifications for the complex physiology of TNF. Cell 53:45-53.

70. Tang P, Hung MC, Klostergaard J. 1996. Human pro-tumor necrosis factor is a homotrimer. Biochemistry 35:8216-25.

71. Adrain C, Zettl M, Christova Y, Taylor N, Freeman M. 2012. Tumor necrosis factor signaling requires iRhom2 to promote trafficking and activation of TACE. Science 335:225-8.

72. McIlwain DR, Lang PA, Maretzky T, Hamada K, Ohishi K, Maney SK, Berger T, Murthy A, Duncan G, Xu HC, Lang KS, Haussinger D, Wakeham A, Itie-Youten A, Khokha R, Ohashi PS, Blobel CP, Mak TW. 2012. iRhom2 regulation of TACE controls TNF-mediated protection against Listeria and responses to LPS. Science 335:229-32.

73. Grell M, Douni E, Wajant H, Lohden M, Clauss M, Maxeiner B, Georgopoulos S, Lesslauer W, Kollias G, Pfizenmaier K, Scheurich P. 1995. The transmembrane form of tumor necrosis factor is the prime activating ligand of the 80 kDa tumor necrosis factor receptor. Cell 83:793-802.

74. Brenner D, Blaser H, Mak TW. 2015. Regulation of tumour necrosis factor signalling: live or let die. Nat Rev Immunol 15:362-74.

75. Ofengeim D, Yuan J. 2013. Regulation of RIP1 kinase signalling at the crossroads of inflammation and cell death. Nat Rev Mol Cell Biol 14:727-36.

76. Yuan J, Amin P, Ofengeim D. 2019. Necroptosis and RIPK1-mediated neuroinflammation in CNS diseases. Nat Rev Neurosci 20:19-33.

77. Kerr JF, Wyllie AH, Currie AR. 1972. Apoptosis: a basic biological phenomenon with wide-ranging implications in tissue kinetics. Br J Cancer 26:239-57.

78. Vandenabeele P, Galluzzi L, Vanden Berghe T, Kroemer G. 2010. Molecular mechanisms of necroptosis: an ordered cellular explosion. Nat Rev Mol Cell Biol 11:700-14.

79. Laster SM, Wood JG, Gooding LR. 1988. Tumor necrosis factor can induce both apoptic and necrotic forms of cell lysis. J Immunol 141:2629-34.

80. Wertz IE, O'Rourke KM, Zhou H, Eby M, Aravind L, Seshagiri S, Wu P, Wiesmann C, Baker R, Boone DL, Ma A, Koonin EV, Dixit VM. 2004. De-ubiquitination and ubiquitin ligase domains of A20 downregulate NF-kappaB signalling. Nature 430:694-9.

81. Wang L, Du F, Wang X. 2008. TNF-alpha induces two distinct caspase-8 activation pathways. Cell 133:693-703.

82. Hitomi J, Christofferson DE, Ng A, Yao J, Degterev A, Xavier RJ, Yuan J. 2008. Identification of a molecular signaling network that regulates a cellular necrotic cell death pathway. Cell 135:1311-23.

83. Carrington PE, Sandu C, Wei Y, Hill JM, Morisawa G, Huang T, Gavathiotis E, Wei Y, Werner MH. 2006. The structure of FADD and its mode of interaction with procaspase-8. Mol Cell 22:599-610.

84. Feoktistova M, Geserick P, Kellert B, Dimitrova DP, Langlais C, Hupe M, Cain K, MacFarlane M, Hacker G, Leverkus M. 2011. cIAPs block Ripoptosome formation, a RIP1/caspase-8 containing intracellular cell death complex differentially regulated by cFLIP isoforms. Mol Cell 43:449-63.

85. Bertrand MJ, Milutinovic S, Dickson KM, Ho WC, Boudreault A, Durkin J, Gillard JW, Jaquith JB, Morris SJ, Barker PA. 2008. cIAP1 and cIAP2 facilitate cancer cell survival by functioning as E3 ligases that promote RIP1 ubiquitination. Mol Cell 30:689-700.

86. Vanden Berghe T, Linkermann A, Jouan-Lanhouet S, Walczak H, Vandenabeele P. 2014. Regulated necrosis: the expanding network of non-apoptotic cell death pathways. Nat Rev Mol Cell Biol 15:135-47.

87. Su L, Quade B, Wang H, Sun L, Wang X, Rizo J. 2014. A plug release mechanism for membrane permeation by MLKL. Structure 22:1489-500.

88. Slee EA, Zhu H, Chow SC, MacFarlane M, Nicholson DW, Cohen GM. 1996. Benzyloxycarbonyl-Val-Ala-Asp (OMe) fluoromethylketone (Z-VAD.FMK) inhibits apoptosis by blocking the processing of CPP32. Biochem J 315 (Pt 1):21-4.
89. Beug ST, Beauregard CE, Healy C, Sanda T, St-Jean M, Chabot J, Walker DE, Mohan A, Earl N, Lun X, Senger DL, Robbins SM, Staeheli P, Forsyth PA, Alain T, LaCasse EC, Korneluk RG. 2017. Smac mimetics synergize with immune checkpoint inhibitors to promote tumour immunity against glioblastoma. Nat Commun 8.
90. Matton A, Buydens P, Finne E, Govaerts J, Vanhaelst L. 1991. Analysis of the receptor specificity of tolerance induction in stress versus opioid-related prolactin secretion in rats. J Endocrinol 128:281-5.
91. Degterev A, Huang Z, Boyce M, Li Y, Jagtap P, Mizushima N, Cuny GD, Mitchison TJ, Moskowitz MA, Yuan J. 2005. Chemical inhibitor of nonapoptotic cell death with therapeutic potential for ischemic brain injury. Nat Chem Biol 1:112-9.
92. Degterev A, Maki JL, Yuan J. 2013. Activity and specificity of necrostatin-1, small-molecule inhibitor of RIP1 kinase. Cell Death Differ 20:366.
93. Takahashi N, Duprez L, Grootjans S, Cauwels A, Nerinckx W, DuHadaway JB, Goossens V, Roelandt R, Van Hauwermeiren F, Libert C, Declercq W, Callewaert N, Prendergast GC, Degterev A, Yuan J, Vandenabeele P. 2012. Necrostatin-1 analogues: critical issues on the specificity, activity and in vivo use in experimental disease models. Cell Death Dis 3:e437.
94. Auperin DD, Romanowski V, Galinski M, Bishop DH. 1984. Sequencing studies of pichinde arenavirus S RNA indicate a novel coding strategy, an ambisense viral S RNA. J Virol 52:897-904.
95. Lee KJ, Novella IS, Teng MN, Oldstone MB, de La Torre JC. 2000. NP and L proteins of lymphocytic choriomeningitis virus (LCMV) are sufficient for efficient transcription and replication of LCMV genomic RNA analogs. J Virol 74:3470-7.
96. Riviere Y, Ahmed R, Southern PJ, Buchmeier MJ, Dutko FJ, Oldstone MB. 1985. The S RNA segment of lymphocytic choriomeningitis virus codes for the nucleoprotein and glycoproteins 1 and 2. J Virol 53:966-8.
97. Hastie KM, Igonet S, Sullivan BM, Legrand P, Zandonatti MA, Robinson JE, Garry RF, Rey FA, Oldstone MB, Saphire EO. 2016. Crystal structure of the prefusion surface glycoprotein of the prototypic arenavirus LCMV. Nat Struct Mol Biol 23:513-521.

98. Eichler R, Lenz O, Strecker T, Eickmann M, Klenk HD, Garten W. 2003. Identification of Lassa virus glycoprotein signal peptide as a trans-acting maturation factor. EMBO Rep 4:1084-8.

99. Cao W, Henry MD, Borrow P, Yamada H, Elder JH, Ravkov EV, Nichol ST, Compans RW, Campbell KP, Oldstone MB. 1998. Identification of alpha-dystroglycan as a receptor for lymphocytic choriomeningitis virus and Lassa fever virus. Science 282:2079-81.

100. Salvato MS, Shimomaye EM. 1989. The completed sequence of lymphocytic choriomeningitis virus reveals a unique RNA structure and a gene for a zinc finger protein. Virology 173:1-10.

101. Salvato M, Shimomaye E, Oldstone MB. 1989. The primary structure of the lymphocytic choriomeningitis virus L gene encodes a putative RNA polymerase. Virology 169:377-84.

102. Welsh RM, Seedhom MO. 2008. Lymphocytic choriomeningitis virus (LCMV): propagation, quantitation, and storage. Curr Protoc Microbiol Chapter 15:Unit 15A 1.

103. Janeway CA, Jr., Medzhitov R. 2002. Innate immune recognition. Annu Rev Immunol 20:197-216.

104. Takeuchi O, Akira S. 2010. Pattern recognition receptors and inflammation. Cell 140:805-20.

105. Kawai T, Akira S. 2010. The role of pattern-recognition receptors in innate immunity: update on Toll-like receptors. Nat Immunol 11:373-84.

106. Kumar H, Kawai T, Akira S. 2011. Pathogen recognition by the innate immune system. Int Rev Immunol 30:16-34.

107. Steinman RM, Cohn ZA. 1973. Identification of a novel cell type in peripheral lymphoid organs of mice. I. Morphology, quantitation, tissue distribution. J Exp Med 137:1142-62.

108. Banchereau J, Steinman RM. 1998. Dendritic cells and the control of immunity. Nature 392:245-52.

109. Akira S, Uematsu S, Takeuchi O. 2006. Pathogen recognition and innate immunity. Cell 124:783-801.

110. Clark GJ, Angel N, Kato M, Lopez JA, MacDonald K, Vuckovic S, Hart DN. 2000. The role of dendritic cells in the innate immune system. Microbes Infect 2:257-72.

111. Chehimi J, Starr SE, Kawashima H, Miller DS, Trinchieri G, Perussia B, Bandyopadhyay S. 1989. Dendritic cells and IFN-alpha-producing cells are two

functionally distinct non-B, non-monocytic HLA-DR+ cell subsets in human peripheral blood. Immunology 68:486-90.

112. Hemmi H, Akira S. 2005. TLR signalling and the function of dendritic cells. Chem Immunol Allergy 86:120-135.
113. Liu YJ. 2005. IPC: professional type 1 interferon-producing cells and plasmacytoid dendritic cell precursors. Annu Rev Immunol 23:275-306.
114. Xia CQ, Peng R, Chernatynskaya AV, Yuan L, Carter C, Valentine J, Sobel E, Atkinson MA, Clare-Salzler MJ. 2014. Increased IFN-alpha-producing plasmacytoid dendritic cells (pDCs) in human Th1-mediated type 1 diabetes: pDCs augment Th1 responses through IFN-alpha production. J Immunol 193:1024-34.
115. Swiecki M, Gilfillan S, Vermi W, Wang Y, Colonna M. 2010. Plasmacytoid dendritic cell ablation impacts early interferon responses and antiviral NK and CD8(+) T cell accrual. Immunity 33:955-66.
116. Jung S, Unutmaz D, Wong P, Sano G, De los Santos K, Sparwasser T, Wu S, Vuthoori S, Ko K, Zavala F, Pamer EG, Littman DR, Lang RA. 2002. In vivo depletion of CD11c+ dendritic cells abrogates priming of CD8+ T cells by exogenous cell-associated antigens. Immunity 17:211-20.
117. Nathan CF, Hibbs JB, Jr. 1991. Role of nitric oxide synthesis in macrophage antimicrobial activity. Curr Opin Immunol 3:65-70.
118. Nathan CF. 1987. Secretory products of macrophages. J Clin Invest 79:319-26.
119. Nathan C. 2008. Metchnikoff's Legacy in 2008. Nat Immunol 9:695-8.
120. Rabinovitch M. 1995. Professional and non-professional phagocytes: an introduction. Trends Cell Biol 5:85-7.
121. Gordon S. 2016. Phagocytosis: An Immunobiologic Process. Immunity 44:463-475.
122. Delamarre L, Pack M, Chang H, Mellman I, Trombetta ES. 2005. Differential lysosomal proteolysis in antigen-presenting cells determines antigen fate. Science 307:1630-4.
123. Savina A, Amigorena S. 2007. Phagocytosis and antigen presentation in dendritic cells. Immunol Rev 219:143-56.
124. Mills CD, Kincaid K, Alt JM, Heilman MJ, Hill AM. 2000. M-1/M-2 macrophages and the Th1/Th2 paradigm. J Immunol 164:6166-73.
125. Mackaness GB. 1977. Cellular immunity and the parasite. Adv Exp Med Biol 93:65-73.

126. O'Shea JJ, Murray PJ. 2008. Cytokine signaling modules in inflammatory responses. Immunity 28:477-87.

127. Mosser DM, Edwards JP. 2008. Exploring the full spectrum of macrophage activation. Nat Rev Immunol 8:958-69.

128. Mebius RE, Kraal G. 2005. Structure and function of the spleen. Nat Rev Immunol 5:606-16.

129. Kohyama M, Ise W, Edelson BT, Wilker PR, Hildner K, Mejia C, Frazier WA, Murphy TL, Murphy KM. 2009. Role for Spi-C in the development of red pulp macrophages and splenic iron homeostasis. Nature 457:318-21.

130. Gordon S, Taylor PR. 2005. Monocyte and macrophage heterogeneity. Nat Rev Immunol 5:953-64.

131. Elomaa O, Kangas M, Sahlberg C, Tuukkanen J, Sormunen R, Liakka A, Thesleff I, Kraal G, Tryggvason K. 1995. Cloning of a novel bacteria-binding receptor structurally related to scavenger receptors and expressed in a subset of macrophages. Cell 80:603-9.

132. Borges da Silva H, Fonseca R, Pereira RM, Cassado Ados A, Alvarez JM, D'Imperio Lima MR. 2015. Splenic Macrophage Subsets and Their Function during Blood-Borne Infections. Front Immunol 6:480.

133. Kraal G, Janse M. 1986. Marginal metallophilic cells of the mouse spleen identified by a monoclonal antibody. Immunology 58:665-9.

134. Miyake Y, Asano K, Kaise H, Uemura M, Nakayama M, Tanaka M. 2007. Critical role of macrophages in the marginal zone in the suppression of immune responses to apoptotic cell-associated antigens. J Clin Invest 117:2268-78.

135. Perez OA, Yeung ST, Vera-Licona P, Romagnoli PA, Samji T, Ural BB, Maher L, Tanaka M, Khanna KM. 2017. CD169(+) macrophages orchestrate innate immune responses by regulating bacterial localization in the spleen. Sci Immunol 2.

136. Honke N, Shaabani N, Cadeddu G, Sorg UR, Zhang DE, Trilling M, Klingel K, Sauter M, Kandolf R, Gailus N, van Rooijen N, Burkart C, Baldus SE, Grusdat M, Lohning M, Hengel H, Pfeffer K, Tanaka M, Haussinger D, Recher M, Lang PA, Lang KS. 2011. Enforced viral replication activates adaptive immunity and is essential for the control of a cytopathic virus. Nat Immunol 13:51-7.

137. Shinde PV, Xu HC, Maney SK, Kloetgen A, Namineni S, Zhuang Y, Honke N, Shaabani N, Bellora N, Doerrenberg M, Trilling M, Pozdeev VI, van Rooijen N, Scheu S, Pfeffer K, Crocker PR, Tanaka M, Duggimpudi S, Knolle P, Heikenwalder M,

Ruland J, Mak TW, Brenner D, Pandyra AA, Hoell JI, Borkhardt A, Haussinger D, Lang KS, Lang PA. 2018. Tumor Necrosis Factor-Mediated Survival of CD169(+) Cells Promotes Immune Activation during Vesicular Stomatitis Virus Infection. J Virol 92.

138. Xu HC, Huang J, Khairnar V, Duhan V, Pandyra AA, Grusdat M, Shinde P, McIlwain DR, Maney SK, Gommerman J, Lohning M, Ohashi PS, Mak TW, Pieper K, Sic H, Speletas M, Eibel H, Ware CF, Tumanov AV, Kruglov AA, Nedospasov SA, Haussinger D, Recher M, Lang KS, Lang PA. 2015. Deficiency of the B cell-activating factor receptor results in limited CD169+ macrophage function during viral infection. J Virol 89:4748-59.

139. Nolte MA, Arens R, Kraus M, van Oers MH, Kraal G, van Lier RA, Mebius RE. 2004. B cells are crucial for both development and maintenance of the splenic marginal zone. J Immunol 172:3620-7.

140. Khairnar V, Duhan V, Maney SK, Honke N, Shaabani N, Pandyra AA, Seifert M, Pozdeev V, Xu HC, Sharma P, Baldin F, Marquardsen F, Merches K, Lang E, Kirschning C, Westendorf AM, Haussinger D, Lang F, Dittmer U, Kuppers R, Recher M, Hardt C, Scheffrahn I, Beauchemin N, Gothert JR, Singer BB, Lang PA, Lang KS. 2015. CEACAM1 induces B-cell survival and is essential for protective antiviral antibody production. Nat Commun 6:6217.

141. Junt T, Moseman EA, Iannacone M, Massberg S, Lang PA, Boes M, Fink K, Henrickson SE, Shayakhmetov DM, Di Paolo NC, van Rooijen N, Mempel TR, Whelan SP, von Andrian UH. 2007. Subcapsular sinus macrophages in lymph nodes clear lymph-borne viruses and present them to antiviral B cells. Nature 450:110-4.

142. Cooper MD, Alder MN. 2006. The evolution of adaptive immune systems. Cell 124:815-22.

143. Weigert MG, Cesari IM, Yonkovich SJ, Cohn M. 1970. Variability in the lambda light chain sequences of mouse antibody. Nature 228:1045-7.

144. Tonegawa S. 1976. Reiteration frequency of immunoglobulin light chain genes: further evidence for somatic generation of antibody diversity. Proc Natl Acad Sci U S A 73:203-7.

145. Oettinger MA, Schatz DG, Gorka C, Baltimore D. 1990. RAG-1 and RAG-2, adjacent genes that synergistically activate V(D)J recombination. Science 248:1517-23.

146. Davis MM, Chien YH, Gascoigne NR, Hedrick SM. 1984. A murine T cell receptor gene complex: isolation, structure and rearrangement. Immunol Rev 81:235-58.

147. Pieper K, Grimbacher B, Eibel H. 2013. B-cell biology and development. J Allergy Clin Immunol 131:959-71.

148. Fairfax KA, Kallies A, Nutt SL, Tarlinton DM. 2008. Plasma cell development: from B-cell subsets to long-term survival niches. Semin Immunol 20:49-58.

149. Nutt SL, Hodgkin PD, Tarlinton DM, Corcoran LM. 2015. The generation of antibody-secreting plasma cells. Nat Rev Immunol 15:160-71.

150. Tokoyoda K, Egawa T, Sugiyama T, Choi BI, Nagasawa T. 2004. Cellular niches controlling B lymphocyte behavior within bone marrow during development. Immunity 20:707-18.

151. Schneider P, MacKay F, Steiner V, Hofmann K, Bodmer JL, Holler N, Ambrose C, Lawton P, Bixler S, Acha-Orbea H, Valmori D, Romero P, Werner-Favre C, Zubler RH, Browning JL, Tschopp J. 1999. BAFF, a novel ligand of the tumor necrosis factor family, stimulates B cell growth. J Exp Med 189:1747-56.

152. Thompson JS, Bixler SA, Qian F, Vora K, Scott ML, Cachero TG, Hession C, Schneider P, Sizing ID, Mullen C, Strauch K, Zafari M, Benjamin CD, Tschopp J, Browning JL, Ambrose C. 2001. BAFF-R, a newly identified TNF receptor that specifically interacts with BAFF. Science 293:2108-11.

153. Basso K, Dalla-Favera R. 2012. Roles of BCL6 in normal and transformed germinal center B cells. Immunol Rev 247:172-83.

154. Klein U, Casola S, Cattoretti G, Shen Q, Lia M, Mo T, Ludwig T, Rajewsky K, Dalla-Favera R. 2006. Transcription factor IRF4 controls plasma cell differentiation and class-switch recombination. Nat Immunol 7:773-82.

155. Tumanov A, Kuprash D, Lagarkova M, Grivennikov S, Abe K, Shakhov A, Drutskaya L, Stewart C, Chervonsky A, Nedospasov S. 2002. Distinct role of surface lymphotoxin expressed by B cells in the organization of secondary lymphoid tissues. Immunity 17:239-50.

156. Rennert PD, Browning JL, Mebius R, Mackay F, Hochman PS. 1996. Surface lymphotoxin alpha/beta complex is required for the development of peripheral lymphoid organs. J Exp Med 184:1999-2006.

157. De Togni P, Goellner J, Ruddle NH, Streeter PR, Fick A, Mariathasan S, Smith SC, Carlson R, Shornick LP, Strauss-Schoenberger J, et al. 1994. Abnormal development of peripheral lymphoid organs in mice deficient in lymphotoxin. Science 264:703-7.

158. Banks TA, Rouse BT, Kerley MK, Blair PJ, Godfrey VL, Kuklin NA, Bouley DM, Thomas J, Kanangat S, Mucenski ML. 1995. Lymphotoxin-alpha-deficient mice.

Effects on secondary lymphoid organ development and humoral immune responsiveness. J Immunol 155:1685-93.

159. Shlomchik MJ, Weisel F. 2012. Germinal center selection and the development of memory B and plasma cells. Immunol Rev 247:52-63.
160. Victora GD, Nussenzweig MC. 2012. Germinal centers. Annu Rev Immunol 30:429-57.
161. Stavnezer J, Amemiya CT. 2004. Evolution of isotype switching. Semin Immunol 16:257-75.
162. Scollay R, Smith J, Stauffer V. 1986. Dynamics of early T cells: prothymocyte migration and proliferation in the adult mouse thymus. Immunol Rev 91:129-57.
163. Petrie HT. 2003. Cell migration and the control of post-natal T-cell lymphopoiesis in the thymus. Nat Rev Immunol 3:859-66.
164. Gaud G, Lesourne R, Love PE. 2018. Regulatory mechanisms in T cell receptor signalling. Nat Rev Immunol 18:485-497.
165. Smith-Garvin JE, Koretzky GA, Jordan MS. 2009. T cell activation. Annu Rev Immunol 27:591-619.
166. Rosendahl Huber S, van Beek J, de Jonge J, Luytjes W, van Baarle D. 2014. T cell responses to viral infections - opportunities for Peptide vaccination. Front Immunol 5:171.
167. Zhang S, Zhang H, Zhao J. 2009. The role of CD4 T cell help for CD8 CTL activation. Biochem Biophys Res Commun 384:405-8.
168. Bevan MJ. 2004. Helping the CD8(+) T-cell response. Nat Rev Immunol 4:595-602.
169. Lopez JA, Susanto O, Jenkins MR, Lukoyanova N, Sutton VR, Law RH, Johnston A, Bird CH, Bird PI, Whisstock JC, Trapani JA, Saibil HR, Voskoboinik I. 2013. Perforin forms transient pores on the target cell plasma membrane to facilitate rapid access of granzymes during killer cell attack. Blood 121:2659-68.
170. de Saint Basile G, Menasche G, Fischer A. 2010. Molecular mechanisms of biogenesis and exocytosis of cytotoxic granules. Nat Rev Immunol 10:568-79.
171. Smyth MJ, Trapani JA. 1998. The relative role of lymphocyte granule exocytosis versus death receptor-mediated cytotoxicity in viral pathophysiology. J Virol 72:1-9.
172. Moskophidis D, Lechner F, Pircher H, Zinkernagel RM. 1993. Virus persistence in acutely infected immunocompetent mice by exhaustion of antiviral cytotoxic effector T cells. Nature 362:758-61.

173. Gallimore A, Glithero A, Godkin A, Tissot AC, Pluckthun A, Elliott T, Hengartner H, Zinkernagel R. 1998. Induction and exhaustion of lymphocytic choriomeningitis virus-specific cytotoxic T lymphocytes visualized using soluble tetrameric major histocompatibility complex class I-peptide complexes. J Exp Med 187:1383-93.

174. Zajac AJ, Blattman JN, Murali-Krishna K, Sourdive DJ, Suresh M, Altman JD, Ahmed R. 1998. Viral immune evasion due to persistence of activated T cells without effector function. J Exp Med 188:2205-13.

175. Barber DL, Wherry EJ, Masopust D, Zhu B, Allison JP, Sharpe AH, Freeman GJ, Ahmed R. 2006. Restoring function in exhausted CD8 T cells during chronic viral infection. Nature 439:682-7.

176. Blackburn SD, Shin H, Haining WN, Zou T, Workman CJ, Polley A, Betts MR, Freeman GJ, Vignali DA, Wherry EJ. 2009. Coregulation of CD8+ T cell exhaustion by multiple inhibitory receptors during chronic viral infection. Nat Immunol 10:29-37.

177. Kaech SM, Tan JT, Wherry EJ, Konieczny BT, Surh CD, Ahmed R. 2003. Selective expression of the interleukin 7 receptor identifies effector CD8 T cells that give rise to long-lived memory cells. Nat Immunol 4:1191-8.

178. Tag CG, Sauer-Lehnen S, Weiskirchen S, Borkham-Kamphorst E, Tolba RH, Tacke F, Weiskirchen R. 2015. Bile duct ligation in mice: induction of inflammatory liver injury and fibrosis by obstructive cholestasis. J Vis Exp doi:10.3791/52438.

179. Chiang JYL, Ferrell JM. 2018. Bile Acid Metabolism in Liver Pathobiology. Gene Expr 18:71-87.

180. Makishima M, Okamoto AY, Repa JJ, Tu H, Learned RM, Luk A, Hull MV, Lustig KD, Mangelsdorf DJ, Shan B. 1999. Identification of a nuclear receptor for bile acids. Science 284:1362-5.

181. Kawamata Y, Fujii R, Hosoya M, Harada M, Yoshida H, Miwa M, Fukusumi S, Habata Y, Itoh T, Shintani Y, Hinuma S, Fujisawa Y, Fujino M. 2003. A G protein-coupled receptor responsive to bile acids. J Biol Chem 278:9435-40.

182. Kountouras J, Billing BH, Scheuer PJ. 1984. Prolonged bile duct obstruction: a new experimental model for cirrhosis in the rat. Br J Exp Pathol 65:305-11.

183. Georgiev P, Jochum W, Heinrich S, Jang JH, Nocito A, Dahm F, Clavien PA. 2008. Characterization of time-related changes after experimental bile duct ligation. Br J Surg 95:646-56.

184. Jurikova M, Danihel L, Polak S, Varga I. 2016. Ki67, PCNA, and MCM proteins: Markers of proliferation in the diagnosis of breast cancer. Acta Histochem 118:544-52.

185. Xia JL, Dai C, Michalopoulos GK, Liu Y. 2006. Hepatocyte growth factor attenuates liver fibrosis induced by bile duct ligation. Am J Pathol 168:1500-12.

186. Canbay A, Feldstein AE, Higuchi H, Werneburg N, Grambihler A, Bronk SF, Gores GJ. 2003. Kupffer cell engulfment of apoptotic bodies stimulates death ligand and cytokine expression. Hepatology 38:1188-98.

187. Gehring S, Dickson EM, San Martin ME, van Rooijen N, Papa EF, Harty MW, Tracy TF, Jr., Gregory SH. 2006. Kupffer cells abrogate cholestatic liver injury in mice. Gastroenterology 130:810-22.

188. Novobrantseva TI, Majeau GR, Amatucci A, Kogan S, Brenner I, Casola S, Shlomchik MJ, Koteliansky V, Hochman PS, Ibraghimov A. 2005. Attenuated liver fibrosis in the absence of B cells. J Clin Invest 115:3072-82.

189. Yoshiji H, Kuriyama S, Miyamoto Y, Thorgeirsson UP, Gomez DE, Kawata M, Yoshii J, Ikenaka Y, Noguchi R, Tsujinoue H, Nakatani T, Thorgeirsson SS, Fukui H. 2000. Tissue inhibitor of metalloproteinases-1 promotes liver fibrosis development in a transgenic mouse model. Hepatology 32:1248-54.

190. Miyazaki T, Ise M, Seo H, Niwa T. 1997. Indoxyl sulfate increases the gene expressions of TGF-beta 1, TIMP-1 and pro-alpha 1(I) collagen in uremic rat kidneys. Kidney Int Suppl 62:S15-22.

191. Gandhi CR. 2017. Hepatic stellate cell activation and pro-fibrogenic signals. J Hepatol 67:1104-1105.

192. Seki E, De Minicis S, Osterreicher CH, Kluwe J, Osawa Y, Brenner DA, Schwabe RF. 2007. TLR4 enhances TGF-beta signaling and hepatic fibrosis. Nat Med 13:1324-32.

193. Tarrats N, Moles A, Morales A, Garcia-Ruiz C, Fernandez-Checa JC, Mari M. 2011. Critical role of tumor necrosis factor receptor 1, but not 2, in hepatic stellate cell proliferation, extracellular matrix remodeling, and liver fibrogenesis. Hepatology 54:319-27.

194. Kocabayoglu P, Lade A, Lee YA, Dragomir AC, Sun X, Fiel MI, Thung S, Aloman C, Soriano P, Hoshida Y, Friedman SL. 2015. beta-PDGF receptor expressed by hepatic stellate cells regulates fibrosis in murine liver injury, but not carcinogenesis. J Hepatol 63:141-7.

195. Nevzorova YA, Tolba R, Trautwein C, Liedtke C. 2015. Partial hepatectomy in mice. Lab Anim 49:81-8.

196. Chanutin A, Gjessing EC. 1949. The effect of partial hepatectomy, thermal injury, and beta-chloroethyl vesicants on the lipides of plasma and plasma fractions of rats. J Biol Chem 178:1-5.

197. Taub R. 2004. Liver regeneration: from myth to mechanism. Nat Rev Mol Cell Biol 5:836-47.

198. Tao Y, Wang M, Chen E, Tang H. 2017. Liver Regeneration: Analysis of the Main Relevant Signaling Molecules. Mediators Inflamm 2017:4256352.

199. Fausto N. 2000. Liver regeneration. J Hepatol 32:19-31.

200. Fausto N, Campbell JS, Riehle KJ. 2006. Liver regeneration. Hepatology 43:S45-53.

201. Michalopoulos GK. 2007. Liver regeneration. J Cell Physiol 213:286-300.

202. Bohm F, Kohler UA, Speicher T, Werner S. 2010. Regulation of liver regeneration by growth factors and cytokines. EMBO Mol Med 2:294-305.

203. Wang B, Kaufmann B, Engleitner T, Lu M, Mogler C, Olsavszky V, Ollinger R, Zhong S, Geraud C, Cheng Z, Rad RR, Schmid RM, Friess H, Huser N, Hartmann D, von Figura G. 2019. Brg1 promotes liver regeneration after partial hepatectomy via regulation of cell cycle. Sci Rep 9:2320.

204. Wang X, Kiyokawa H, Dennewitz MB, Costa RH. 2002. The Forkhead Box m1b transcription factor is essential for hepatocyte DNA replication and mitosis during mouse liver regeneration. Proc Natl Acad Sci U S A 99:16881-6.

205. Schmidt-Arras D, Rose-John S. 2016. IL-6 pathway in the liver: From physiopathology to therapy. J Hepatol 64:1403-15.

206. Lee SY, Buhimschi IA, Dulay AT, Ali UA, Zhao G, Abdel-Razeq SS, Bahtiyar MO, Thung SF, Funai EF, Buhimschi CS. 2011. IL-6 trans-signaling system in intra-amniotic inflammation, preterm birth, and preterm premature rupture of the membranes. J Immunol 186:3226-36.

207. Cressman DE, Greenbaum LE, DeAngelis RA, Ciliberto G, Furth EE, Poli V, Taub R. 1996. Liver failure and defective hepatocyte regeneration in interleukin-6-deficient mice. Science 274:1379-83.

208. Fazel Modares N, Polz R, Haghighi F, Lamertz L, Behnke K, Zhuang Y, Kordes C, Haussinger D, Sorg UR, Pfeffer K, Floss DM, Moll JM, Piekorz RP, Ahmadian MR, Lang PA, Scheller J. 2019. IL-6 Trans-signaling Controls Liver Regeneration After Partial Hepatectomy. Hepatology doi:10.1002/hep.30774.

209. Li W, Liang X, Kellendonk C, Poli V, Taub R. 2002. STAT3 contributes to the mitogenic response of hepatocytes during liver regeneration. J Biol Chem 277:28411-7.

210. Yang L, Magness ST, Bataller R, Rippe RA, Brenner DA. 2005. NF-kappaB activation in Kupffer cells after partial hepatectomy. Am J Physiol Gastrointest Liver Physiol 289:G530-8.

211. Cornell RP. 1985. Restriction of gut-derived endotoxin impairs DNA synthesis for liver regeneration. Am J Physiol 249:R563-9.

212. Cornell RP. 1985. Gut-derived endotoxin elicits hepatotrophic factor secretion for liver regeneration. Am J Physiol 249:R551-62.

213. Strey CW, Markiewski M, Mastellos D, Tudoran R, Spruce LA, Greenbaum LE, Lambris JD. 2003. The proinflammatory mediators C3a and C5a are essential for liver regeneration. J Exp Med 198:913-23.

214. Selzner N, Selzner M, Odermatt B, Tian Y, Van Rooijen N, Clavien PA. 2003. ICAM-1 triggers liver regeneration through leukocyte recruitment and Kupffer cell-dependent release of TNF-alpha/IL-6 in mice. Gastroenterology 124:692-700.

215. Akerman P, Cote P, Yang SQ, McClain C, Nelson S, Bagby GJ, Diehl AM. 1992. Antibodies to tumor necrosis factor-alpha inhibit liver regeneration after partial hepatectomy. Am J Physiol 263:G579-85.

216. Yamada Y, Kirillova I, Peschon JJ, Fausto N. 1997. Initiation of liver growth by tumor necrosis factor: deficient liver regeneration in mice lacking type I tumor necrosis factor receptor. Proc Natl Acad Sci U S A 94:1441-6.

217. Yamada Y, Webber EM, Kirillova I, Peschon JJ, Fausto N. 1998. Analysis of liver regeneration in mice lacking type 1 or type 2 tumor necrosis factor receptor: requirement for type 1 but not type 2 receptor. Hepatology 28:959-70.

218. Ware CF. 2005. Network communications: lymphotoxins, LIGHT, and TNF. Annu Rev Immunol 23:787-819.

219. Fu YX, Huang G, Wang Y, Chaplin DD. 1998. B lymphocytes induce the formation of follicular dendritic cell clusters in a lymphotoxin alpha-dependent fashion. J Exp Med 187:1009-18.

220. Tumanov AV, Kuprash DV, Nedospasov SA. 2003. The role of lymphotoxin in development and maintenance of secondary lymphoid tissues. Cytokine Growth Factor Rev 14:275-88.

221. Anders RA, Subudhi SK, Wang J, Pfeffer K, Fu YX. 2005. Contribution of the lymphotoxin beta receptor to liver regeneration. J Immunol 175:1295-300.

222. Knight B, Yeoh GC. 2005. TNF/LTalpha double knockout mice display abnormal inflammatory and regenerative responses to acute and chronic liver injury. Cell Tissue Res 319:61-70.

223. Tumanov AV, Koroleva EP, Christiansen PA, Khan MA, Ruddy MJ, Burnette B, Papa S, Franzoso G, Nedospasov SA, Fu YX, Anders RA. 2009. T cell-derived lymphotoxin regulates liver regeneration. Gastroenterology 136:694-704 e4.

224. Sorg UR, Behnke K, Degrandi D, Reich M, Keitel V, Herebian D, Deenen R, Beyer M, Schultze JL, Kohrer K, Gabbert HE, Mayatepek E, Haussinger D, Pfeffer K. 2016. Cooperative role of lymphotoxin beta receptor and tumor necrosis factor receptor p55 in murine liver regeneration. J Hepatol 64:1108-1117.

225. Benvenuti S, Comoglio PM. 2007. The MET receptor tyrosine kinase in invasion and metastasis. J Cell Physiol 213:316-25.

226. Lindroos PM, Zarnegar R, Michalopoulos GK. 1991. Hepatocyte growth factor (hepatopoietin A) rapidly increases in plasma before DNA synthesis and liver regeneration stimulated by partial hepatectomy and carbon tetrachloride administration. Hepatology 13:743-50.

227. Pediaditakis P, Lopez-Talavera JC, Petersen B, Monga SP, Michalopoulos GK. 2001. The processing and utilization of hepatocyte growth factor/scatter factor following partial hepatectomy in the rat. Hepatology 34:688-93.

228. Patijn GA, Lieber A, Schowalter DB, Schwall R, Kay MA. 1998. Hepatocyte growth factor induces hepatocyte proliferation in vivo and allows for efficient retroviral-mediated gene transfer in mice. Hepatology 28:707-16.

229. Block GD, Locker J, Bowen WC, Petersen BE, Katyal S, Strom SC, Riley T, Howard TA, Michalopoulos GK. 1996. Population expansion, clonal growth, and specific differentiation patterns in primary cultures of hepatocytes induced by HGF/SF, EGF and TGF alpha in a chemically defined (HGM) medium. J Cell Biol 132:1133-49.

230. Paranjpe S, Bowen WC, Bell AW, Nejak-Bowen K, Luo JH, Michalopoulos GK. 2007. Cell cycle effects resulting from inhibition of hepatocyte growth factor and its receptor c-Met in regenerating rat livers by RNA interference. Hepatology 45:1471-7.

231. Huh CG, Factor VM, Sanchez A, Uchida K, Conner EA, Thorgeirsson SS. 2004. Hepatocyte growth factor/c-met signaling pathway is required for efficient liver regeneration and repair. Proc Natl Acad Sci U S A 101:4477-82.

232. Romero-Gallo J, Sozmen EG, Chytil A, Russell WE, Whitehead R, Parks WT, Holdren MS, Her MF, Gautam S, Magnuson M, Moses HL, Grady WM. 2005. Inactivation of TGF-beta signaling in hepatocytes results in an increased proliferative response after partial hepatectomy. Oncogene 24:3028-41.

233. Kiso S, Kawata S, Tamura S, Inui Y, Yoshida Y, Sawai Y, Umeki S, Ito N, Yamada A, Miyagawa J, Higashiyama S, Iwawaki T, Saito M, Taniguchi N, Matsuzawa Y, Kohno K. 2003. Liver regeneration in heparin-binding EGF-like growth factor transgenic mice after partial hepatectomy. Gastroenterology 124:701-7.

234. Kong B, Sun R, Huang M, Chow MD, Zhong XB, Xie W, Lee YH, Guo GL. 2018. Fibroblast Growth Factor 15-Dependent and Bile Acid-Independent Promotion of Liver Regeneration in Mice. Hepatology 68:1961-1976.

235. Lohela M, Bry M, Tammela T, Alitalo K. 2009. VEGFs and receptors involved in angiogenesis versus lymphangiogenesis. Curr Opin Cell Biol 21:154-65.

236. Ohkohchi. N MS, Takahashi. K. 2012. Platelet and Liver Regeneration doi: 10.5772/25422.

237. Luhur A, Buddika K, Ariyapala IS, Chen S, Sokol NS. 2017. Opposing Post-transcriptional Control of InR by FMRP and LIN-28 Adjusts Stem Cell-Based Tissue Growth. Cell Rep 21:2671-2677.

238. Morris AG, Lin YL, Askonas BA. 1982. Immune interferon release when a cloned cytotoxic T-cell line meets its correct influenza-infected target cell. Nature 295:150-2.

239. Liu Z, Ge Y, Wang H, Ma C, Feist M, Ju S, Guo ZS, Bartlett DL. 2018. Modifying the cancer-immune set point using vaccinia virus expressing re-designed interleukin-2. Nat Commun 9:4682.

240. Pfeffer K, Matsuyama T, Kundig TM, Wakeham A, Kishihara K, Shahinian A, Wiegmann K, Ohashi PS, Kronke M, Mak TW. 1993. Mice deficient for the 55 kd tumor necrosis factor receptor are resistant to endotoxic shock, yet succumb to L. monocytogenes infection. Cell 73:457-67.

241. Tummers B, Green DR. 2017. Caspase-8: regulating life and death. Immunol Rev 277:76-89.

242. Weinlich R, Green DR. 2014. The two faces of receptor interacting protein kinase-1. Mol Cell 56:469-80.

243. Dillon CP, Weinlich R, Rodriguez DA, Cripps JG, Quarato G, Gurung P, Verbist KC, Brewer TL, Llambi F, Gong YN, Janke LJ, Kelliher MA, Kanneganti TD, Green DR.

2014. RIPK1 blocks early postnatal lethality mediated by caspase-8 and RIPK3. Cell 157:1189-202.

244. Rickard JA, O'Donnell JA, Evans JM, Lalaoui N, Poh AR, Rogers T, Vince JE, Lawlor KE, Ninnis RL, Anderton H, Hall C, Spall SK, Phesse TJ, Abud HE, Cengia LH, Corbin J, Mifsud S, Di Rago L, Metcalf D, Ernst M, Dewson G, Roberts AW, Alexander WS, Murphy JM, Ekert PG, Masters SL, Vaux DL, Croker BA, Gerlic M, Silke J. 2014. RIPK1 regulates RIPK3-MLKL-driven systemic inflammation and emergency hematopoiesis. Cell 157:1175-88.

245. Newton K, Dugger DL, Wickliffe KE, Kapoor N, de Almagro MC, Vucic D, Komuves L, Ferrando RE, French DM, Webster J, Roose-Girma M, Warming S, Dixit VM. 2014. Activity of protein kinase RIPK3 determines whether cells die by necroptosis or apoptosis. Science 343:1357-60.

246. Polykratis A, Hermance N, Zelic M, Roderick J, Kim C, Van TM, Lee TH, Chan FKM, Pasparakis M, Kelliher MA. 2014. Cutting edge: RIPK1 Kinase inactive mice are viable and protected from TNF-induced necroptosis in vivo. J Immunol 193:1539-1543.

247. Kondylis V, Polykratis A, Ehlken H, Ochoa-Callejero L, Straub BK, Krishna-Subramanian S, Van TM, Curth HM, Heise N, Weih F, Klein U, Schirmacher P, Kelliher M, Pasparakis M. 2015. NEMO Prevents Steatohepatitis and Hepatocellular Carcinoma by Inhibiting RIPK1 Kinase Activity-Mediated Hepatocyte Apoptosis. Cancer Cell 28:582-598.

248. Dara L, Johnson H, Suda J, Win S, Gaarde W, Han D, Kaplowitz N. 2015. Receptor interacting protein kinase 1 mediates murine acetaminophen toxicity independent of the necrosome and not through necroptosis. Hepatology 62:1847-57.

249. Deutsch M, Graffeo CS, Rokosh R, Pansari M, Ochi A, Levie EM, Van Heerden E, Tippens DM, Greco S, Barilla R, Tomkotter L, Zambirinis CP, Avanzi N, Gulati R, Pachter HL, Torres-Hernandez A, Eisenthal A, Daley D, Miller G. 2015. Divergent effects of RIP1 or RIP3 blockade in murine models of acute liver injury. Cell Death Dis 6:e1759.

250. Gunther C, He GW, Kremer AE, Murphy JM, Petrie EJ, Amann K, Vandenabeele P, Linkermann A, Poremba C, Schleicher U, Dewitz C, Krautwald S, Neurath MF, Becker C, Wirtz S. 2016. The pseudokinase MLKL mediates programmed hepatocellular necrosis independently of RIPK3 during hepatitis. J Clin Invest 126:4346-4360.

251. Filliol A, Piquet-Pellorce C, Le Seyec J, Farooq M, Genet V, Lucas-Clerc C, Bertin J, Gough PJ, Dimanche-Boitrel MT, Vandenabeele P, Bertrand MJ, Samson M. 2016.

RIPK1 protects from TNF-alpha-mediated liver damage during hepatitis. Cell Death Dis 7:e2462.

252. Kondylis V, Pasparakis M. 2019. RIP Kinases in Liver Cell Death, Inflammation and Cancer. Trends Mol Med 25:47-63.

253. Afonso MB, Rodrigues PM, Simao AL, Ofengeim D, Carvalho T, Amaral JD, Gaspar MM, Cortez-Pinto H, Castro RE, Yuan J, Rodrigues CM. 2016. Activation of necroptosis in human and experimental cholestasis. Cell Death Dis 7:e2390.

254. Roychowdhury S, McMullen MR, Pisano SG, Liu X, Nagy LE. 2013. Absence of receptor interacting protein kinase 3 prevents ethanol-induced liver injury. Hepatology 57:1773-83.

255. Gautheron J, Vucur M, Reisinger F, Cardenas DV, Roderburg C, Koppe C, Kreggenwinkel K, Schneider AT, Bartneck M, Neumann UP, Canbay A, Reeves HL, Luedde M, Tacke F, Trautwein C, Heikenwalder M, Luedde T. 2014. A positive feedback loop between RIP3 and JNK controls non-alcoholic steatohepatitis. EMBO Mol Med 6:1062-74.

256. Afonso MB, Rodrigues PM, Carvalho T, Caridade M, Borralho P, Cortez-Pinto H, Castro RE, Rodrigues CM. 2015. Necroptosis is a key pathogenic event in human and experimental murine models of non-alcoholic steatohepatitis. Clin Sci (Lond) 129:721-39.

257. Xu D, Jin T, Zhu H, Chen H, Ofengeim D, Zou C, Mifflin L, Pan L, Amin P, Li W, Shan B, Naito MG, Meng H, Li Y, Pan H, Aron L, Adiconis X, Levin JZ, Yankner BA, Yuan J. 2018. TBK1 Suppresses RIPK1-Driven Apoptosis and Inflammation during Development and in Aging. Cell 174:1477-1491 e19.

258. Weisz ED, Towheed A, Monyak RE, Toth MS, Wallace DC, Jongens TA. 2018. Loss of Drosophila FMRP leads to alterations in energy metabolism and mitochondrial function. Hum Mol Genet 27:95-106.

259. Leboucher A, Pisani DF, Martinez-Gili L, Chilloux J, Bermudez-Martin P, Van Dijck A, Ganief T, Macek B, Becker JAJ, Le Merrer J, Kooy RF, Amri EZ, Khandjian EW, Dumas ME, Davidovic L. 2019. The translational regulator FMRP controls lipid and glucose metabolism in mice and humans. Mol Metab 21:22-35.

260. McLennan Y, Polussa J, Tassone F, Hagerman R. 2011. Fragile x syndrome. Curr Genomics 12:216-24.

261. Darnell JC, Van Driesche SJ, Zhang C, Hung KY, Mele A, Fraser CE, Stone EF, Chen C, Fak JJ, Chi SW, Licatalosi DD, Richter JD, Darnell RB. 2011. FMRP stalls

ribosomal translocation on mRNAs linked to synaptic function and autism. Cell 146:247-61.

262. Liu XS, Wu H, Krzisch M, Wu X, Graef J, Muffat J, Hnisz D, Li CH, Yuan B, Xu C, Li Y, Vershkov D, Cacace A, Young RA, Jaenisch R. 2018. Rescue of Fragile X Syndrome Neurons by DNA Methylation Editing of the FMR1 Gene. Cell 172:979-992 e6.

263. Yang G, Parkhurst CN, Hayes S, Gan WB. 2013. Peripheral elevation of TNF-alpha leads to early synaptic abnormalities in the mouse somatosensory cortex in experimental autoimmune encephalomyelitis. Proc Natl Acad Sci U S A 110:10306-11.

264. Beattie EC, Stellwagen D, Morishita W, Bresnahan JC, Ha BK, Von Zastrow M, Beattie MS, Malenka RC. 2002. Control of synaptic strength by glial TNFalpha. Science 295:2282-5.

265. Stellwagen D, Malenka RC. 2006. Synaptic scaling mediated by glial TNF-alpha. Nature 440:1054-9.

266. Odeh M, Sabo E, Srugo I, Oliven A. 2005. Relationship between tumor necrosis factor-alpha and ammonia in patients with hepatic encephalopathy due to chronic liver failure. Ann Med 37:603-12.

267. Sandgren EP, Palmiter RD, Heckel JL, Daugherty CC, Brinster RL, Degen JL. 1991. Complete hepatic regeneration after somatic deletion of an albumin-plasminogen activator transgene. Cell 66:245-56.

268. Bauer J, Ganter U, Geiger T, Jacobshagen U, Hirano T, Matsuda T, Kishimoto T, Andus T, Acs G, Gerok W, et al. 1988. Regulation of interleukin-6 expression in cultured human blood monocytes and monocyte-derived macrophages. Blood 72:1134-40.

269. Izumi T, Imai J, Yamamoto J, Kawana Y, Endo A, Sugawara H, Kohata M, Asai Y, Takahashi K, Kodama S, Kaneko K, Gao J, Uno K, Sawada S, Kalinichenko VV, Ishigaki Y, Yamada T, Katagiri H. 2018. Vagus-macrophage-hepatocyte link promotes post-injury liver regeneration and whole-body survival through hepatic FoxM1 activation. Nat Commun 9:5300.

270. Amemiya H, Kono H, Fujii H. 2011. Liver regeneration is impaired in macrophage colony stimulating factor deficient mice after partial hepatectomy: the role of M-CSF-induced macrophages. J Surg Res 165:59-67.

271. Moseman EA, Iannacone M, Bosurgi L, Tonti E, Chevrier N, Tumanov A, Fu YX, Hacohen N, von Andrian UH. 2012. B cell maintenance of subcapsular sinus

macrophages protects against a fatal viral infection independent of adaptive immunity. Immunity 36:415-26.

272. Shaabani N, Duhan V, Khairnar V, Gassa A, Ferrer-Tur R, Haussinger D, Recher M, Zelinskyy G, Liu J, Dittmer U, Trilling M, Scheu S, Hardt C, Lang PA, Honke N, Lang KS. 2016. CD169(+) macrophages regulate PD-L1 expression via type I interferon and thereby prevent severe immunopathology after LCMV infection. Cell Death Dis 7:e2446.

273. Peters M, Blinn G, Jostock T, Schirmacher P, Meyer zum Buschenfelde KH, Galle PR, Rose-John S. 2000. Combined interleukin 6 and soluble interleukin 6 receptor accelerates murine liver regeneration. Gastroenterology 119:1663-71.

274. van der Kuyl AC, van den Burg R, Zorgdrager F, Groot F, Berkhout B, Cornelissen M. 2007. Sialoadhesin (CD169) expression in CD14+ cells is upregulated early after HIV-1 infection and increases during disease progression. PLoS One 2:e257.

275. Holt AP, Stamataki Z, Adams DH. 2006. Attenuated liver fibrosis in the absence of B cells. Hepatology 43:868-71.

276. Schiemann B, Gommerman JL, Vora K, Cachero TG, Shulga-Morskaya S, Dobles M, Frew E, Scott ML. 2001. An essential role for BAFF in the normal development of B cells through a BCMA-independent pathway. Science 293:2111-4.

277. Davies LC, Jenkins SJ, Allen JE, Taylor PR. 2013. Tissue-resident macrophages. Nat Immunol 14:986-95.